UNCLASSIFIED

AD 295 464

UNCLASSIFIED

ASD-TDR-62-165
Volume I

CATALOGED BY ASTIA
AS AD No. 295464

295 464

STUDY OF A SONIC LOAD RECORDER

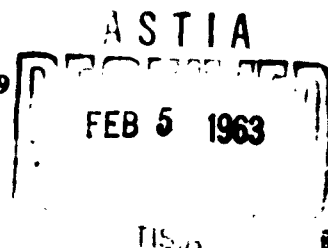TECHNICAL DOCUMENTARY REPORT ASD-TDR-62-165

VOLUME I

November 1962

Flight Dynamics Laboratory

Aeronautical Systems Division

Air Force Systems Command

Wright-Patterson Air Force Base, Ohio

Project No. 1370, Task No. 137005

ASTIA

FEB 5 1963

TIS...

NOTICES

When Government drawings, specifications, or other data are used for any purpose other than in connection with a definitely related Government procurement operation, the United States Government thereby incurs no responsibility nor any obligation whatsoever; and the fact that the Government may have formulated, furnished, or in any way supplied the said drawings, specifications, or other data, is not to be regarded by implication or otherwise as in any manner licensing the holder or any other person or corporation, or conveying any rights or permission to manufacture, use, or sell any patented invention that may in any way be related thereto.

ASTIA release to OTS not authorized.

Qualified requesters may obtain copies of this report from the Armed Services Technical Information Agency, (ASTIA), Arlington Hall Station, Arlington 12, Virginia.

Copies of this report should not be returned to the Aeronautical Systems Division unless return is required by security considerations, contractual obligations, or notice on a specific document.

D

FOREWORD

Volume I covers the period of work from January through December 1961. This work was concerned with the study and design of an instrument to monitor sonic loads. Volume II covers the period of work from January to July 1962 during which the design of an instrument to monitor the response of aircraft panels was considered.

ABSTRACT

The feasibility of a compact instrument to measure the accumulated acoustic exposure of a flight vehicle is considered. The output data of the instrument will aid the estimation of fatigue life. A study of the conditions and parameters involved together with general requirements of the instrument is presented. Design criteria are discussed such as techniques for amplitude analysis, sampling and accumulation of data in a directly readable and usable form. A specific design of a breadboard model of the sonic recorder is given with test and performance data under laboratory conditions. A discussion of the effects of temperature, vibration, and power supply variations is also included. Complete circuit diagrams are provided.

PUBLICATION REVIEW

This report has been reviewed and is approved.

FOR THE COMMANDER

WALTER J. MYKYTOW
Chief, Dynamics Branch
Flight Dynamics Laboratory

TABLE OF CONTENTS

LIST OF FIGURES

ASD-TDR-62-165
Volume I

LIST OF FIGURES FOR APPENDIX A.

LIST OF FIGURES FOR APPENDIX B.

LIST OF TABLES

LIST OF SYMBOLS

a	bandwidth of narrowest filter
A	correlation area
α	fatigue exponent
b	percentage modulation
B	gain
B+, B-	voltage supplies
C	constant
db	decibels
D	damage accumulation
δ	sampling pulse
δ^*	boundary layer momentum thickness
ϵ	strain
η	damping factor
f	frequency
FM	frequency modulation
G	transfer function
h	altitude
θ	lifetime of turbulence
I	correlation integral
KC	1000 cycles per second
m	bias voltage
M	mach number

M'	surface density
μ	mean value
N	life
ω	angular frequency ($2\pi f$)
$\Delta\omega$	frequency deviation
p	pressure
P	probability
q	dynamic pressure
Q	selectivity
ρ	ambient density of air
S(t)	periodic waveform
$S_o(f)$	spectral density
SPL	sound pressure level in db re .0002 dynes/cm^2
σ	standard deviation
t	time variable
T	period
τ	duration of a maximum
u	free stream velocity
v	velocity
V	voltage
VCO	voltage controlled oscillator
ϕ	characteristic function
x, y	spatial variables

SECTION I

INTRODUCTION

Knowledge of the sonic induced loads to which a flight vehicle is subjected during its lifetime is required for structural fatigue analysis in flight vehicle design. This study investigates the requirements for a device which will provide a useful description of sonic induced loads at a point on operational aircraft. This information is presently estimated using accumulated data of engine rpm, ambient temperature, etc. However, there are many other factors which determine the sound pressure level at a point from this excitation. Hence it is beneficial to accumulate sound pressure data directly.

The sonic recorder is a compact instrumentation system which will measure the sound pressure at a point, filter the signal into frequency bands, detect the resulting signal, and then record a measure of the length of time the signal has spent within given levels. Since this device is to be carried in a flight vehicle, it is necessary to process and store only the most important (from a fatigue viewpoint) characteristics of the signal. Thus, it is necessary to limit the range of frequencies and the range of the amplitudes for which the system must record and store duration information. Furthermore, it is important to estimate the durations in various amplitude and frequency ranges in order to provide an adequate, but not excessively large, memory capacity for the recorder.

This study has been accomplished in two phases. Phase I examined the feasibility of the recorder system and set forth the requirements. The results of this work are contained in Section II of Volume I. Phase II considered the design of an instrument to meet the requirements. This design was verified by the construction of a breadboard system. Sections III and IV discuss the results of Phase II.

SECTION II

STUDY OF REQUIREMENTS FOR THE SONIC LOAD HISTORY RECORDER

·The level, the spectrum, and the duration characteristics of sonic loads on aircraft are discussed in Section A. The responses of aircraft structures to these loads are estimated in Section B. On the basis of the information in Sections A and B, design requirements are derived for the sonic load history recorder.

A.   NOISE EXCITATION

1.   Introduction

The noise exposure at a point or the response of a structure at a point can be described by three independent characteristics: (1) a measure of the level, (2) a measure of the frequency (cps) distribution, and (3) a measure of the distribution of the time spent, for each frequency, in various level increments. In order to minimize the size and weight of the Sonic Load History Recorder (SLHR) it is necessary to limit the range of levels, the range of frequencies, and the range of durations to those of importance to sonic fatigue of flight vehicle structures. An efficient data storage system can be achieved if the maximum anticipated noise levels, their spectra, and their relative durations are known. In this section, attempts are made to estimate these quantities in order to provide the basis for the design of an efficient data storage system.

The distribution of noise levels for a contemporary aircraft are estimated on the basis of operational data supplied by the Aeronautical Systems Division of the U. S. Air Force. The distribution of noise levels will approximate the distribution of anticipated responses provided the relation between excitation and response is near a linear one. No attempt is made here to determine an absolute distribution of response or noise input. The important result is the relative durations in contiguous amplitude level bands, that is, the "shape" of the distribution.

2.   Maximum Noise Levels

The primary objective during the initial studies was to attempt to find, as a function of frequency, the maximum excitations which are likely to be encountered on contemporary and future aircraft. Consideration has been given to both the noise from jet and rocket engines and the noise arising from pressure fluctuations in the boundary layer.

a)   Jet and Rocket Engine Noise

Noise from the exhaust of jet engines is the most important con-
tributor to sonic fatigue of aircraft structures. When the engines are
mounted in pods, the aircraft control structures are generally located
in the most intense near field noise of the jet. The fatigue problem
is not so acute for aircraft with the engines mounted in the fuselage
with the jet exhaust orifice in the tail of the aircraft.

Consideration of the level and frequency distribution of acoustic
noise in the near field of jet aircraft suggests that the most severe
sonic exposure for contemporary aircraft is probably found on the B-58
which has afterburning J-79 engines.* An octave band spectrum of the
maximum sound pressure levels found near the surface of structures on
the B-58 with afterburner operation in shown in Fig. 1, (Ref. 1). If
we allow about 6 db for (1) growth in engine performance, (2) increase
in noise outputs during certain adverse environmental conditions, and
(3) uncertainty, then the maximum expected levels of jet engine noise
for the SLHR are as given in curve 2 in Fig. 1. These maximum levels
will occur only during infrequent ground maintenance procedures.

The jet noise incident on surfaces of the aircraft will decrease
as the aircraft accelerates to takeoff speed. Typically, a fighter
will reach its climb speed in less than one minute after brake release.
For a bomber or tanker the climb speed may not be reached for two or
perhaps three minutes after release. In either case the noise levels
during climb (say 400-500 knots IAS) will be from 5 to 15 db below the
levels on the ground since the noise generated depends upon the seventh
or eighth power of the jet exhaust velocity with respect to the
surrounding air. A prediction of the decrease in noise level with air
speed is obtained upon the net thrust-mass flow-air speed-velocity
characteristics of contemporary engines. An example is given in Section
3 below.

Noise from rocket exhaust is slightly higher. Figure 1 indicates
levels measured at the lower end of a missile (Atlas) near the rocket
nozzle, (Ref. 2). Levels much higher than this are not expected in the
near field, although the total power radiated by larger rockets may be
considerably higher.

_____

* Another example of severe exposure is in fighter aircraft such as
  the F-101 which has engines buried in the wing root.

b) Aerodynamic Noise Levels

The pressure fluctuations in boundary layers have been investigated in wind tunnels and in flight for subsonic velocities. Few measurements have been made in wind tunnels in supersonic unaccelerated flows. The supersonic data do not appear to be self-consistent. We follow the common procedure of using a subsonic relationship to extrapolate into the supersonic regime.

The overall root-mean-square pressure fluctuations in the boundary layer are given by $\sqrt{p^2} = C_1 \times q$, in which q is the dynamic pressure $(1/2 \, \rho \, v^2)$, ρ is the ambient density of the air, v is the true airspeed of the aircraft, and C_1 is a dimensionless constant whose value is about 6×10^{-3}. This formula represents an average over the known information for subsonic pressure fluctuations. In terms of overall sound pressure level (SPL_{OA}) in db re .0002 dynes/cm^2, the mean square pressure can be expressed as

$$SPL_{OA} = 20 \log_{10}(q) + 86 \text{ db}$$

where q is in lbs/ft^2 and a 3 db safety factor is included. Since ρ is a function of altitude the overall sound pressure levels expected in various flight regimes can be calculated and presented on a graph on which the flight regimes of space vehicles can be superimposed. Such a presentation is given in Fig. 2. This curve is based on the ICAO standard atmosphere as given in NASA TN #3182 (h<65,000 ft.), and on the NASA tentative upper atmosphere (NASA TN #1200) (h>65,000 ft.). A curve (M=1) divides the figure into subsonic and supersonic regimes as a reminder that the estimates are based on subsonic data and that they may be subject to large uncertainties in the supersonic range.

Most flight vehicles are limited in their performance by the maximum dynamic pressure (q) which the structure can tolerate. A maximum q curve for an aircraft would also be a fixed overall pressure curve, at least in the subsonic regime. For example, a q of 1000 lbs/ft2 corresponds to an overall sound pressure level of 146 db. A q of 2000 lbs/ft2 would be an overall sound pressure level of 152 db. Preliminary estimates of aerodynamic noise levels suggest that these may not be an important source of aircraft fatigue.

Precise theoretical estimates cannot be made in view of the large
uncertainties in the prediction of the parameters of the boundary layer
which influence the noise. The pressure fluctuations in any particular
situation may be influenced in an unknown manner by aircraft geometry,
flight attitude, skin roughness, and interaction of shock waves with
the boundary layer. These problems will arise in both the subsonic and
supersonic regimes.

Contemporary aircraft seem to be limited to a q of at most 2000
lbs/ft^2. The corresponding overall SPL would then be predicted to be
about 152 db. If future vehicles were designed to exceed this figure
by a factor of two, then the corresponding SPL might be 6 db greater

The spectra of the aerodynamic sound pressure levels are less well
predictable than the overall level. There is general agreement that
the sound pressure level spectrum (on a per cycle basis) is approximately
flat up to some frequency, f_o, and decreases rapidly at higher frequen-
cies. Various studies and experiments indicate

$$f_o \sim C \frac{u}{\delta^*}$$

where u is the free stream velocity and δ^* is the boundary layer momentum
thickness, and C lies between 0.1 and 1.0, apparently depending on Mach
number. This result implies that for typical aircraft flight regimes,
frequencies up to 10 KC may be important in determining the overall
SPL. (Ref. 3)

3. **Distribution of Jet Noise Levels for a Contemporary Aircraft**

An attempt here is made to estimate the duration vs. level distri-
bution of the jet noise levels for a contemporary aircraft. No attempt
is made to obtain a corresponding estimate for aerodynamic noise because
sufficiently detailed operational information is not available and the
state of the art for predicting boundary layer noise does not allow such
estimates to be accurate enough to be useful

Under ASD Contract No. AF 33(616)-7066 data have been obtained
which describe statistical histories of engine ground operations for
three RB-47E aircraft. These data were reduced and analyzed by the
Battelle Memorial Institute and presented in a letter progress report
dated June 10, 1960. The engine data are given as the time spent in
various rpm categories. The time history of the acoustic noise at a
point on the aircraft is derived in this section from these data and
from the data contained in Model Specification for the J-47 engines by
the procedures given in WADC TR 58-343. (Ref. 3).

a)   Engine Operating Time on the Ground

The engine operations have been divided in five categories on the basis of engine rpm. The amount of time the engine spends in each rpm category while on the ground is given in the Battelle Report. The average values for the No. 4 engine are given in Table I below. The average number of hours an aircraft spends on the ground with the No. 4 engine in each rpm category are given for each one-thousand hours of flight time.

TABLE I

APPROXIMATE NO. 4 ENGINE GROUND TIME
IN HRS/1000 HOURS OF FLIGHT

(AVERAGE OF DATA FROM BATTELLE REPORT)

Category	1	2	3	4	5
rpm range (% of max)	0-80	80-90	90-95	95-98	98-100
time in hrs/1000 flt hrs	140	2	0.3	0.2	5.0

Engine ground time includes operations with the aircraft stationary and some time with the aircraft accelerating for takeoff and decelerating after landing.

b)   Noise Levels for RPM Categories

A position on the trailing edge of the wing near the highest levels from the No. 4 engine is selected as a point to investigate the relative duration of noise levels. For part of the investigation the duration at various noise levels is of importance. The absolute levels are only of secondary importance. We have therefore not attempted to take into account the acoustic effects of ground reflections, of pressure doubling at the wing surface, of the two adjacent engines on one another, etc.

SPL's in octave bands of frequency for each rpm category are given in Table II below. It is assumed here that the aircraft is stationary and that the temperature is 59°F.

TABLE II

SOUND PRESSURE LEVELS ON AN RB-47 WING SURFACE
FOR VARIOUS ENGINE SPEEDS

Speed Category	rpm (% of max)	Octave Bands of Frequency - cps							
		20 75	75 150	150 300	300 600	600 1200	1200 2400	2400 4800	4800 10KC
5	98-100	122	126	130	134	137	135	132	129
4	95-98	121	125	129	133	136	134	131	128
3	90-95	114	118	122	126	129	127	124	121
2	80-90	107	111	115	119	119	116	113	110

No attempt has been made to estimate the noise levels for Category No. 1 (0 to 80% rpm) since the range of rpm is too large to obtain a reasonable estimate. Furthermore, the usual prediction methods do not generally apply at low rpm conditions since combustor noise, compressor noise, and other noise sources may prevail over the jet noise. Noise levels 5 db or more below the maximum value in any band are of no consequence to the fatigue problem and the lower levels offer no useful information. A study of the time spent in the various engine categories and at the indicated sound pressure levels shows that the only information of any real interest to the fatigue problem is the time spent in the highest category, (see Section II.B.2).

The SPL's on the wing corresponding to the highest engine category will be affected by the speed of the aircraft and the ambient temperature. These effects are considered in the following sections.

c) Temperature-Induced Noise Level Variations

The Battelle Report includes a distribution of ambient temperatures weighted for the time an engine was in rpm category No. 5. These data indicate that the mean temperature while an aircraft was operating was about 65°F. The distribution was approximately normal with a standard deviation of about 20°F. The variation of SPL with temperature was derived from the mass flow and thrust variations indicated in the Model Specification for the J-47 engine. In the temperature range from 0°F to 100°F the SPL is found to increase an average of about 1 db* for each 20°F decrease in temperature. This approximate result is consistent with measured data in the literature.

---

* Actually the change of SPL with temperature is somewhat greater at high temperatures than at low temperatures.

We have derived the distribution of SPL's by considering the mean temperature to be 59°F rather than 65°F since engine data is given at 59°F. The distribution will not be at all affected and a great deal of simplicity is obtained for the calculations. The results are given in Table III. This table indicates the SPL will be at the normal 59°F level for 38% of the 5 hours/1000 hours of flight, one db higher 24% of the 5 hours/1000 hours of flight, etc.

TABLE III

SPL VARIATIONS OWING TO TEMPERATURE VARIATIONS

SPL in db re 59°F level	+3	+2	+1	0	-1	-2	-3
Percent of time	1	12	24	38	24	12	1

These results apply of course only when considering operations over a full year since the mean temperature will vary from season to season.

d)   Aircraft Speed-Induced Variations in Noise Level

The forward motion of an aircraft reduces the jet velocity relative to the surrounding air and thereby decreases the noise radiated by the engine. Thus as the aircraft accelerates during takeoff, the sound pressure levels continually decrease even though the engine is kept at a constant power setting. A further decrease in SPL will occur when the aircraft engine power setting is reduced to a climb power after takeoff.

The change in SPL has been calculated using engine information given in the manufacturer's model specifications and the techniques outlined in WADC TR 58-343. The calculations were carried out for eight octave bands. The results are given for two octave bands in Fig. 3. In both bands the noise level has dropped about 5 db when the aircraft has accelerated to 100 knots. At the takeoff speed, about 160 knots, the SPL's have dropped about eight db. A power reduction from maximum to maximum continous power (96% rpm) causes a further reduction of about 7 db.

The time history of the noise on a takeoff can be derived if the acceleration of the aircraft is known. The acceleration for an RB-47E is assumed to be about 4 ft/sec^2 on the basis of limited information, (Ref. 4). This figure is consistent with the power to weight ratio of the aircraft.

The time history of the SPL during takeoff is given in Fig. 4. This figure was derived from the assumed acceleration and the data presented in Fig. 3. The results in Fig. 4 apply only for the 600-1200 cps band. Similar results could be derived for the other bands. If the ambient temperature were higher, the SPL vs. the time curve would be lower than the curve shown, but the time to takeoff would be somewhat longer owing to the loss of thrust and the higher takeoff speed. We will assume the change in takeoff time is negligible in the following section in order to derive a distribution of levels in this band when the effects of motion and temperature on SPL are both considered.

e) Level Distribution

As noted earlier, the Battelle Report states that about 5 hours/1000 hours of flight are spent in engine category No. 5. This engine ground time includes both operations with the aircraft stationary and accelerating during takeoff. In order to estimate the SPL distribution it is necessary to separate time spent in these two operations. This was done by dividing the average flight time into 1000 to obtain the average number of flights and takeoffs/1000 hours of flight. The average flight was given as about 6.5 hours so that one could expect an average of about 155 takeoffs in each 1000 hours of flight. Since a takeoff involves a ground run of about 65 seconds, operations during takeoff roll account for about 2.8 hours of engine operation in category No. 5. The remaining 2.2 hours are static operations such as maintenance operations and pre-brake-release run-ups before takeoff.

Some of the engine time on the ground in category No. 5 can be accounted for by "touch-and-go" operations. According to the Battelle Report this time is a very small fraction of the total time in category No. 5 and may be neglected.

The level distribution per 1000 hours of flight for the 600-1200 cps band is presented in Fig. 5. The contributions to the various levels have been coded to distinguish between static operations and takeoff operations. The SPL's from static operations are symmetrically distributed about the value of 137 because a linear relation between SPL and the normally distributed temperature has been assumed. The takeoff operations are also assumed to have the same temperature distribution, but the resulting SPL's are biased because the effects of acceleration cause the lower levels to occur more frequently than the higher levels. From a fatigue viewpoint only the range of levels between the highest level (140 db) and the most frequently occurring high level (137 db) are of interest.

It would appear from this example that a 5 db range for the level distributor in a sonic load history recorder would be adequate if the maximum levels were known precisely. A greater range must be used, however, because of our ignorance of the maximum noise levels.

B.   RESPONSE OF AIRCRAFT PANELS TO NOISE FIELDS

The pressure level and spectrum at a point provide necessary, but
not complete information for deriving the response of a panel to jet
or rocket exhaust noise fields. A direction of propagat: ҳ is gener-
ally needed for accurate prediction of the response. However, for the
important case of excitation of a fundamental mode at low* frequencies,
direction of propagation is not important. Also, the maximum possible
responses can be estimated by assuming the most "efficient" angle of
incidence occurred. A pressure level and its spectrum then provide
useful information for design against fatigue by jet and rocket noise.
However, propagation direction is important for precise calculation
of response.

The response to boundary layer pressure fluctuations (aerodynamic
noise) is more complex. The response of a panel depends vitally on
the space-time correlation of pressures over the panel and consequently
prediction of fatigue life is almost impossible from only pressure
level and spectrum information obtained from measurements at a single
point unless additional information leading to space-time correlation
is obtained.

In this section we consider the response of panels to (1) jet
and rocket noise, and (2) to aerodynamic noise and the ratio of the
response to these two noises from the viewpoint of the possibility of
obtaining useful information from a sonic load history recorder.

---

*   When the wavelength of sound is much greater than a characteristic
panel length.

1. <u>Dynamic Response of Aircraft Panels</u>

The mean square velocity of a panel excited by an acoustic noise from jets and rockets depends upon the intensity of the exciting pressure, its frequency, and the angle of incidence. The mean square velocity may be written as, (Ref. 6)

$$\bar{v}_1^2(x,y) = \frac{\pi G^2 S_o(f_{mn}) \phi_n^2(x) \phi_m^2(y)}{2 \eta \omega_{mn} (M')^2}$$ (1)

in which

$\bar{v}_1^2(x,y)$ is the mean square velocity at some point on the panel,

$S_o(f_{mn})$ is the spectral density of the exciting pressure, near f_{mn},

ω_{mn} is a resonance frequency $(2\pi f_{mn})$,

$\phi_n^2(x)$ is a characteristic function which describes the spatial variation of $\bar{v}_1^2$ in the x direction,

$\phi_m^2(y)$ describes the spatial variation of $\bar{v}_1^2$ in the y direction,

G^2 is a function which describes the dependence of $\bar{v}_1^2$ on the angle of incidence of the sound on the plate (see below),

η is a hysteretic damping factor,

M' is the surface density of the panel.

We shall consider the maximum value of the mean square velocity over the plate and let $\phi_n^2(x)$ and $\phi_m^2(y)$ have their maximum value of unity.

G^2 is a "transfer" function which depends on angle of incidence. For a "one-dimensional" long, narrow plate, the transfer function is given in Fig. 6. The point to be made is that the prediction of the velocity and hence the strain depends strongly on angle of incidence at high frequencies for the fundamental mode and at all frequencies for higher order modes. For a two-dimensional plate, G^2 has a maximum value of 1 for m and n>1. For m and n equal to 1, the value of G^2 is about 1.6. We shall assume G^2 is unity for a comparison later with aerodynamic excitation. We therefore write

$$\bar{v}^2_{1 \text{ max}} \doteq \frac{\pi S_o(f_{mn})}{2\eta\omega_{mn}(M')^2} \tag{2}$$

The response of panels to the turbulent pressure fluctuations in the boundary layer depends upon a different set of variables. Again allowing the characteristic functions to have their maximum value, the mean square velocity of a plate subjected to a turbulent pressure fluctuation in a boundary layer can be written as, (Ref. 5)

$$\bar{v}^2_2 = \frac{A \, p^2 I_{mn}(0)}{(M')^2 A_p} \tag{3}$$

in which

A   is a correlation area which is a measure of the size of a turbulent eddy,

p^2 is the (overall) mean square pressure fluctuation,

M'   is the surface density,

A_p is the area of the plate,

$I_{mn}(0)$ is a time correlation integral.

This result may be somewhat surprising in that the spectrum of the noise excitation does not appear explicitly. The mathematical model from which the correlation integrals were derived implies that the spectrum is white. Measurements corroborate the model up to at least 5 or 10 KC depending upon the flight regime. This result is important in the design of a recorder since it implies that it is only necessary to measure the overall SPL. This result simply states the cross-correlation of pressures at two different points is important, but the auto-correlation of the pressure at a single point is not important.

The mean square velocity will have a maximum value when the correlation function has a maximum. The maximum value of $I_{mn}(0)$ depends upon the ratio of the velocity at which the turbulent eddies are convected across a panel, u_c, to the bending wave velocity, c_b. When $u_c/c_b = 1$, there is a (high frequency mode) maximum and when $u_c/c_b \gg 1$ there is another (low frequency mode) maximum. We consider the latter condition for the special case of low damping,

$$I_{mn}(0) = \frac{4\theta}{\omega_{mn}\eta(1+\omega^2\theta^2)} \qquad \omega_{mn}\eta\theta \ll 1 \qquad (4)$$

in which θ is the statistical lifetime of the turbulence.

If we further assume that $\omega^2\theta^2 \ll 1$ which will be the relevant case for low frequencies, then

$$\bar{v}^2_{2\ max} = \frac{4A\ p^2\theta}{A_p\eta\omega_{mn}(M')^2} \qquad (5)$$

Obviously the response of a panel depends very strongly on whether acoustic noise or aerodynamic noise is the excitation, as comparison of Eq. (2) and Eq. (5) indicates.

A feasible sonic load recorder can give estimates of a mean square pressure (p^2) and of the pressure spectrum density [$S_0(f_{mn})$], but not the source of these pressures. In order to estimate the vibration response of the panel from the SLHR data it is imperative to decide whether these pressure signals were caused by aerodynamic noise or by acoustic noise.

Computations have been performed for the maximum response at a low frequency mode of a panel excited by a "white" noise with a mean square pressure p^2, a spectrum level $S_0(f_{mn})$ and with a 5 KC bandwidth, first assuming the noise originated from a jet and then assuming the noise came from boundary layer turbulence on a flight at 30,000 ft. at about Mach 1.* The rms velocity for acoustic jet excitation was about 30 times the rms velocity for the boundary layer turbulence. This indicates that if a pressure arose from an aerodynamic boundary

* θ was estimated at 10^{-4} seconds, $A = 10^{-3}$ ft^2, $A_p = 1$ ft^2 for these flight conditions (Ref. 7).

layer source, and we incorrectly assume it arose from an acoustic source, we would predict a root mean square velocity (and a root mean square strain) about 30 times greater than the actual value. The ratio may be as small as 10 or as large as 100. Uncertainties in the values of boundary layer parameters prevent a more accurate estimate. It is clear, however, that the recorder must distinguish between acoustic noises and boundary layer noises if unambiguous data are to be obtained.

2. Fatigue Damage

The vibration response to noise gives rise to vibrations and consequent strains in the panel. The root mean square strain resulting from jet noise may be shown to be proportional to the root mean square velocity of the panel. Thus for strains (ϵ) induced by jet noise at a resonance we may write (from Eq. (2))*

$$\epsilon_{rms} \sim \frac{S_o (f_{mn})^{1/2}}{f_{mn}^{1/2}} \tag{6}$$

The partial fatigue damage accumulation (D) owing to a resonance may be expressed as

$$D \sim \epsilon_{rms}^{\alpha} \cdot f_{mn} \cdot t \quad , \tag{7}$$

where f_{mn} is a resonance frequency and t is the time in seconds. The number of cycles of stress at a level ϵ_{rms} is then $f_{mn}t$. The exponent is experimentally determined from constant stress, fatigue life tests. The value of α is somewhere between 8 and 25. We shall assume it is only 8, to find the widest possible range of levels of interest.

---

* An interesting result by Ungar (Ref. 8) shows $\epsilon_{max} \approx \sqrt{3} \, v_{max}/c_L$ for a wide class of vibrating systems. Strain is then just proportional to a "Mach Number" referred to longitudinal wave velocity.

Substituting the first proportionality into the second yields

$$D \sim [S_o(f_{mn})]^{\alpha/2} \; t \Big/ f_{mn}^{(\alpha/2-1)}$$
$$\sim [S_o(f_{mn})]^4 \; t \Big/ f_{mn}^3$$

(8)

D is thus proportional to the fourth power of the power spectral density and inversely proportional to the cube of frequency. The dependence on the fourth power of the power spectral density means that the range of levels which must be stored in the recorder is quite small. It also means they must be accurately known.

From the point of view of damage accumulation and considering operational data discussed in Section A, it would appear that a range of levels of 5 db would be adequate for the recorder if one could always predict exactly the maximum signal which would be encountered.

Signals a small level below the maximum levels are not very important. Suppose, for example, that a noise signal with a spectrum level of 150 db causes a damage of D_1 units (arbitrary) in one minute. If the noise level is now decreased 10 db, what will be the length of time required for the same degree of damage if frequency is held constant? Since the power spectral density is decreased by a factor of 10, the damage per unit time is decreased by a factor of 10^4. The exposure time at 140 db for a damage equal to D_1 will have, therefore, to be 10,000 times longer, or 16 hours. Thus, for example, if afterburner operations on the ground occur for one minute, then operations at a condition 10 db lower will be considered important only if they last about 16 hours for each minute of afterburner operation.

A similar decrease in damage per unit time is obtained by increasing frequency (while holding the spectrum level constant). For example, if a damage of D_2 units occur in one minute of frequency, f_{mn}, then the damage rate at a frequency 10 f_{mn} will be decreased by a factor of 1000, assuming the spectrum level is the same at 10 f_{mn} as at f_{mn}. For jet and rocket noise we can expect that a peak in the spectrum density will occur somewhere between 100 and 500 cps for existing and future engines. Above this peak the spectrum level will decrease at about 6 db per octave. The fundamental resonance frequencies of most aircraft structures will lie within the same frequency range. Beyond either the peak in the spectrum density or beyond the first mode the damage rate will decrease at an extremely high rate. Considering present and future aircraft design a frequency range of a sonic load history recorder, from 100 to 1000 cps would appear adequate to contain all of the information relative to fatigue life.

Similar arguments can be derived for limiting the level and the spectrum of the strains induced by aerodynamic noise. The partial damage for aerodynamic noise will be

$$D \sim \left(\sqrt{\overline{p^2}} \right)^8 \Big/ f_{mn}^3 \tag{9}$$

The damage is independent of the spectrum (because of the model assumed) but D still depends on the f_{mn}^{-3} so excitation of high frequency modes cannot be important.

C.   DESIGN STUDY

1.   Basic Recorder Systems

To this point we have considered the levels, spectra and duration vs. level distribution of acoustic excitation. We have also considered the response and fatigue damage which may result from these excitations. With this information and by considering the application for data obtainable from various designs, we can outline the requirements to some possible sonic load history recorders.

We have considered in detail only systems which measure an excitation or a response at a single point. No consideration has been given to the possibility of correlating (in real time) signals from two or more points on the aircraft. Useful correlation measurements, particularly in the aerodynamic noise area, can be made only under long-time quasi-steady state conditions. In addition, provisions must be made for variable time delay between the signals and for a variable spacing between transducers. These requirements are beyond the potentialities of a useful, lightweight, unattended compact field instrument.

We have considered the assets and liabilities of four types of recorders. System No. 1 would measure pressure but would store information only about jet and rocket noise. System No. 2 would measure pressure and would store information about jet and aerodynamic noise in separate memories. System No. 3 would measure strain and would store data about the response of the panel to jet and aerodynamic noise and other sources of dynamic strain. System No. 4 would measure both pressure and strain and would store separately information about the excitation and the response. The relative merits of these four systems can be seen from a consideration of the applications of the resulting data.

.

a) Applications of Data Obtained from Basic Recorder Systems

Applications of the data outlined from the SLHR are diagrammatically outlined in Fig. 7. If a pressure transducer is used the load history $\overline{p_1^2}$ is obtained from the recorder. This history is then used to derive a history of the velocity of the panel by theoretical techniques which require additional information about the surface density of the panel, its resonance frequencies, the damping at each resonance frequency, and the angle of incidence of the exciting sound field.

The velocity history so obtained can then be used to find the desired stress history from which a life, N_1, can be estimated. The process of going from a velocity history to a stress history requires further information about the thickness of the material, the stress concentrations, and of course assumptions must be made concerning the linearity (or lack thereof) of the panel. The cumulative errors involved in going from a pressure history to a stress history may be quite large because the pressure history at a point does not provide sufficient information for very accurate calculations of stress at a point. This application of pressure histories is indicated by the solid line in Fig. 7.

Another application for the data would be to predict the fatigue life of Panel No. 2 by predicting the pressure history for Panel No. 2 from the history for No. 1 and from other physical factors which will affect the ratio of p_2/p_1. Panel No. 2 may be another panel on the same aircraft or a panel on another aircraft. With the pressure history of Panel No. 2 in hand, one can repeat the process outlined above to obtain the life N_2 of Panel No. 2. This is the dashed curve in Fig. 7. These are applications of data from recorder System 1.

System No. 2 would record both jet and aerodynamic noise and offers the same applications of the data on System No. 1. More uncertainty is involved than before even if the distinction between aerodynamic noise and jet noise is complete. In order to make any estimate of the response of the panel to the aerodynamic noise, we need to know the aircraft speed and altitude at the time the recorded pressures were generated. Then on the basis of extremely limited data one could attempt a prediction of resulting vibration history, strain history, and fatigue life.

System No. 3 would measure and store the strain response and has some distinct advantages from an applications viewpoint. For this version we concentrate on the response of the panel and neglect entirely the sonic load. Prediction of the fatigue life of Panel No. 1 is then much more accurate than for either of the previous versions. The output of such a system is the strain history itself and the prediction of fatigue life is much more direct and accurate. The several involved steps which tend to cumulate errors in the predicted stress history are avoided completely.

17

Furthermore, the prediction of fatigue life (N_2) for a second panel need be no harder for System No. 3 than for Systems 1 and 2. One can estimate the ratio of the new pressure excitation, $\overline{p_2^2}$, to the pressure estimated for Panel No. 1, $\overline{p_1^2}$. This step is about as accurate as the corresponding step of going from $\overline{p_1^2}$ to $\overline{p_2^2}$.

With a response measurement system one does not know whether the measured strain corresponds to jet noise, aerodynamic noise, or to aerodynamic instability such as the flutter of extended flaps under high speed descents. However, it is important to know the strains themselves, even though their source may not be known. Without knowing the strains from all sources it will not be possible to predict fatigue life accurately.

If a response history is recorded, then distinguishing between the various types of excitation is not so important. In a sense the panel solves the response equations (see Section II.C.1) for us. The response measurements have a great deal of merit. This device might show directly whether or not aerodynamic noise is important to the fatigue problem. This would be done without understanding the structure of the noise field (i.e., space and time correlations, convection velocities and data characteristics). The conclusion that aerodynamic noise is important might be obtained from measurements on a single aircraft. Of course, the negative conclusion that aerodynamic noise is not important would be obtained only after many measurements of many panels on aircraft flying many flight regimes.

System No. 4 would measure both the exciting pressure and the response. A comparison of the measured distribution of pressures with the measured distribution of responses may be a very useful tool. First, such a comparison can aid in determining whether or not a linear relationship exists between the exciting pressure and the response. Second, the presence of significant responses without corresponding excitations might indicate that other sources of dynamic strain are as important as acoustic excitation. Third, a high degree of correlation between dynamic strain and pressure would indicate that other sources of excitation are not important. Clearly, such a system would be more advantageous than either a pressure or response system alone.

b) Discrimination Between Aerodynamic and Jet Noise

In Sections A and B we have shown that (1) in areas on an aircraft where fatigue is an important problem, the jet noise levels will generally be higher than the aerodynamic noise levels, and (2) that the response to aerodynamic noise is, under reasonable appropriate assumptions, much lower than the response to jet noise. It has been pointed out that it is unlikely that very large increases in aerodynamic noise level will take place since the maximum q and, therefore, the maximum

aerodynamic noise levels appear to be limited. We have further noted that the pressure data obtained from a sonic load history recorder will be useful and unambiguous only if there is a way to discriminate between jet noise and aerodynamic noise (Section II.B.1). Unless positive measures are incorporated to distinguish between the two signals, there will always remain some unresolvable ambiguities.

One way to remove the ambiguity would be to use a switching device which is activated by an indicated air speed device. This switching device would de-activate the recorder system (recorder System No. 1) or switch between one storage element which would store jet noise information and another storage element which would store aerodynamic noise information (recorder System No. 2). There is no doubt that more information about the levels of aerodynamic noise are needed, particularly in the supersonic regime. Here information is also needed in relations between the size, convection speed, and lifetime of the turbulent eddies in the boundary layer and the relation of these parameters to the resulting response. The sonic load history recorder, as presently conceived does not appear to be the most appropriate method to obtain additional information. More elaborate instrumentation and more control of the experimental conditions are needed.

    c)   <u>Summary</u>

A recording system or systems which gather both strain and acoustic information is desired (System No. 4). To procced with the feasibility study, a pressure measuring system will be breadboarded to demonstrate the realizability of the instrumentation techniques. This is essentially a System No. 1, but is also half of a System No. 4. The remainder of the System No. 4 will be pursued as the next phase of this work and is not reported herein.

The next section discusses requirements for individual pieces of equipment necessary to realize a pressure measuring recorder for jet noise.

2.   <u>Specific Requirements for the Recorder</u>

    a)   <u>Transducer</u>

Histories of fatigue failures for aircraft structures indicate that excitations below 135 db overall sound pressure level are not of interest to fatigue problems (Ref. 9). The maximum noise levels which may be expected are of the order of 170-180 db overall, even when considering future space vehicles. Thus the total dynamic range for the microphone must be about 45 db. The frequency range of interest is from 75 cps to 1200 cps. The response of the microphone should be essentially independent of frequency (within about ±1 db) in this frequency range.

The range of temperature to which the transducer is exposed will depend on the ambient temperature of the air and on the temperature rise of the air when it is accelerated by the moving aircraft. The maximum temperature rise above ambient is given in Fig. 8. On the aircraft structure the temperature rise will generally be less than that indicated in Fig. 8 owing to incomplete acceleration, conduction of heat away from the skin, reradiation of thermal energy, and other considerations.

b)   Filters and Detectors   .

As observed in Section II.B.2., the frequency range of interest to the acoustical fatigue problem is from about 100 to 1000 cps. For jet noise this frequency range could be encompassed satisfactorily by four octave band filters covering the frequency range from 75-1200 cps.

The dynamic range from the lowest signal to the highest signal should be at least 15 db and, if possible, 20 db referred to the input, (40 db at the output if a squaring device is used). In general, it would be more desirable to have a squaring device. However, for jet noise, studies are available which relate the mean square value to the average value of the rectified signal and the difference is sufficiently small and sufficiently well predictable so that a linear detector could be used.

The time constants of the detector smoothing circuit cannot be too long. On a typical takeoff the rate of change of SPL with time was found to be about 7 seconds per db during acceleration during takeoff roll. Similar, more highly powered aircraft accelerate faster and will have a correspondingly faster decrease with time. During the increase of engine speed from idle to maximum before takeoff, the rate of change of SPL with time will be also greater than 7 seconds/db. A time constant of a few seconds will smooth the signal sufficiently without introducing such a large lag that the duration data is suspect for short maximum levels occurring during pre-takeoff run-up or maintenance run-ups. The only signals that will be lost by a time constant of this order are the transients associated with rocket ignition or the "hard" lighting afterburners.

These excitation transients have a large peak factor. However they are of very short duration and hence the peak factor in the response may be assumed to be small. To the authors' knowledge no field measurements have been made to ascertain the importance of these transients to the fatigue problem. These transients could be measured only if the time constants of the smoothing circuit were much less than one second. It is doubtful that an attempt can be made to assess the importance of the response transients to fatigue through the application of a sonic load recorder.

c) <u>Level Discriminator</u>

The range of levels of interest to the fatigue life of a structure have been shown to be small. Further, the range of significant levels (those between the maximum level expected and most frequently occurring level just below the maximum) for jet noise which may be encountered has been shown to be small. A range of 5 or 6 db from maximum contains all of the level-duration information of importance. A larger range will be required in the level recorder because the maximum level in each band will not be exactly known even if a preliminary field test is carried out to adjust the gain in each filter channel appropriately.

It is recommended that the discriminator have 6 windows each 2 db wide. The maximum resulting uncertainty will then be +1 db owing to the finite window size. This represents a compromise between a wide dynamic range (and many storage elements) and the flexibility necessary to allow for uncertainty in levels in the field. It is expected that adjustments of gain in each filter channel will have to be made in the field to use this narrow range effectively.

d) <u>Information Storage</u>

The damage accumulation rate depends on a high power of spectrum level or overall pressure $\left[S_0(f)^{\alpha/2} \text{ or } \overline{p^2}^{\alpha/2} \right]$, and on the first power of the duration (time) for signals of the same frequency. This implies that signals of relatively infrequent occurrence will be of as much importance as signals which occur at lower levels much more often. Table IV below illustrates this quantitatively.

TABLE IV

DURATION OR NUMBER OF OCCURRENCES FOR EQUAL DAMAGE

$S(f)$ or $\overline{p^2}$ in db re highest level	$S(f)$ or $\overline{p^2}$ relative values	Duration or Number Of Occurrences for Equal Damage	
		$\alpha = 8$	$\alpha = 16$
-6	1	256	63,000
-5	1.26	100	10,000
-4	1.59	45	2,000
-3	2	16	256
-2	2.5	6.4	41
-1	3.2	2.6	68
0	4	1	1

In deriving filter bandwidth requirements an exponent of eight $(\alpha/2 = 4)$ was used as a conservative practice. Here an exponent of 16 must be chosen for a conservative result since the duration of occurrence for equal damage at lower levels increases with α.

The data in Fig. 5 suggest that the maximum signal may be 3 db greater than the most frequently occurring signal. Thus Table IV indicates a dynamic range of 256 is required overall. That is, one storage unit must be capable of storing 256 samples at 3 db below the maximum and another storage unit 3 db away must be able to distinguish the single, equally important sample 3 db higher.

A design goal for the recorder is that it be capable of operation without being attended for a period of three months. The memory should then be capable of storing information for that period of time without being saturated. The estimation of the required storage capacity depends directly upon the utilization of the aircraft. This will be different for different types of aircraft and for different commands (SAC, ADC, ATC, etc.). A crude order of magnitude estimate can be made for the RB-47E data in the Battelle Report referenced in Section II.A.3.

These data indicate that an average of 4.1 flights per month are flown, which implies that there are on the average about 80 hours flown in a three-month period. Allowing a factor of about four for uncertainties, we might have a maximum of 300 hours of flight in a three-month period.

From Fig. 5, we obtain the time per 1000 hours of flight that the signal stays within a set of 2 db windows as follows:

Filter	SPL Level	Hrs/1000 Hrs.	Seconds/300 Hrs.
600-1200 cps	141-142	0	0
	139-140	0.2	216
	137-138	1.7	1840
	135-136	1.25	1350
	133-134	0.7	750

The values in the last column represent the maximum expectation based on the data above with a factor of 4 allowance for uncertainties. We must provide this maximum storage time and permit a wide range of readings from a few seconds at high levels (above 140 db SPL) to a few thousand seconds at the most probable SPL. If temperature variations were not important, it would be possible that all of the accumulated time between 133 db and 142 db might be spent in a single level. The accumulated time in a single level might then be about 4000 seconds.

An analysis of the data in other octave bands would yield the same sort of distribution. Again, note that this result is an order of magnitude estimate of the storage requirements based on operational data from three RB-47E aircraft at a particular SAC base. Ultimately the rate of aircraft utilization will determine how many months the recorder can operate. Ample provision has been made in the storage design to account for large variations in aircraft utilization rate.

SECTION III

DESIGN OF THE SONIC LOAD HISTORY RECORDER

A. BASIC CONCEPTS

In this section consideration is given to (1) the technique of implementing the amplitude distribution, (2) the possibility of time sharing the amplitude analyzer between the four octave bands, and (3) the accumulator requirements.

1. Amplitude Distributor

The function of the Amplitude Distributor is to sort the rms amplitudes from the octave band filters and send them to the correct accumulators of the display. This can be accomplished by using a set of amplitude "windows." A signal with an amplitude between the upper and lower edges of the "window" falls through and is recorded. Signals with amplitudes higher or lower fall into windows above or below. The total spread of all the window levels is 12 decibels (as recommended in Section II) with each window 2 db wide. This range of levels will record only the highest and discard the low ones. This is consistent with life expectation under fatigue tests where life is a very strong function of the amplitude of the excitation.

The Amplitude Distributor may be realized by at least three different techniques: gating circuits, frequency modulation and filters, and amplitude modulation and limiting. The latter technique has been successfully used in the design of a laboratory probability density analyzer (Ref. 12) in which a single gating circuit is used by applying a variable bias to the detected signal level to obtain windows. High frequency AM carriers are required in this technique and bias and gate stabilities with wide environmental fluctuation need be considered.

The first technique (gating circuits) would consist of a set of trigger circuits set at amplitude levels to correspond to the desired windows. Here again the long term dc stability of the trigger circuits over wide environmental fluctuations would be a serious consideration.

In the frequency modulation technique the window edges are converted to the cut-off frequencies of bandpass filters. The windows would consist of a set of bandpass filters. This technique would take advantage of the large effort expended by industry to make FM telemetry components small and reliable for airborne applications. The fact that multiple side bands are produced by FM techniques could be minimized by keeping the modulation index low so the side bands higher than the first few are rapidly attenuated. This technique has the advantage that the amplitude information is converted to frequency

ASD-TDR-62-165
Volume I

information, reducing the requirement for high amplitude stability in the components following the voltage controlled oscillator and avoiding dc amplifiers in the analyzer. In addition, the band pass filters can be selected to match a wide variety of equivalent window sizes.

The spectrum of the FM output of a VCO with a pure tone input is well known (Ref. 13). It is a spectrum with lines spaced by the fundamental frequency of the pure tone, and having amplitudes determined by Bessel functions of the frequency deviation ratio. It follows that spectrum lines are present all through the frequency deviation range. Also, it can be shown that the amplitude of the spectrum is higher at frequency deviations corresponding to the amplitude of the pure tone. When the sum of two different pure tones is applied at the input of the VCO, the spectrum of the output becomes complicated. A simple superposition does not apply.

For the application considered here, a square wave input to the VCO would yield sufficient information for the feasibility study, since the detected signal will approach this. The analytical solution here is amenable to a closed form.

A carrier of frequency ω_c is modulated by the square wave $S(t)$ of Fig. 9 giving

$$e(t) = \cos\ [\omega_c t + b\Delta\omega \int S(t)\ dt] \tag{10}$$

where

$e(t)$	=	output voltage
b	=	percentage modulation
$\pm\Delta\omega$	=	allowed frequency deviation
ω_c	=	carrier frequency in radians per second.

We assume that the carrier frequency is a high harmonic of the fundamental frequency of the square wave ω_0. This slight restriction is a convenience to simplify the algebra. It follows that $e(t)$ is periodic of fundamental frequency ω_0; Eq. (10) can therefore be expanded into a Fourier series:

$$e(t) = \sum_{n=-\infty}^{+\infty} a_n\ \epsilon^{in\omega_0 t} \tag{11}$$

25

$$a_n = \frac{1}{2T} \int_{-\frac{T}{2}}^{+\frac{T}{2}} e(t) \, \epsilon^{in\omega_o t} \, dt$$

$$= \frac{1}{2T} \int_{-\frac{T}{2}}^{+\frac{T}{2}} \left(\epsilon^{+iF_1(t)} + \epsilon^{-iF_2(t)} \right) dt \qquad (12)$$

where

$$F_1(t) = (\omega_c - n\omega_o)t + b\Delta\omega \int S(t) \, dt \qquad (13)$$

$$F_2(t) = (\omega_c + n\omega_o)t + b\Delta\omega \int S(t) \, dt \qquad (14)$$

From Figure 9 we have,

$$\int S(t) \, dt = -\frac{T}{4} + t \quad ; \quad 0 < t < \frac{T}{2}$$

$$= -\frac{T}{4} - t \quad ; \quad -\frac{T}{2} < t < 0 \qquad (15)$$

The evaluation of Eq. (12) using Eqs. (13), (14), and (15) yields a line spectrum with spacing equal to the fundamental frequency of the square wave. The amplitude of the spectrum is highest near the frequencies $\omega_c - b\Delta\omega$ and $\omega_c + b\Delta\omega$ as shown in Fig. 10.

The lines decrease in amplitude away from the frequencies $(\omega_c - b\Delta\omega)$ or $(\omega_c + b\Delta\omega)$. It follows that the filter bandwidth required to capture unambiguously this spectrum has to be 5 to 10 times the fundamental frequency of the square wave input.

The average selectivity Q of the narrow band filters (windows) following the VCO can be set assuming equal bandwidth for all filters as:

$$Q = \frac{k\,\omega_c}{2\Delta\omega} \tag{16}$$

which is equal to the number of windows (k) divided by the total frequency deviation ratio $\frac{2\Delta\omega}{\omega_c}$. For example, consider a frequency deviation $\frac{2\Delta\omega}{2\pi}$ of 6,600 cps (which corresponds to the standard RDB Telemetry Channel "A") with a center frequency ω_c of 22,000 cps. Consider six amplitude windows. Here

$$Q_{ave.} = \frac{6 \times 22,000}{6,600} = 20.$$

The average selectivity is the Q if all the filters had equal bandwidths. However, those required in the amplitude analyzer are spaced logarithmically in 2 db increments. This can be given by

$$\frac{2\Delta\omega}{2\pi} = a + 1.26a + (1.26)^2 a + (1.26)^3 a + (1.26)^4 a + (1.26)^5 a = 11.54a$$

where "a" is the bandwidth in cps of the narrowest filter. For this example, a = 572 cps. This corresponds to a maximum selectivity for this example of about 22,000/572 = 38. This selectivity is realizable at these frequencies with relatively small components.

The maximum frequency of square wave input for the above example is

$$f_{o_{max}} = \frac{572\ cps}{10} = 57.2\ cps.$$

Since the minimum duration of a pressure pulse expected to the sonic recorder is 3 seconds, the above input bandwidth is more than adequate. Therefore no difficulty is expected from spectrum spreading of the frequency modulation.

Although the derivation given above satisfies the bandwidth and Q requirements from a quasi-steady state point of view, it is necessary to check the rise time capability of the narrowest bandpass filter.

The envelope of the response of a single narrow band filter has a time constant equal to 2/(Bandwidth) where the bandwidth is in radians per second. For the case considered above, this time constant is much less than a millisecond. This reponse time is negligible for the purposes of the sonic recorder.

ASD-TDR-62-165
Volume I

2. **Time Sharing**

It would be desirable to time share the amplitude distributor
between the four different octave band outputs. Otherwise, four separate
amplitude distributors would be required.

Those SPL levels which occur least frequently will introduce the
most inaccuracy if time sharing is used. The maximum rms values are
more infrequent than the intermediate levels. The minimum time dura-
tion of a certain rms level can be set as either (1) the minimum
expected time that the signal takes to pass through a window, or (2) the
minimum time that the signal is likely to stay at a certain maximum.
For the first case we have that (1) an RB-47 plane during runway acceler-
ation sees its SPL from jet noise decrease by about 1 db per 7 seconds.
A fighter plane will have about three to four times this acceleration.
For a window size of 2 db the RB-47 plane gives an equivalent duration
of SPL within a window of approximately 14 seconds. For a fighter plane,
this time duration is reduced to about three to four seconds. For the
second case, we will assume that, for maxima of SPL, the minimum duration
of these maxima is also three to four seconds. The number of flights
expected in a three-month period varies considerably with the aircraft.
For reasonably active crafts about 12 flights per three-month period are
expected. It is assumed that for less active aircrafts the use of the
sonic recorder is not considered or justified. Therefore, a minimum
requirement of having to sample 12 maxima of SPL each of duration of at
least 3 seconds is set.

The possibility of obtaining a measure of accumulated time which
falls within prescribed uncertainty limits is derived from a binomial
distribution. Different cases are considered, depending on the relative
values of the period T of the sampling function and the duration τ of
the maxima to be sampled. See Fig. 11 for nomenclature. We consider
the following cases where τ is kept constant.

$$
\begin{array}{lll}
\text{I} & : & \tau < T \\
\text{II} & : & T < \tau < 2T \\
\text{III} & : & kT < \tau < (k+1)T
\end{array}
$$

Each case introduces uncertainties of its own. From this analysis
an acceptable T is determined, since the minimum value of τ is fixed.
Also imposed is the requirement that $\delta \ll \tau$. (δ = sample duration).

Case I. $\tau < T$

Since there is equal probability that the sampling pulse δ will
fall anywhere within τ, the net time measured, on the average is $\delta\tau/T$.
The probability (P) of catching the maximum SPL of duration τ when
sampling once during the period T is:

$$ P = \frac{\tau}{T} $$

For a number n of such independent trials (when n corresponds to the number of flights), the mean (μ) of the number of samples is:

$$\mu = nP.$$

The standard deviation (σ) about this mean is:

$$\sigma = \sqrt{nP\,(1-P)}$$

The ratio of the standard deviation to the mean is:

$$\frac{\sigma}{\mu} = \sqrt{\frac{(1-P)}{nP}} = \sqrt{\frac{1-\tau/T}{n\ \tau/T}}$$

This is a measure of the scatter around the mean value, and thereby gives a measure of the possible error spread caused by sampling. Therefore σ/μ should be minimized. A value of σ/μ of not more than 5% would be acceptable.

Case II. $T<\tau<2T$

The probability of getting at least one sample is unity. The probability P' of getting another sample after having obtained one is:

$$P' = \frac{\tau-T}{T}$$

Therefore the mean value μ of the number of successes is:

$$\mu = n\,(1+P')$$

The standard deviation is contributed only by the probability of the second success:

$$\sigma = \sqrt{nP'\,(1-P')}$$

Finally, the ratio σ/μ becomes

$$\frac{\sigma}{\mu} = \sqrt{\frac{P'\ (1-P')}{n}} \times \frac{1}{1+P'}$$

$$= \sqrt{\frac{\left|\frac{\tau}{T} - 1\right|\left|2 - \frac{\tau}{T}\right|}{n}} \times \frac{T}{\tau}$$

Case III. $kT < \tau < (k+1)T$

We can repeat the same process and obtain

$$P' = \frac{\tau - kT}{T}$$

$$\mu = n\ (k+P')$$

$$\sigma = \sqrt{nP'\ (1-P')}$$

$$\frac{\sigma}{\mu} = \sqrt{\frac{P'\ (1-P')}{n}} \times \frac{1}{k+P'}$$

$$= \frac{T}{\tau} \sqrt{\frac{\left|\frac{\tau}{T} - k\right|\left|1 + k - \frac{\tau}{T}\right|}{n}}$$

These ratios σ/μ show that the uncertainty in sampling is reduced inversely with the square root of the number of samples. In addition, it decreases almost directly with the ratio τ/T. The value of σ/μ has been calculated for different ratios of τ/T using $n = 12$. The results are shown in Fig. 11b. Clearly when $\tau/T = 1, 2, 3 \ldots$ the error σ/μ is zero; however this result assumes that τ is accurately known, which is certainly not the case. It follows that the envelope of the curve of Fig. 11b, shown as a dashed line, should be used as the expected error σ/μ. Using the criterion that σ/μ should be less than 5% we obtain from the envelope curves of Fig. 11b that τ/T should be 3 or more. Since τ is set as at least 3 seconds we obtain that the sampling period T should not be more than one second.

The duration δ of the sampling pulse should be a fraction of the sampling period such that T/δ is equal to or greater than the number of channels sampled. For 4 channels, δ becomes equal to (or less than) 0.25 second.

This error contribution of sampling was computed using the estimated minimum number of maximum occurrences of 12, each of 3 seconds duration. For larger values of n and τ the sampling uncertainty will be less than 5%. It is therefore possible and desirable to time share the input to the amplitude analyzer at the rate of one sample per second from each of the four octave band channels.

3. Accumulation and Display

Many devices and techniques have been examined for accumulation and display of data. These were grouped into two categories: (1) those that stored events with reference to the time that it occurred, and (2) those that accumulated the total number of events that occurred over a period of time. In general, those techniques of (1) consists of traveling media on which events were recorded such as punched tape, magnetic tape, or a photographic process. Devices included in (2) are electrochemical elapsed time indicators, electromechanical counters or elapsed time indicators, and electronic counters. The items of (1) were less advantageous than those of (2) because they did not yield a display without further manipulation and were generally more difficult to use in severe environments. The devices of (2) are discussed further below.

The electrochemical indicators presently available have an operational temperature range less than that required for the sonic load recorder. In addition, their dynamic range is only about 30 to 1. These are not suited for this application.

The most reliable and simple group of accumulators for severe environments is the electromechanical devices. The electromechanical counter can be actuated by discrete pulses which move an electromagnetic actuator (solenoid), or by a motor which is turned on and off as in an Elapsed Time Indicator. This has the advantage over electronic counters of giving a direct reading of the accumulated count and of reliably retaining the count when power is off.

The Elapsed Time Indicator has a severe limitation because of the start and stop time of the motor. For example, if power is applied to the motor for a duration d and the angular rotation of the motor is measured from the instant the pulse is applied to the time the motor is stopped, we get:

$$\text{relative error} = \frac{a_1}{T} e^{-\frac{T}{a_1}}$$

where a_1 is the ratio of the moment of inertia of the motor to its viscous damping with a linear torque speed characteristic assumed. This error is positive, meaning that the total motor rotation will be larger than if a motor with $a_1 = 0$ were used. This error becomes less than 2 percent when the ratio a_1/T is greater than 3. If a_1/T becomes unity, the error is 37%. In practice, one should not measure periods T of duration less than 3 a_1.

The requirements for accumulation and display are simply handled by an electromechanical counter. A counting rate of one count per second and a total count of a few thousand per channel is required. This allows a margin of five over that estimated for the RB-47E data on page 23. That data also included a margin of four, allowing a total factor of twenty.

B.   SYSTEM DESCRIPTION

A recorder system for accumulating jet noise data using the distributor technique and the sampling presented in Section III.A. is discussed here. Figure 12 illustrates the functional blocks of this system.* These blocks are

a.   Data Acquisition
b.   Time Sharing
c.   Amplitude Distributor
d.   Output Matrix

In the Data Acquisition block, the microphone signal is amplified, filtered into four octave bands, and detected. The signal is switched off by the Aerodynamic Noise Discriminator (simply an altitude-speed switch) when certain altitudes and speeds are exceeded.

The need for aerodynamic noise discrimination was discussed in Section II. In addition it is necessary to de-activate the microphone signal at higher altitudes to eliminate the effects of temporary microphone sensitivity changes due to a decrease of ambient pressure. This

---

*   Detailed circuit diagrams of each of the individual blocks of Fig. 12 are given in Appendix A.

discrimination is accomplished with two switches in series: a dynamic pressure switch operating at Mach 0.3 and an altitude switch operating at 7000 feet. Both switches must be closed for the microphone signal to be analyzed by the sonic recorder. Thus only data below 7000 feet and below a speed of Mach 0.3 are analyzed.

The microphone preamplifier has the required high input impedance and low noise floor for the type of microphone selected and the expected sound pressure levels. Calibrated attenuators and fine level adjustments are provided. The detector yields the same d.c. output for sine waves or octave bands of noise with the same true rms values. This is important since calibration will be performed with sine waves.

The Time Sharing System samples sequentially the outputs of the four detectors, feeds these samples into the Amplitude Distributor, and finally directs the outputs of the Distributor to the Output Matrix. All the gates are controlled by a 4 cps clock which is suitably divided and decoded to produce gating control signals of a quarter of a second duration in the proper sequence to sample and record each channel once per second. Channel indicating lamps are provided for use during calibration and check out.

The Amplitude Distributor consists of a voltage-controlled oscillator (VCO), a set of six filters (corresponding to amplitude windows), followed by six peak detectors which trigger a corresponding set of six Schmidt triggers.

The VCO receives the time-shared signals from the four rms detectors and converts the level of these signals into proportional frequency deviations. A bias voltage of 1.66 volts is subtracted from the detector outputs to permit maximum use of the input voltage range (0-5 volts) of the VCO. The input voltage range of the VCO can then be made to correspond to six windows each 2 db wide giving a total range of 12 db. The value of this bias voltage is established as follows.

Consider an input voltage V_1 applied to an active network with gain G and bias voltage y. It is desired that an increase of V_1 by 12 db (a factor of 4) change the output of the network from zero to five volts. Two equations result:

$$(V_1) \ (B) + m = 0 \text{ volts}$$

$$(4V_1) \ (B) + m = 5 \text{ volts} \tag{17}$$

Here V_1 corresponds to the rms voltage from the microphone, B to the gain of the data acquisition equipment (including the detector), and m the bias voltage. Solution of the two equations yields the following results:

$$m = -5/3 \text{ volts}$$

$$B V_1 = 5/3 \text{ volts} \tag{18}$$

Hence the unique value required for the bias is -1.66 volts and the useful range of the detector output is from 1.66 volts to 6.66 volts.

If it is desired to have sound pressure levels from 145 db to 170 db re .0002 μbar correspond to the highest window level, B must be adjustable over a range of 35 db. However, a greater range will in fact be required to accommodate microphones of different sensitivities.

An input of zero volts to the VCO corresponds to 18,700 cps at the output and an input of five volts corresponds to a 25,300 cps output. Linear variations of input voltage within this range result in a linear shift of output frequency. The bandpass filters have bandwidths equivalent to 2 db windows, as discussed earlier. The peak detectors follow the envelope of the signal from the associated bandpass filters. Since the frequency is very close to being single valued (see Section III.A.1), only one detector is excited at any given time. The Schmidt triggers sense whether a detector output above a certain level is present. Upon firing, the trigger output voltage changes of the order of 10 volts in a few microseconds. This is the command that a count should be recorded in the counter of that particular amplitude window.

The Output Matrix consists of a four by six matrix of electromechanical impulse counters. Separate power transistors drive each row and each column of the matrix, requiring a total of ten power transistors. The six rows correspond to the six amplitude windows of the Amplitude Distributor and are controlled by the outputs of the Schmidt triggers. The four columns correspond to the four octave bands and are cycled by the Time Sharing control circuitry.

In addition to the blocks shown in Fig. 12, a Total Elapsed Time Indicator is necessary. The Elapsed Time Indicator is operated whenever the aircraft engines are operating and is used as the normalizing factor. For example, 347 counts in a given window correspond to the number of seconds a signal is present in the window (one sample is taken each second). If the total elapsed time were 463 hours, then the data would indicate that the octave band SPL had occurred 748 seconds per 1000 hours of aircraft operation.

SECTION IV

BREADBOARD SYSTEM

A represe.itation of the systems described in Section III has
been designed and constructed as a breadboard to insure feasibility
and correct functional operation. The breadboard consists of three
chassis and two readout packages as shown in Figure 13.

The three chassis include the Amplitude Distributor, Time-Sharing
Equipment, and Data Acquisition. The Output Matrix is contained in
the readout packages, (except for the row and column drivers which are
mounted on the Time Sharing Chassis). One readout package contains
room for the twenty-four electromagnetic counters, although only six
were mounted in the breadboard. The other readout package contains
substitution lamps that are used during calibration and set-up.
Modular circuits have been employed where practical for the breadboard
system. The circuits have been mounted on 4" by 6" epoxy boards of
the type shown in Figure 14.

Silicon transistors and diodes are used with conservative dissi-
pation derating to permit operation at ambient temperatures up to at
least +75°C. The electromechanical impulse counters have been care-
fully selected to insure good operation under adverse environments.

In the following paragraphs the circuitry for each of the basic
functions is discussed and measured data given.

A. DATA ACQUISITION

Many of the requirements for this equipment such as input
impedance, noise, and gain are set by the type of transducer used
and its sensitivity. The transducer type considered is a flush
mounted ceramic microphone. Flush mounting is desirable when measur-
ing sonic noise on a surface exposed to a high air velocity. A
ceramic type of microphone is simple, rugged, and more reliable than
either condenser or diaphragm types. The sensitivity of some avail-
able ceramic microphones is adequate for the range of SPL to be
measured and the maximum temperature can exceed 500°F. These micro-
phones are completely sealed and therefore unaffected by humidity.
A specific type of ceramic microphone is discussed in Appendix B.

The Data Acquisition System has been designed for greater
stability than that expected for currently available microphones
under adverse environmental conditions. Thus improved types of
ceramic microphones can still be used effectively with this record-
ing system.

It should be emphasized that a specific location of the microphone for a given application will undoubtedly dictate certain microphone characteristics. These specific requirements cannot be considered here, but provision can be made in the Data Acquisition equipment to operate with different microphone sensitivities and capacities. If a different microphone is desired, its selection should be based on the following considerations: acoustic sensitivity, electrical capacity, frequency response, vibration sensitivity, temperature sensitivity, and ambient pressure sensitivity.

The Data Acquisition System is designed to operate with microphones having a capacity of 1500 picofarads or greater and acoustic sensitivities between -110 and -90 db re 1 volt per microbar. The microphone installation will probably require vibration isolation to absolutely insure that the vibration response is insignificant. This is discussed in Section 2 below.

1. Circuit Characteristics

A cathode follower was initially used in the input circuit to the Data Acquisition System to obtain a high input impedance with low electrical noise for capacitive sources. The vacuum tube used (the only one in the recorder) was the recently developed nuvistor, which is very small and constructed with metal and ceramic for high temperature operation. An input impedance of 9 megohms is achieved. This input impedance together with a 1500 picofarad microphone capacity limits the low frequency response to 3 db down at 15 cps.

After the design of the cathode follower circuit was completed, a new solid state device became available. This is the silicon field-effect transistor which can be operated at high impedance with low noise. An input circuit utilizing this device has been designed and is included in Appendix B. An input impedance of ten megohms and a lower frequency of about ten cps at 3 db down with 1500 pfd is available from the field effect transistor circuit.

The maximum electrical noise floor tolerable is established by the minimum input signal of interest. Minimum data levels are about 135 db SPL in an octave band. However, it is desirable to calibrate the microphone acoustically at levels of the order of 120 db SPL. For a microphone having a sensitivity of -110 db re 1 volt/μbar, a calibration tone of the 120 db SPL corresponds to -64 db re 1 volt rms. A noise floor of the order of -75 db re 1 volt rms with capacitive input is acceptable. The equivalent input noise of the

Data Acquisition System is less than -80 db re 1 volt rms broadband with a capacitive source of 1000 pfd.* In octave bands the equivalent input noise is less than -90 db re 1 volt rms.

The frequency response for this system up to the octave band filters is shown in Fig. 15. The low frequency end of the data has been adjusted to show the expected attenuation caused by the micro-phone capacity (1500 pfd) with the 9 megohm input impedance.

The linearity of the output from the detectors with respect to a sinusoidal input to the cathode follower is presented in Fig. 16. The transfer function is used between about 1.5 and 7 volts output and is within +1% of the best straight line in this range. The bias which is required to set the 12 db range limits the required range of the detector's output to values above 1.5 volts. Thus the diode non-linearity below 1.5 volts is not significant.

The data shown as crosses (X) in Fig. 16 was taken with a sine wave at 850 cps. The data shown as dots (o) in Fig. 16 was taken with a sum of three sine waves (650 cps, 850 cps, and 1150 cps). The three sine waves had equal amplitudes, resulting in a peak-to-rms ratio of $\sqrt{2}$ x $\sqrt{3}$, which is 8 db. (This sum of sine waves simulates an octave band of random noise; however, the measurements are much easier to make and more accurate because the random fluctuations are limited and the sine wave generators are much more stable than random noise sources. If an octave band of true random noise is used to obtain data similar to those of the dots of Fig. 16, the inherent fluctuations of both the rms value of the noise and its detected value limit the ability to establish these limits to better than +5%; much more elaborate techniques involving a very long integration time would be needed.)

The data of Fig. 16 indicate that the detector as measured needs some slight adjustment (the series resistor, 1.45K ohms of Fig. A-8 should be increased, perhaps to 1.6K ohms) in order to make the detector give equal readings for sine wave and random noise. An adjustment technique for this is given in Appendix B. If the two lines of Fig. 16 are made to coincide, the deviation from the best straight line for either a sine wave or a random signal is less than +2% of the cardinal points within the required detector range.

---

* The field effect transistor circuit noise is less than -100 db re 1 volt rms broadband with 1500 pfd.

The detector discharge time constant is approximately 2.5 seconds. The charge time constant is approximately one second. This is consistent with the maximum rate of change of signal anticipated in Section II. The detector output will drop 8 db in 2.5 seconds (about 0.3 db/sec), considerably quicker than the 7 seconds per db discussed in Section II.

Equation (18) of Section III.B. yielded a criteria for the gain (B) of the Data Acquisition System in the form $B = 5/(3 V_1)$ where V_1 is the input voltage from the microphone. For sound pressure levels of 145 db to 170 db re .0002 μbar full scale, a microphone with a sensitivity of -110 db re 1 μbar would yield voltages of -39 db re 1 volt to -4 db re 1 volt respectively for V_1. Therefore B must be variable between 43 db and 8 db for this particular microphone sensitivity. The forward gain of the system is approximately 60 db without use of any attenuators. Attenuation of up to 60 db can be set to provide the needed variation for B.

2. Influence of Adverse Conditions

a) Power Supply Fluctuations

Tests have been performed with variations of the positive and negative power supplies. No difference in gain was noted from the cathode follower input to the detector input for supply voltage fluctuations from -24 to -30 and +24 to +30 volts, either jointly or individually. A shift of the bias supply was noted on the input of the VCO. For positive supply changes from +26 to +30 volts, the equivalent detector output increased .08 volts. For negative supply variations from -26 to -30 volts, the equivalent detector output decreased by .04 volts. For joint variations of both supply voltages from 26 to 30 volts, the detector output increased .02 volts.

The maximum bias shift above corresponds to .02 volts per volt change of supply voltages. This change has a positive coefficient in that the bias increases for increasing supply voltages. For .05% regulated supplies (readily available for airborne applications), a fluctuation of +15 millivolts is allowed in the supply voltages. Thus a bias change of +0.3 millivolts is expected at the detector output. This is entirely negligible.

b) Ambient Temperature Changes

Brief checks on temperature sensitivities have been performed. From this and from specified data for components, estimation of the variations with temperature can be made.

The preamplifier system is not expected to vary more than ± 0.2 db in gain over the temperature range from $-50^\circ C$ to $+70^\circ C$. This corresponds to an increase of about .003 db per C° rise. Both the nuvistor of the cathode follower and the high gain amplifier are capable of operation at $150^\circ C$.

Temperature compensation has been employed for the biased output of the detectors. Measurements for a temperature change between $27^\circ C$ to $65^\circ C$ indicated no change within the 0.5% (.01 volt) readability of the monitoring equipment. It can be assumed that the coefficient of the bias change is better than 0.25 millivolts/C°. An increase of bias is expected for increasing temperature.

Thus the thermal sensitivity of this equipment can be approximated by two coefficients; $+.0003$ db/C° gain variation; $+0.25$ millivolts/C° bias variation; for deviations from a nominal $25^\circ C$.

c)   <u>Vibration Effects</u>

Vibration sensitivity has been examined for two critical component the microphone and the nuvistor in the cathode follower.

(1)   Cathode Follower

Vibration sensitivity of the nuvistor type* of vacuum tube has bee previously reported (Ref. 14), of the order of -80 db re 1 volt per g at frequencies below 4000 cps. Between 4000 and 10,000 cps, sensitivities of up to -50 db re 1 volt per g occur, primarily about 8000 cps. Since signals beyond 1200 cps are filtered out by the octave bands the vibration sensitivity beyond 1200 cps is only important in that it may overload the following high gain amplifier. Below 1200 cps the equivalent SPL for 10 g acceleration at the cathode follower is 124 db SPL when a microphone having a sensitivity of -110 dbv/μbar is used. From both considerations, above and below 1200 cps, it follows that some vibration isolation of the cathode follower is desirable.

---

*   In Appendix B a substitute circuit employing a field effect transistor is given which will negate vibration effects in the input circuit.

The cathode follower output could utilize a simple RC low pass filter to attenuate the vibration response since it is important at a frequency higher than the response required. This however would not contribute very much since this frequency is only an octave above the required response. A maximum of 6-9 db of attenuation might be realized in this manner.

A better solution is to provide a simple vibration mount for the nuvistor. Large attenuation of vibrations at these high frequencies is not difficult and no undesired limitations occur at frequencies in the pass band. The performance required from this isolation is not critical and can be easily realized.

(2) Microphone

Vibration can deteriorate the data accumulated by direct excitation of the ceramic microphone. It is deemed desirable to provide vibration isolation for the microphone. Brief tests have been performed to evaluate a design of a typical vibration mount. The microphone employed for these tests was a Gulton P420M-6, which has a lower vibration sensitivity than most ceramic microphones since it employs some internal cancellation for vibration compensation.

A vibration mount for the microphone was molded from Silastic ®
silicone rubber. This material has a brittle point of $-100°$F and can withstand up to $400°$F for prolonged periods. This mount and its two part mold are shown in Fig. 17. The thin rubber collar provides compliance in both the vertical and horizontal directions. The microphone fits into the mount with its sensitive surface flush with the collar surface.

Measurements of the mount with the microphone installed indicate a vertical resonance at 15 cps and a horizontal resonance at 25 cps. The behavior is more complex than the combination of two single-degree-of-freedom systems since the compliance is a distributed element. The vibration transmission of the mount is indicated in Fig. 18. A minimum of 15 db of isolation is provided above 75 cps. The increased response at lower frequencies is not significant as illustrated in Fig. 19 where the vibration response of the microphone is considered for 10 g rms excitation. For comparison the response of the Data Acquisition System to a 135 db SPL is given.

B. AMPLITUDE DISTRIBUTOR

1. Circuit Characteristics

The input to the Distributor is the time shared detected voltages from the octave band filters; the input is also modified by a bias supply. The input device of the Distributor is a commercial voltage-controlled-oscillator (VCO) in the Standard IRIG Telemetry Band "A"

($\pm$15% frequency deviation, center frequency 22,000 cps). The input voltage range is from 0 to 5 volts. As previously discussed, the 1.66 volt bias is used to make the 0-5 volt range correspond to a 12 db range of the detector output.

The linearity of the conversion of input voltage to frequency deviation from the VCO has been measured and is given in Fig. 20. The deviation from the best straight line is better than $\pm$1% of value for the measured points.

The bandpass filters represent the equivalent amplitude windows to the frequency modulated signal. The bands corresponding to 12 db range from 18,700 cps to 25,300 cps are:

	Bandwidth	Ideal Band Edges (cps)		Equivalent VCO Input Voltage		
0 - 2 db	2.60%	18,700	19,270	0.0	to	0.43
2 - 4 db	3.27%	19,270	19,990	0.43		0.97
4 - 6 db	4.12%	19,990	20,900	0.97		1.65
6 - 8 db	5.20%	20,900	22,040	1.65		2.51
8 - 10 db	5.56%	22,040	23,480	2.51		3.58
10 - 12 db	8.26%	23,480	25,300	3.58		5.00

A frequency deviation of 1320 cps from the VCO corresponds to one volt variation at its input.

The bandpass filters are adjusted so their response is down approximately 6 db at each band edge. The measured transfer function from the Distributor input to the detected output of the bandpass filter is given in Fig. 21. The outputs of the six bandpass filters are superimposed.

The filters approximately overlap at their 6 db down points. The level at which the trigger fires correspond to about the 4 db down points, so that there is a definite effective gap between each adjacent window. This gap is needed to avoid the possibility of recording simultaneously on two adjacent windows. The gap width

varies with the setting of the trigger voltage level as can be seen from Fig. 21. The gap reduces the 2 db bandwidth of each window to a nominal value of 1.85 db: this is the value to be used in analyzing the results accumulated by the sonic recorder.

The triggers sense if a signal is present within the preceding bandpass filter. They are adjusted to fire at voltages from the detector corresponding to the sloping edges of the bandpass filters.

Since the trigger is fired on the slope of the bandpass filters, the sensitivity of the system to a drift of trigger level is decreased. For example, if triggers were used directly to set the amplitude windows (in place of the bandpass filters), a 0.1 volt drift of the trigger voltage would yield directly a 0.1 volt drift of the amplitude window. When used on the slope of the bandpass filters, the 0.1 volt variation is reduced by a factor of 8 to .0125 volts. The original 0.1 volt variation would be considerable for the first amplitude window whose width is only 0.43 volts.

This reduction in trigger level sensitivity is also advantageous when the hysteresis of the trigger is considered. That is, the trigger fires at a given rising voltage level, but it turns off at a slightly lower level. Typical hysteresis values for good transistor triggers are a few tenths of a volt. If the triggers were used directly to set the amplitude windows, the window edges would be different for rising voltages and falling voltages. For example, if a trigger were set at 0.0 and 0.43 volts for rising voltages, the corresponding window for falling voltages with 0.2 volts hysteresis would be -0.2 and 0.23 volts. Use of the bandpass filter slope would reduce this variation to .025 volts, or the window resulting for a falling voltage would be -0.025 and 0.405. This variation could be reduced further by utilizing bandpass filters with even steeper slopes.

A typical trigger level is shown as a dotted horizontal line in Fig. 21 at +16 db re 1 volt detector output. Everything above the dotted line corresponds to the "on" state, everything below to the "off" state.

The set of six bandpass filters constructed had the 6 db band edges set to within +50 cps. More accurate filter edges could be set, but this was not done during the breadboard tests. Measurements of the amplitude windows resulting from trigger voltages set at 6 +0.5 volts were taken. The window edges and bandwidths are tabulated on the following page.

ASD-TDR-62-165
Volume I

LOWER EDGE CPS	UPPER EDGE CPS	BANDWIDTH CPS	RESULTING WINDOW	IDEAL BW FOR 2 db CPS
18,678	19,244	566	1.99 db	570
19,286	19,942	656	1.83 db	720
20,025	20,857	832	1.83 db	910
20,900	22,015	1115	1.95 db	1140
22,086	23,382	1296	1.80 db	1440
23,527	25,253	1725	1.89 db	182c

The deviation of the resulting window from a nominal value of 1.85 db is directly attributable to the setting of the edges of the bandpass filters. A criteria can be stated for the accuracy of the bandpass filter settings which would be the most severe for the narrowest filter. If we insist upon a window width of 1.85 db +.02 db, the filter edges should be adjusted to within 1.0% of bandwidth. In the narrowest filter this corresponds to a setting of the edges to within 6 cps which can be accomplished using an electronic counter. The other filters would allow correspondingly wider deviations. The accuracy of the effective window widths shown in the preceding Table is adequate in the intended use of the sonic recorder.

2. Influence of Adverse Conditions

    a) Power Supply Fluctuations

The effects of power supply fluctuations were tested in two parts In the first part, we consider as a group the solid state gates, the bias supply and the voltage-to-frequency converter. In the second part, we consider the trigger voltage.

(1) The solid state gates, the bias supply, and the VCO were operated as a unit: the input signal to any one gate was set at a constant dc value, and the VCO output frequency was measured while power supply voltages were changed. This test encompasses the complete transfer of signal from the rms detector output to the output of the VCO.

A positive supply change from +26 to +30 yielded a decrease in equivalent input voltage to the VCO of 0.39 volts. A negative supply change from -26 to -30 yielded a decrease of equivalent input voltage by .003 volts. Changing both supplies together for 26 to 30 volts yielded a decrease of equivalent VCO input signal of 0.39 volts. This corresponds to a maximum decrease of 100 millivolts per volt increase of supply voltage. With +15 millivolt variation in supply voltages (.05% regulation), this results in a fluctuation of +1.5 millivolts equivalent input to the VCO.

(2) Once the information is converted to frequency, power supply variations have no effect except at the trigger voltage. The triggers operate only from the negative supply. The trigger voltage has been measured to vary from 6.3 volts with a -30 volt supply to 5.6 volts with a -26 volt supply. This corresponds to a -0.7 volt change with a -4 volt supply voltage change, or about +0.2 volts/volt.

The effect of this change on the effective window edges must be modified by the slope of the bandpass filters. Thus this is reduced to an equivalent +0.025 volts/volt. For the assumed regulation of .05% of the power supply, this corresponds to a fluctuation of +0.4 millivolts. This is a fixed indeterminancy in the window edges and must be considered as a bias variation.

(3) Collectively, these two coefficients for the Distributor (gates throug̱ᵗ ᵛᵗʸᴄᴏ and triggers) have the following maximum bias variations:

- 1ᴸ _ :ᵛvolts per volt change of B+,
+ 25 ...ᴸᴸᴸivolts per volt change of B-,

or a net resultant bias variation of the input to the VCO of

$\pm$ 1.5 millivolts with B+

$\mp$ 0.40 millivolts with B-

assuming a $\pm$.05% regulation of the B+ and B- supplies.

This net bias variation is indeed an extremely small fraction of the input voltages applied to the VCO in normal operation; this variation is entirely negligible.

b) Temperature

For the solid-state gates, bias supply, and VCO combination, a change from 30°C to 70°C yielded an output frequency change, corresponding to a bias change of about +0.4 millivolts per C°.

Tests with a bandpass filter and trigger combination indicated the following:

Temperature	Lower Edge	Upper Edge	Window Width
$29^{\circ}C$	0.453 volts	0.935 volts	0.482 volts
$85^{\circ}C$	0.422 volts	0.915 volts	0.493 volts

For the $56^{\circ}C$ change, the lower edge decreased 31 millivolts, the upper edge decreased 20 millivolts, and the window width increased by 11 millivolts. During this test, the trigger voltage decreased by about 0.05 volts for the 56°C change. This would tend to lower the lower edge by 50/8 = 6 millivolts and raise the upper edge by 6 millivolts. This would account for part of the shift. The remainder would be a 25 millivolt decrease for the lower edge, a 26 millivolt decrease for the upper edge, and a negligible increase in the window width. Thus the bandpass filters tend to shift slightly, but the bandwidth is maintained nearly constant.

The width of this window is 0.482 volts at $29^{\circ}C$, which corresponds approximately to 2 db. The lower edge has decreased 31 millivolts or 6.5% of the 2 db, and the upper edge has decreased 20 millivolts or 4.2% of the 2 db, for a $56^{\circ}C$ increase of temperature. These shifts are less than -.0003 db/C° for the lower edge and -.002 db/C° for the upper edge. The change in window width would be the difference between these numbers or +.0001 db/C°.

Combination of the temperature effects for the complete Distributor yield the following:

> bias shift of +0.4 millivolts/C°
> lower window edge shift of -.003 db/C°
> upper window edge shift of -.002 db/C°
> window width shift of +.001 db/C°

for temperature shifts about $25^{\circ}C$ nominal.

These results can be converted into extreme changes corresponding to the two extremes of temperature:

> $-50^{\circ}C$ to $25^{\circ}C$
> $25^{\circ}C$ to $70^{\circ}C$

For the lower extreme of temperature we have a bias shift of 30 millivolts and net window width change of -0.075 db. The bias shift corresponds to - $\frac{30}{490}$ or -6% of the 2 db windows or -.012 db. At the higher extreme of temperature the changes are smaller than for the lower extremes. It follows that these total changes, which are less than 0.1 db of any 2 db window, are rather small and almost negligible.

C. TIME SHARING AND OUTPUT MATRIX

These two blocks of circuits deal with digital logic transfer rather than sensitivity variations. As logic circuits they either operate reliably or they do not. If they fail, they introduce gross errors which are readily recognized in the following tests.

One of the logic circuits, (the gates between the rms detectors and the VCO,) has a small scale effect directly on the signal, caused by power supplies and temperature variations. These effects were included in discussion and tests of the Amplitude Distributor (see Section IV.B).

1. Circuit Characteristics

The circuit diagrams are shown on Fig. A-13 to A-15. The clock is the timing source for the time sharing. It operates at a rate of 4 pulses per second. These pulses are applied to two multivibrators which provide outputs at 2 pulses per second and 1 pulse per second. Various combinations of these outputs are applied to the "AND" gates of the four decoders so that each of the four decoders are energized in sequence for a 250 millisecond interval. The resulting operation is illustrated in Fig. 22. The decoder outputs then provide unique signals to control the time sharing between the octave bands.

As indicated by Fig. 12, the decoder outputs control the solid-state gates. The performance of the gates is critical and they must perform as much like ideal switches as possible, and be as uniform as possible since four are used in sequence. Errors introduced by the offset voltage and difference in saturation resistance of the gates are at most 8 millivolts between the four gates at full scale output. This reduces to 2 millivolts at the minimum signal. Thus a conservative estimate of the gain error is .2% or .02 db for these gates.

The Output Matrix consists of twenty four counters mounted at the intersection of 6 rows and 4 columns, with 10 driving circuits, one for each row and one for each column. The rows correspond to the amplitude window and are controlled by the Schmidt triggers. The columns correspond to octave bands and are controlled by the time sharing system.

The driving circuits are really more correctly called transistor switches. They switch from non-conduction to conduction when a control signal is received. In the conducting state the transistor is saturated, appearing as a very low resistance (10 ohms) between the counter and the supply voltage. Any given counter has two switches in series with it, one between it and +28 volts and the other between it and ground. Thus both switches must conduct before the counter can be activated.

The impulse counters used are Mil-Spec hermetically sealed units. They have an electrical resistance of 1000 ohms and will actuate anywhere from 18 to 28 volts, (corresponding to currents of 18 to 28 milliamps).

The counter will record a count in 20 milliseconds, which is too rapid for the application. This has been purposely slowed to about 150 milliseconds by shunting each counter with a tantalum capacitor. The capacitor also serves to reduce the voltage transients. The 150 milliseconds response time insures that only one count can be recorded by any given counter in a 250 millisecond interval.

2. Influence of Adverse Conditions

a) Power Supply Fluctuations

The output frequency of the clock decreases .0015 cps for each volt increase in its positive supply voltage (no negative voltage used). For .05% regulation (±15 millivolts) this corresponds to an insignificant frequency change.

The Time Sharing equipment in total has been examined for reliable operation with power supply fluctuations. Reliable operation of the complete unit including a clock, frequency dividers, and decoders for positive supply variations from +26 to +30 volts and from -26 to -30 volts has been obtained. If the supply voltages vary together, reliable operation is available from 25 volts to better than 30 volts. Since power supply regulation of .05% is employed, no difficulty is anticipated in any of the circuitry.

b)   Ambient Temperature Change

The clock frequency decreased .0004 cps for each C^o increase of temperature over the range from 30^oC to 70^oC. For a 100^oC change this would correspond to a frequency shift of only .04 cps. The multivibrator and decoder circuits have operated reliably over the same temperature range.

The impulse counters have been specified by their manufacturer to operate over a temperature range of -50^oC to $+70^oC$.

D.   PROPAGATION OF ERRORS

The SPL measurements accumulated during operation of the sonic recorder will show errors which are unavoidably present in the system. These errors have indeed been minimized by proper selection of a microphone and by careful design and selection of components in the sonic recorder. Nevertheless the errors present in the system are not negligible. However, the errors in the accumulated information should be much less than the actual limits of errors since statistical averaging of errors will occur. The following estimates of errors are cited as 2σ values; that is, 95% of the time the error due to the assigned cause is expected to be within the limits given. The limits given are then estimated to be twice the standard deviation. Independent errors can be combined by taking the square root of the sum of the squares (Ref. 15) of the individual errors.

The errors may be classified into three categories: systematic errors, short term errors, and long term errors.

1.   Systematic Errors

The systematic errors are those inherent in the recorder when all external factors are disregarded. These errors include those associated with calibration, with components within the recorder such as filters, detectors, etc., and errors associated with the time sharing of the Amplitude Distributor.

a)   Calibration

The calibration of the sonic recorder involves an acoustic calibration of the microphone in situ and a voltage calibration of the sonic recorder proper. The acoustic calibration of the microphone involves the accuracy of the acoustic calibrator used and the care with which the calibrator is applied to the microphone. At best the acoustic calibration error would be ± 0.2 db.

The voltage calibration of the recorder proper involves a number of steps (discussed in Appendix B). If these steps are followed carefully, our estimate of the minimum resultant error is ± 0.3 db. This estimate assumes that precision meters (1%), attenuators (1%), and counters are used in calibrating the system.

The acoustic and voltage calibration errors are independent. Combining these independent errors we obtain a 2σ error of ± 0.35 db.

b)   Component Errors

These errors are contributed by the inaccuracies of some functional blocks such as the effective width of the octave band filters, the nonlinearity of the rms detector and the VCO, the effective window widths of the narrow band filters following the VCO.

In the design presented in the preceding sections some of these errors are analyzed. We summarize here these errors.

Data Acquisition: The nonlinearity from input to the output of the rms detectors for random noise was shown to be less than ± 0.2 db of the measured points. The bandwidth of the octave band filters influences the output for random signals in proportion to the square root of the filter bandwidth. This bandwidth can be expected to be within $\pm 2\%$, contributing an uncertainty for random signals of ± 0.1 db. The tops of these filters can be expected to be flat to within ± 0.2 db.

Amplitude Distribution: The nonlinearity from the solid-state gates to the VCO output has been shown to be less than ± 0.1 db. The bandpass filters have been shown to vary in bandwidth less than ± 0.1 db from a nominal width.

The total combination of these independent systematic errors results in a 2σ error of ± 0.39 db.

c)   Sampling Errors

The error introduced by sampling the rms detectors was analyzed in Section III.B. The analysis showed that for 12 maxima of SPL occurring for a duration of 3 seconds, the sampling errors would be less than $\pm 5\%$. In practice each window will sample not only some maxima but also the signals passing through the window. It is almost certain that the sampling error will be appreciably less than $\pm 5\%$ for a reasonably active aircraft. Only after knowledge of the actual number of samples in a given window is known, can we give a better estimate of the sampling error introduced. For the purpose of this discussion the sampling error is taken as ± 0.4 db.

2.   Short Term Errors

        The short term errors are those caused by external factors such
as temperature, power line variations, and vibration. They are likely
to occur within a period of a few hours or days.

        a)   Temperature Effects

        The expected change of ambient temperature (-50°C to $+70^{\circ}$C) will
affect the microphone as well as the recorder operation.

        The temperature sensitivity of a typical ceramic microphone (lead
zirconate titanum) is $+0.18\%/C^{\circ}$ of its acoustic sensitivity. The change
of capacity could be neglected provided the RC time constant of the
preamplifier input resistance and microphone capacity has been chosen
large enough to permit lower frequency response than needed. In the
temperature range of -50°C to 70°C (a change of 120°C) the microphone
sensitivity changes by ± 1.1 db.

        Collecting the temperature sensitivities of the recorder from pre-
vious discussions, we find that the Data Acquisition contributes
$+.00003$ db/C° of gain variation and $+0.25$ millivolts/C° of bias shift.
The Amplitude Distributor contributes $-.0003$ db/C° of window edge
shifts, $+.001$ db/C° of window width shift, and $+0.4$ millivolts/C° of
bias shift.

        The bias shift is most significant to the lowest amplitude window,
which is the least important to fatigue. The total $+0.65$ mv/C° bias
shift alone corresponds to $+40$ mv variations for -50°C to $+70^{\circ}$C temper-
ature variations. In the lowest amplitude window this corresponds to
$+10\%$ of the voltage width of 0.43 volts corresponding to 2 db, or an
equivalent $+0.2$ db. However, in the highest amplitude window with a
voltage width of 1.42 volts corresponding to 2 db, this is equivalent
to only $\pm .06$ db.

        The total gain variation and window edge variations correspond to
about $-.002$ db/C°, or ± 0.12 db for -50°C to $+70^{\circ}$C.

        Thus the total effects for temperature changes from -50°C to $+70^{\circ}$C
can be summarized by:

microphone:	± 1.1 db
recorder (lowest amplitude window):	± 0.32 db
recorder (highest amplitude window):	± 0.18 db

Note that the recorder temperature errors are directly summed since
it can be expected that these will not be independent.

b) Power Supply Variations

The effect of power supply variations are located exclusively in the recorder proper and have been analyzed in previous sections. Power supply regulation of 0.05% is assumed. The Data Acquisition Equipment contributes a bias change of +0.03 millivolts. The Amplitude Distributor contributes +1.9 millivolts of bias fluctuation. These are negligible quantities.

c) Vibration Effects

When proper precautions are taken to vibration isolate the microphone (using for example the vibration mount discussed earlier) and to vibration mount the cathode follower of the preamplifier, any vibration up to 10 g's of the microphone or of the sonic recorder should have no measurable effect on the recorded signals. We assume here that an adequate packaging of the sonic recorder is realized in production.

3. Long Term Errors

The long term errors are those which do not have a cyclic nature but are more characterized by a long term drift. We can divide these into two groups: those errors which can be compensated by a recalibration and those which cannot.

In the first group belongs the long term sensitivity drift of the ceramic microphone (which should be less than 0.1 db in a ceramic material which has been properly cycled in temperature), gain drifts of the amplifier because of permanent changes in feedback resistors, bias drifts, drift of the center frequency of the VCO, and bias drift of the trigger circuits. All these changes can be compensated for by a periodic calibration. It is anticipated that these changes will be very small and that calibration should not be needed more often than perhaps every 2 or 3 months.

In the second group belongs the drift of the bandwidths of octave band and narrow band filters, and the rms detector series resistor. These items are very stable and no adjustments are anticipated.

4. Accumulated Errors

The preceding discussions have enumerated many sources of errors and have estimated these in terms of the greatest error expected under operational conditions. These errors have been estimated as 2σ values. These can be combined to yield an estimated overall error for the package. The recorder itself excluding the microphone yields:

ASD-TDR-62-165
Volume I

$$2\sigma_{\text{low window}} = \sqrt{(.035)^2 + (.039)^2 + (.032)^2}$$

$$= \pm 0.61 \text{ db}$$

$$2\sigma_{\text{hi window}} = \sqrt{(.035)^2 + (.039)^2 + (.018)^2}$$

$$= \pm 0.55 \text{ db.}$$

Including the microphone as contributing an independent error raises the value to ±1.25 db. This assumption of independence for the microphone is reasonable since it and the recorder package will be physically located in different environments.

To summarize, the error contribution from the recorder is expected to be less than ±0.6 db with a 95% confidence level. The inclusion of the microphone error raises the overall error to ±1.25 db.

E. SYSTEM EVALUATION

The system from the solid-state gates to the impulse counters has been examined with a very low-frequency triangular wave input applied in parallel to the four solid-state gates. The amplitude of the triangular wave was large enough to extend above the highest window edge and below the lowest window edge. Since the triangular wave spends equal time at all amplitudes within its excursions, the counts accumulated should ideally be directly proportional to the width of each amplitude window. The sampling was employed during these tests.

A triangular wave with a period of 49.492 seconds and amplitude varying between 0.6 volts and 7.1 volts was used. The counters were read at t + 70 minutes, t + 150 minutes, t + 455 minutes, and t + 650 minutes. After each reading the counters were checked to see that all were counting appropriately. No malfunctions occurred.

The resultant data is presented in Table V. Three major columns are given: the counts received in the counter during the tests, the counts expected from measurements of the amplitude windows, and the percent difference between the two. The triangular wave input slope (6.5 volts in about 25 seconds) is about 0.26 volts per second. This corresponds to approximately a 1.5 second signal duration in the narrowest band and a 5 second signal duration in the widest band.

52

TABLE V

ACCUMULATED COUNTS RECEIVED FOR TRIANGULAR WAVE INPUT

Time in Mins.	Counts Received				Counts Expected				% of Difference			
Amplitude Windows	t+70	t+150	t+455	t+650	t+70	t+150	t+455	t+650	t+70	t+150	t+455	t+650
0-2 db	305	667	2264	3070	284	636	2185	2970	+7.4	+4.9	+3.6	+3.4
2-4 db	338	753	2597	3522	329	738	2530	3435	+2.7	+2.1	+2.7	+2.5
4-6 db	426	948	3268	4444	417	931	3210	4345	+2.2	+1.8	+1.8	+2.3
6-8 db	545	1220	4243	5768	559	1250	4300	5830	-2.5	-2.4	-1.6	-1.1
8-10 db	656	1446	4966	6744	652	1455	5010	6790	+0.6	+0.6	-0.9	-0.7
10-12 db	847	1889	6543	8894	862	1925	6620	8990	-1.5	-1.9	-1.3	-1.1

53

Experimental errors of several types are included in this test. First, the synchronism between the periodic triangular wave and the sampling time will cause a slow cycling of the number of pulses recorded as the input waveform slowly shifts with respect to the sampling time. For the period of 49.492 seconds of the triangular wave, a cycle will repeat when the 0.492 seconds matches an integer value of seconds. This would happen in about 500 periods of the triangular wave, or about 450 minutes. This will impose an oscillating error upon the data, the period of oscillation being approximately 7-1/2 hours. A true stationary test should last many times 7-1/2 hours. It follows that the test results are probably biased by the initial conditions. This would not be a problem if a random signal were being analyzed.

The error in determining the actual window width used to compute the expected counts contributes a constant error to the data. This error is about +10 cps in the bandwidth of the filters. The percentage error decreases as the bandwidth increases. This is characteristic of the remaining errors at t + 650 minutes. This error could be greatly reduced by a more accurate determination of the filter widths during manufacture.

In addition the errors contributed by sampling at one second intervals must also be considered. This is an error which decreases with the square root of the number of counts accumulated. After very many counts this error is insignificant. The most serious contribution of this error will be tne narrowest (0-2 db) window at t + 70 minutes. It is calculated that the ratio of the standard deviation to mean value ($\frac{\sigma}{\mu}$) will be approximately 2.5%. For a large family of these tests one would be 68% confident that the error would be within 1σ, or 2.5% above the mean error. The value indicated in the table for the error is 4% above the mean error (3.4%), or a little less than 2σ. This is reasonable for a single sample of a population.

The resulting errors for large numbers of counts approach mean errors which are most likely contributed by measurement error. It is expected that the system as tested which includes sampling errors will be accurate to better than +3%. Table VI clearly suggests this conclusion.

SECTION V

CONCLUSIONS

In the development of the requirements for the recorder system, consideration has been given to the noise levels contributed by jet engines and aerodynamic sources and to the response of aircraft panels to these noise fields. Criteria were set forth which retained the information essential to sonic fatigue. The different responses of panels to aerodynamic noise and to jet noise necessitate the separation of data accumulated from these two noise sources. The jet noise source is generally much more significant in fatigue considerations.

The technique in current use to accumulate information about sonic loads is an indirect one which considers the rpm of the specific jet engines. That technique does not provide data on aerodynamic noise excitation. Use of the sonic recorder herein described would enable more direct and accurate information about the jet noise excitation. Another type of recorder accumulating data on the response of a panel during flight would include both the effects of jet and aerodynamic noise. This response recorder will be pursued as the next phase of this work and will be reported in Volume II of this technical report.

The instrument design reported here accumulates data on the jet sonic excitation experienced at a single point. The performance of the recorder itself yielded smaller errors under the environment than those found in available microphones for this application. It follows that the design should be adequate for use with better microphones when they become available. The small error limits realized in the design of the breadboard were obtained primarily by selecting wherever possible techniques which are inherently insensitive to environment changes and by limiting active components to silicon solid-state devices. The instrument was designed using a unique approach to the amplitude window determination. The amplitude was converted to frequency deviations and the windows to bandpass filters.

The estimated weight and volume of the sonic recorder can be obtained from the weight and volume of our breadboard model. The weight of the instrument exclusive of the packaging and power supplies is less than 15 pounds. The volume of the instrument exclusive of the packaging and power supplies is less than 0.5 cubic feet. It is estimated that the power supplies will weigh 15 pounds and require a volume of 0.1 cubic feet. The power dissipated in the instrument itself is less than 20 watts. If the efficiency of the power supplies is 50%, the net power dissipated in the total package will be less than 40 watts. It would be desirable to isolate thermally the electronics from the power supplies.

The objectives of this effort have been stated in Section I.
The study of Section II provided the criteria needed. The design and
tests of Sections III and IV together with the circuit diagrams of
Appendixes A and B supply the design information needed. The results
of the tests on the breadboard model have shown that the design concepts
and their implementation satisfy the requirements for the sonic
recorder.

LIST OF REFERENCES

1. Mahaffey, P. T., and Smith, K. W., "Method for Predicting Environmental Vibration Levels in Jet-Powered Vehicles," NOISE Control, Vol. 6, No. 4 (1960).

2. Dyer, I., Franken, P. A., and Ungar, E. E., "Noise Environments of Flight Vehicles," NOISE Control, Vol. 6 No. 1 (1960).

3. Franken, P. A, and Kerwin, E. M., Jr., Methods of Flight Vehicle Noise Reduction, WADC TR 58-343, November, 1958.

4. Clark, W. E., Reaction to Aircraft Noise, BBN Report No. 572, USAF Contract No. AF 33(616)-5629.

5. Dyer, I., "Response of Plates to a Decaying and Convecting Random Pressure Field," JASA, Vol. 31, No. 7, July, 1959.

6. Dyer, I., et al. Sonic Fatigue Resistance of Structural Design, BBN Report No. 873, ASD TR-61-262, March, 1961.

7. Private communication from I. Dyer.

8. Ungar, E. E., "Maximum Stresses in Beams and Plates Vibrating at Resonance," ASME Paper No. 61-SA-14 presented at June, 1961 ASME Meeting.

9. Bingman, R. N., "Resonant Fatigue Failures Associated with Noise," Paper presented at SAE Meeting, April, 1960.

10. Willmarth, W. W., "Space-Time Correlations and Spectra of Wall Pressure in a Turbulent Boundary Layer," NASA Memorandum 3-17-59W.

11. Corcos, G. M., Cuthbert, J. W., and Von Winkle, W. A., On the Measurement of Turbulent Pressure Fluctuations With a Transducer of Finite Size, University of California, Institute of Engineering Research, Berkeley, California, Series 82, Issue 12, November, 1959.

12.   Fox, H. L., <u>Probability Density Analyzer, Summary Report</u>, BBN Report No. 895, January, 1962.

13.   Arguimbau, L. B., <u>Vacuum Tubes and Transistors</u>, John Wiley and Sons, 1956.

14.   Noiseux, D. U., Doelling, N., Smith, P.W., Coles, J. J., <u>The Response of Electronics to Intense Sound Fields</u>, BBN Report No. 761, WADD TR 60-754, November, 1960.

15.   Beers, Y., <u>Theory of Error</u>, Addison-Wesley, (1953).
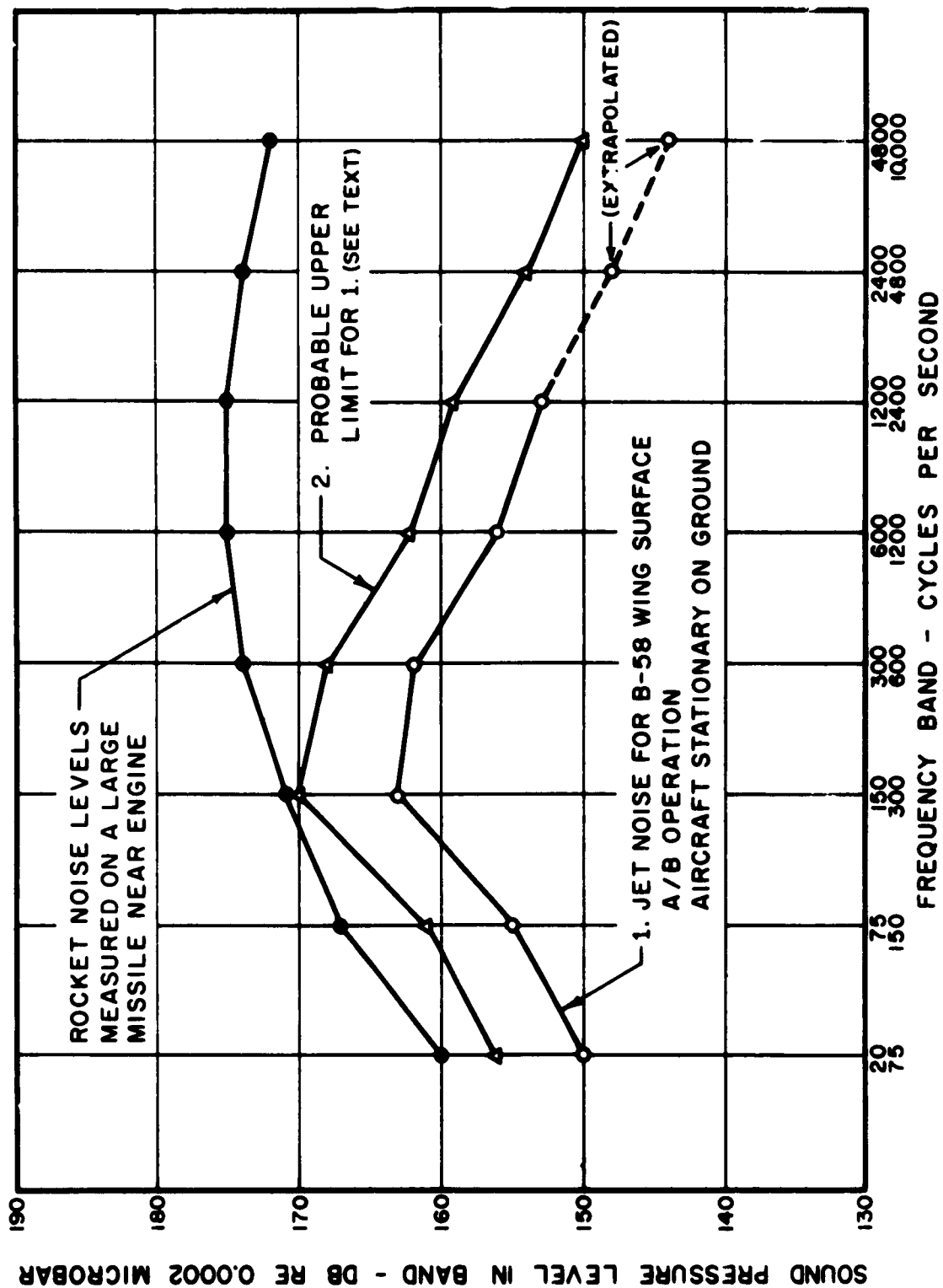
FIG. 1   SOME ESTIMATES OF MAXIMUM NOISE LEVELS FOR
CONTEMPORARY SPACEVEHICLES

59
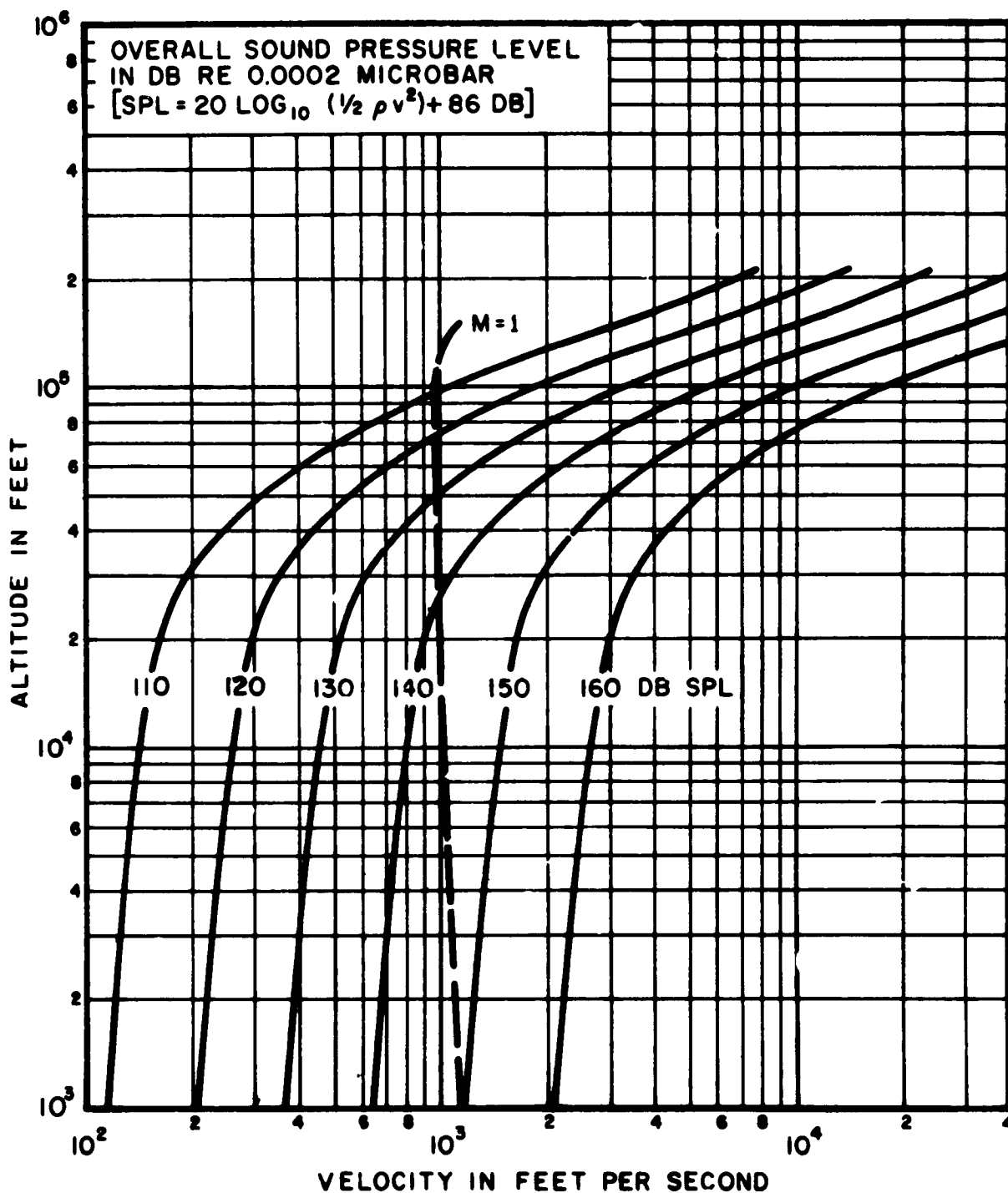
FIG. 2   AERODYNAMIC NOISE LEVELS AS A FUNCTION OF
ALTITUDE AND AIRCRAFT VELOCITY (ICAO STANDARD
ATMOSPHERE)
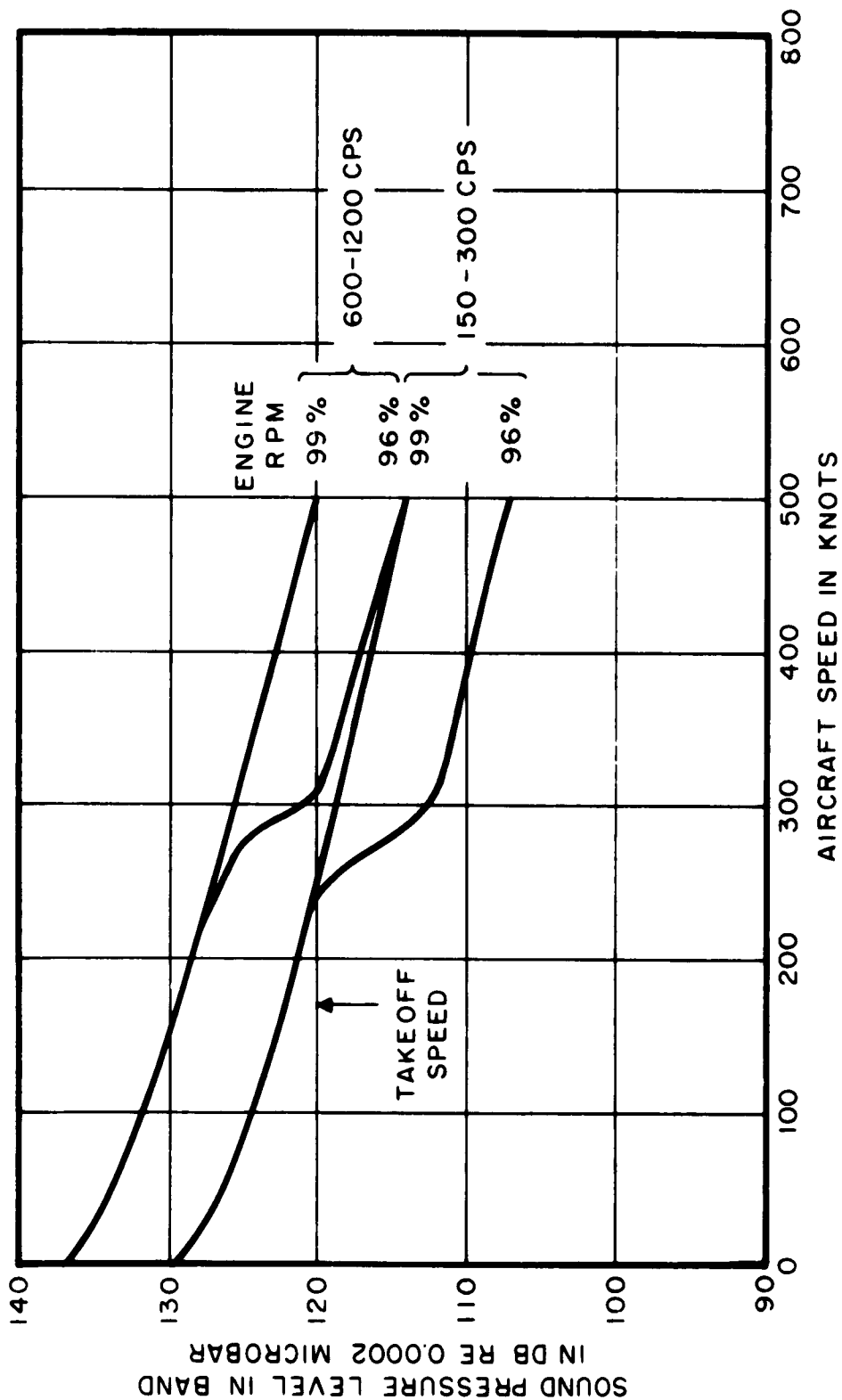
FIG. 3 NOISE LEVELS ON RB-47 WING POSITION AS A FUNCTION OF AIRSPEED – LOW ALTITUDES ONLY
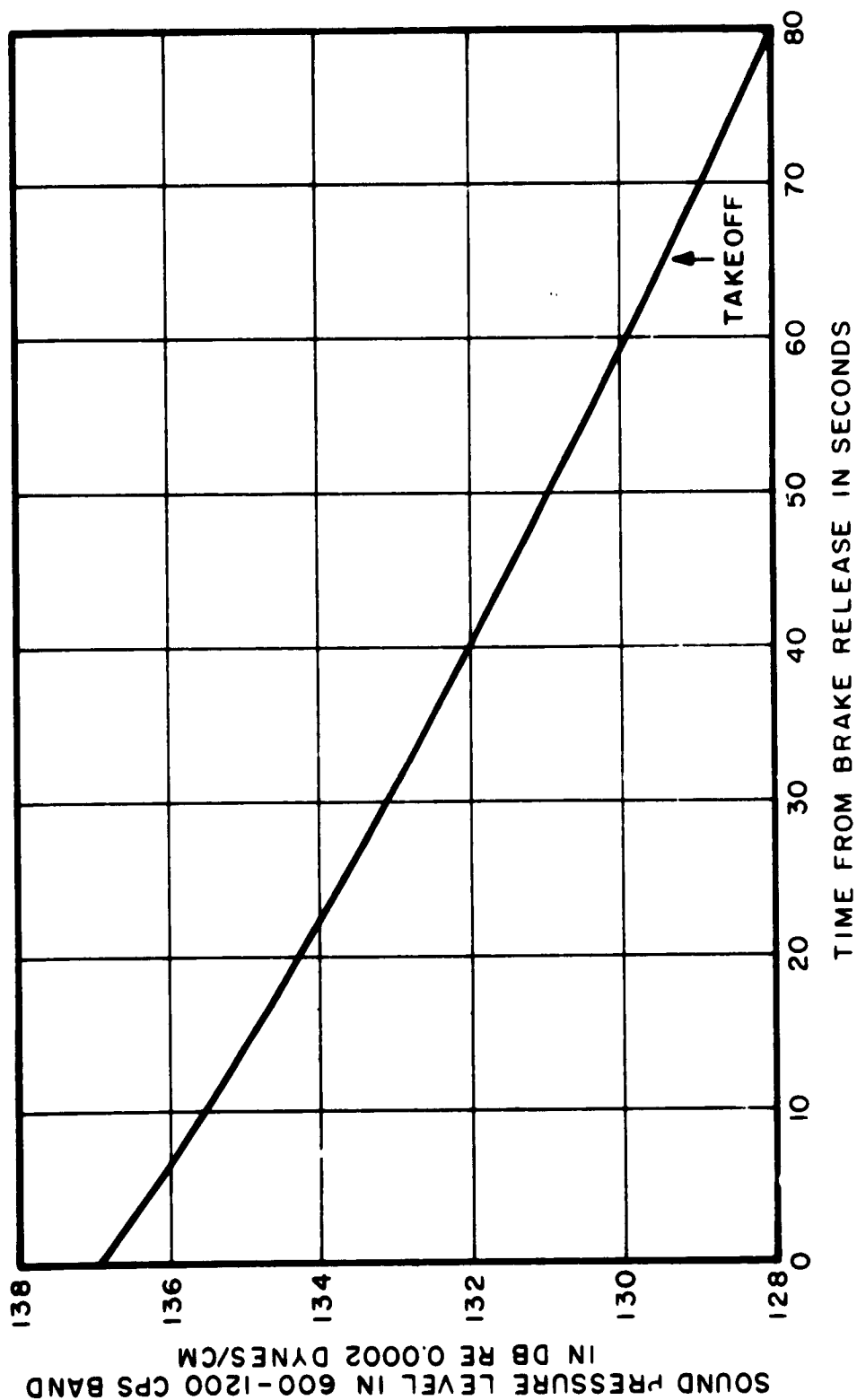
FIG. 4 NOISE LEVELS AS A FUNCTION OF TIME FROM BRAKE RELEASE
FOR AN RB-47 TAKE-OFF-ACCELERATION = 4 FT/SEC^2
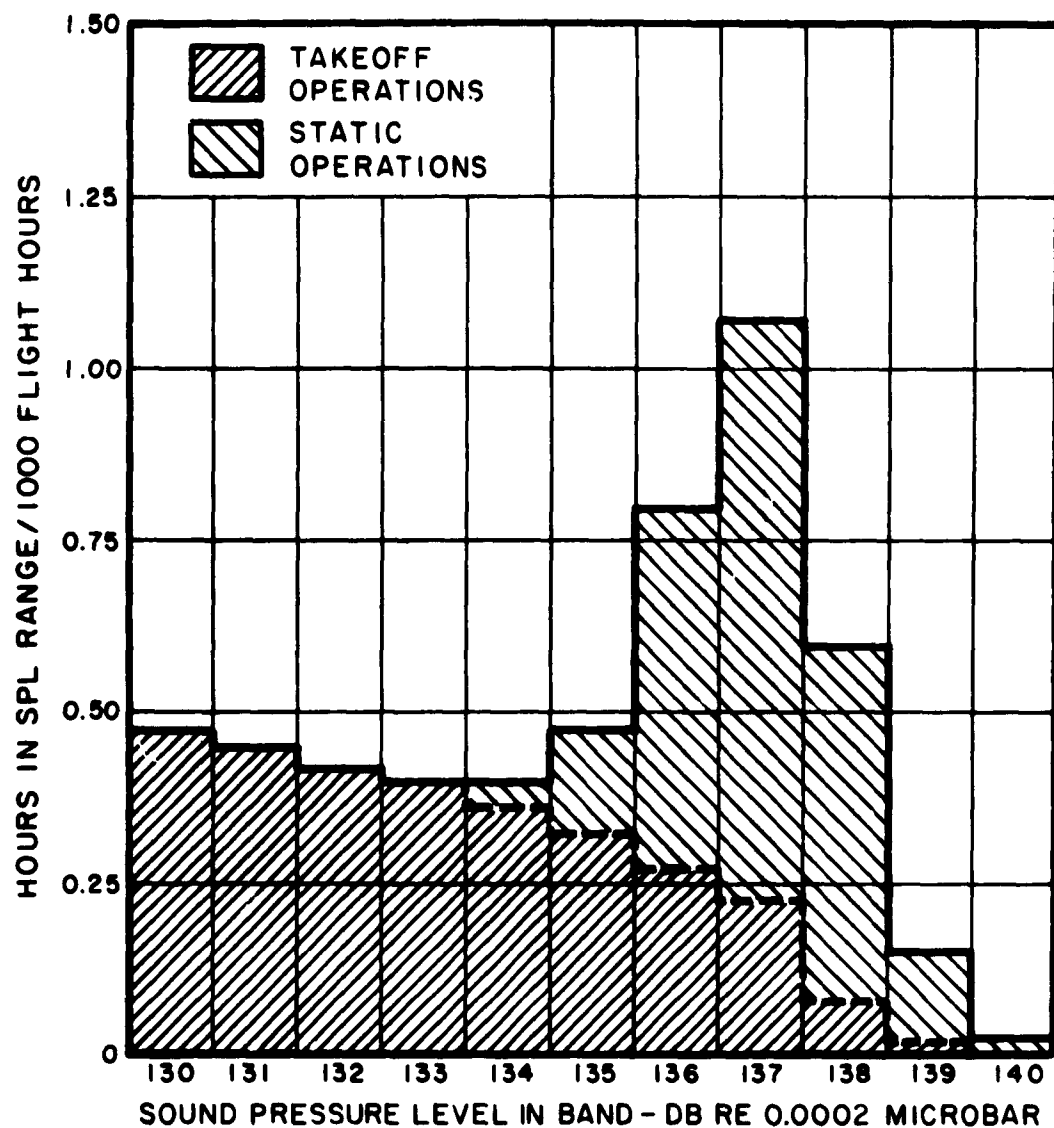
FIG. 5   SOUND PRESSURE LEVEL DISTRIBUTIONS
FOR RB-47 GROUND OPERATIONS
600-1200 CPS BAND
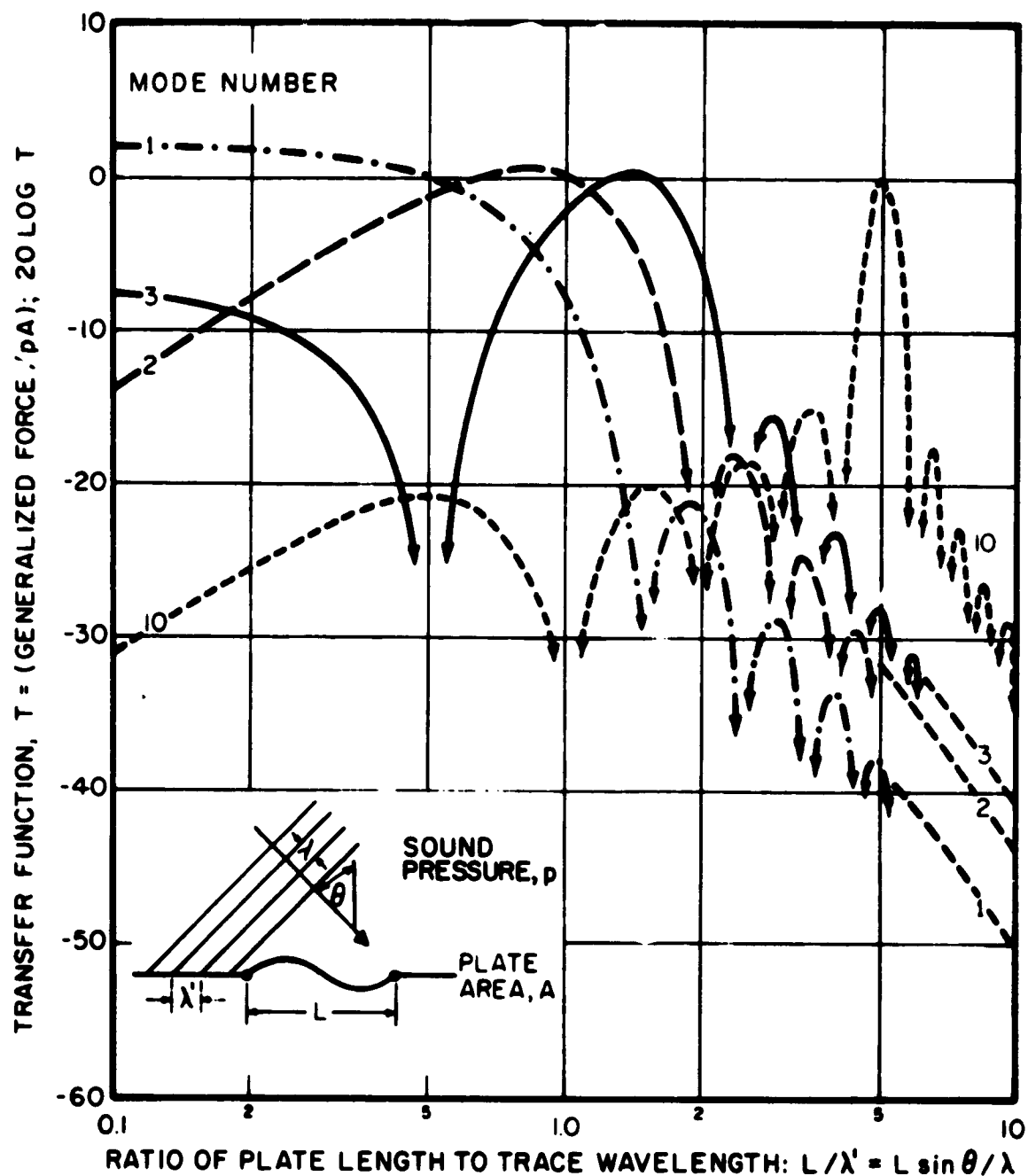
FIG. 6   TRANSFER FUNCTION FOR A SIMPLY SUPPORTED
PLATE, EXCITED BY A PRESSURE FIELD
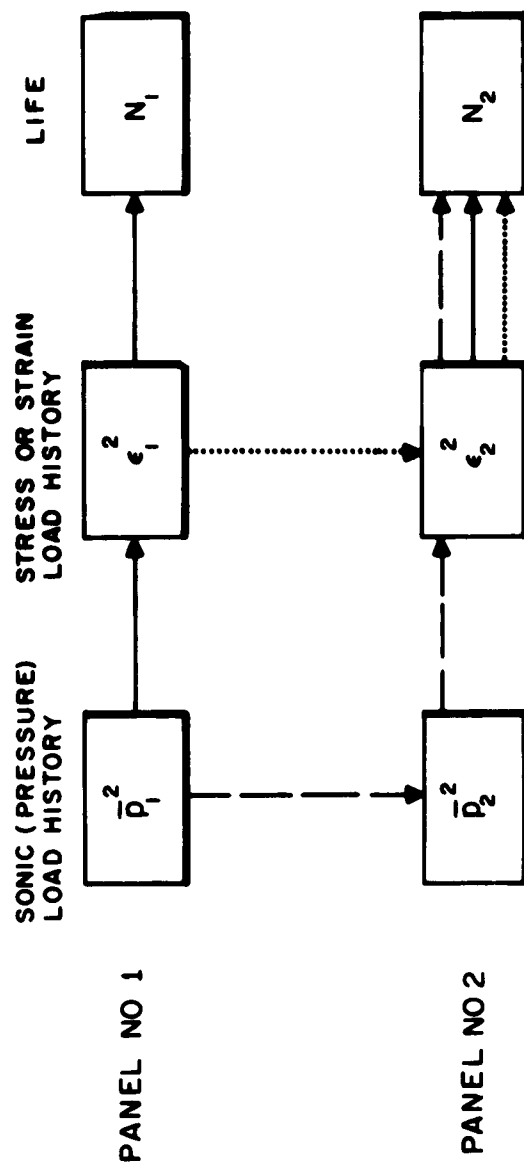
FIG. 7   APPLICATION DIAGRAM FOR SONIC (PRESSURE) LOAD HISTORIES

65
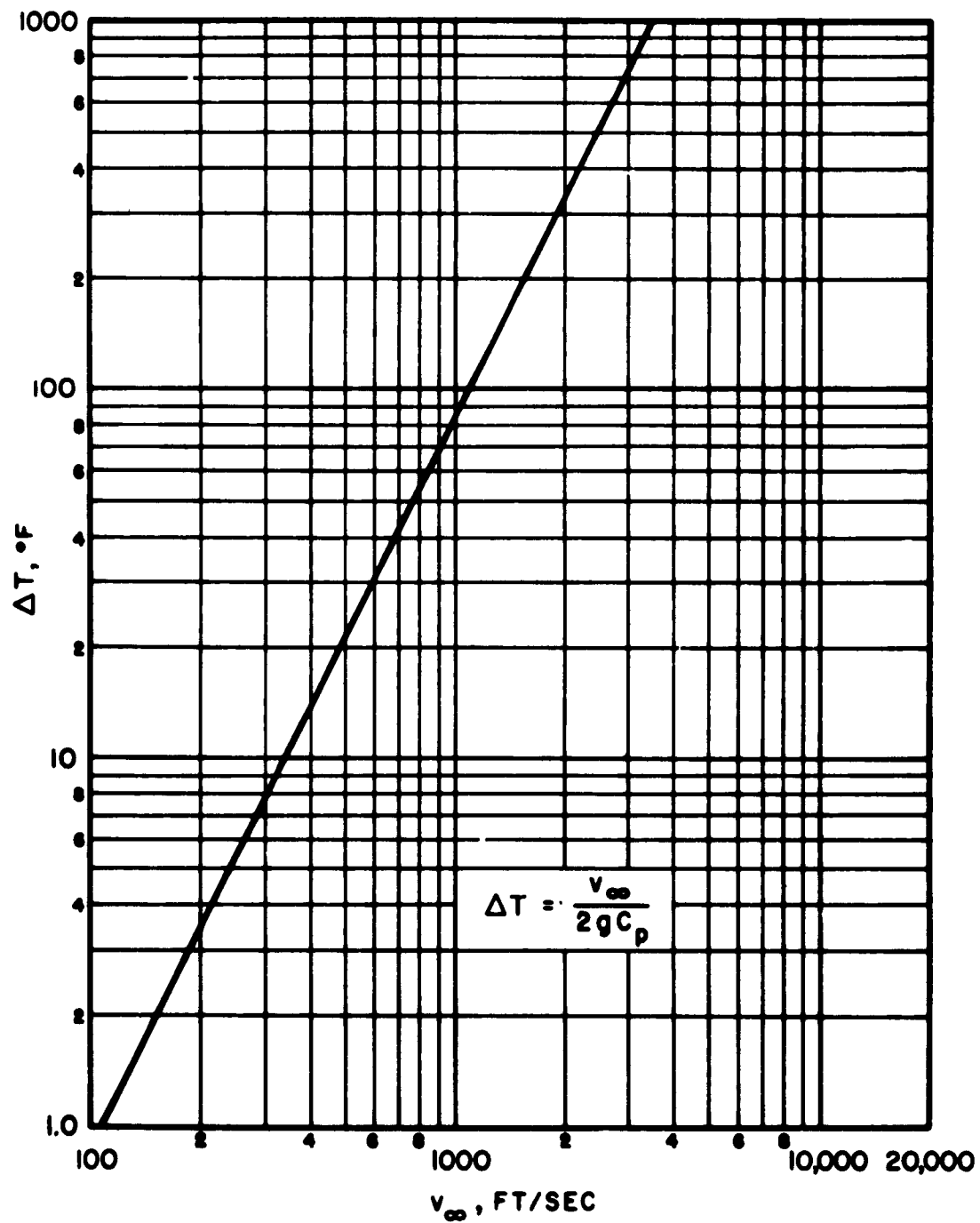
FIG. 8   TEMPERATURE RISE FOR ADIABATIC
DECELERATION OF FLOW
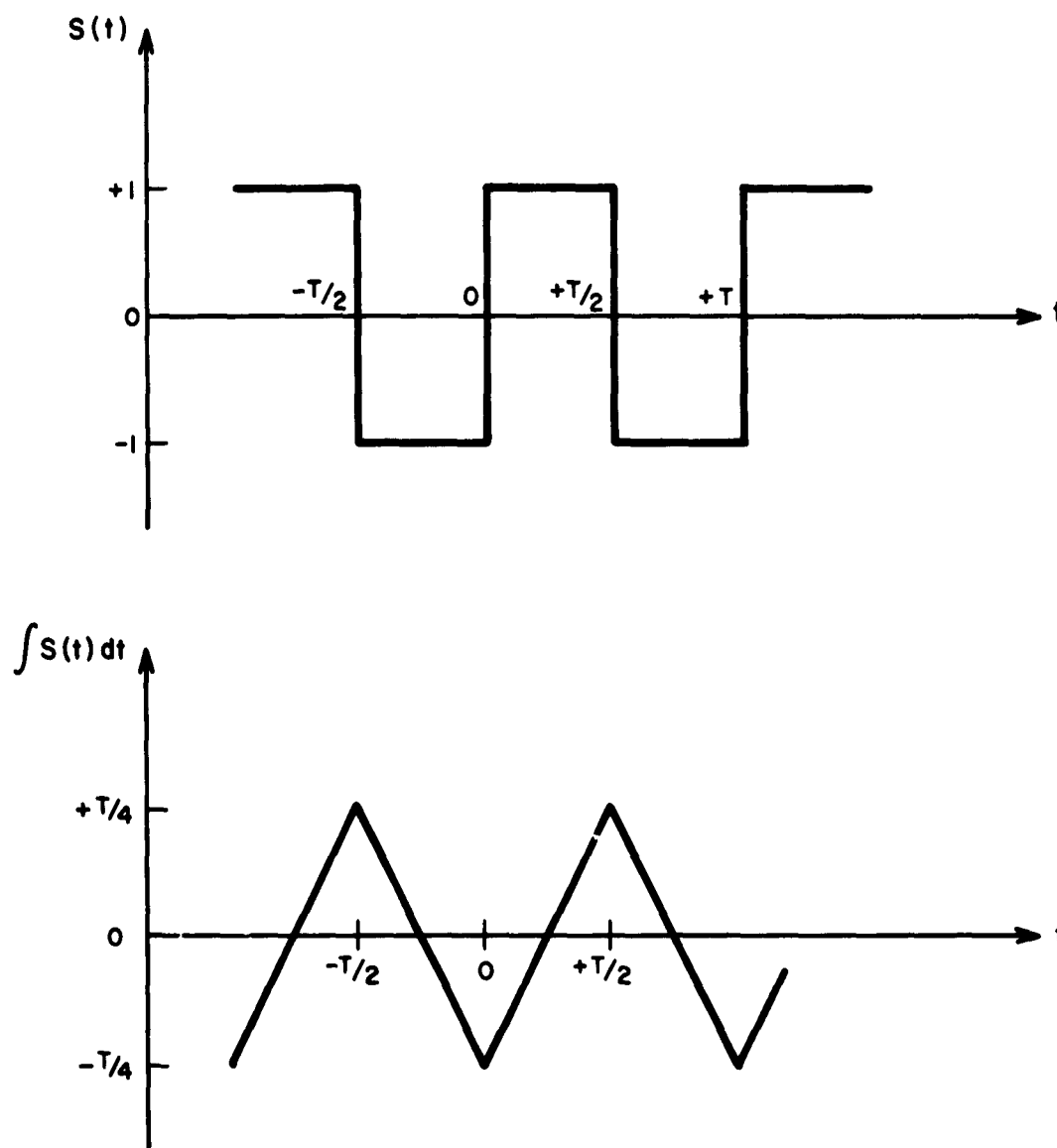
FIG. 9 ILLUSTRATION OF SQUARE WAVE S(t)
AND RESULTING INTEGRAL FOR
EQUATION (6), SECTION III
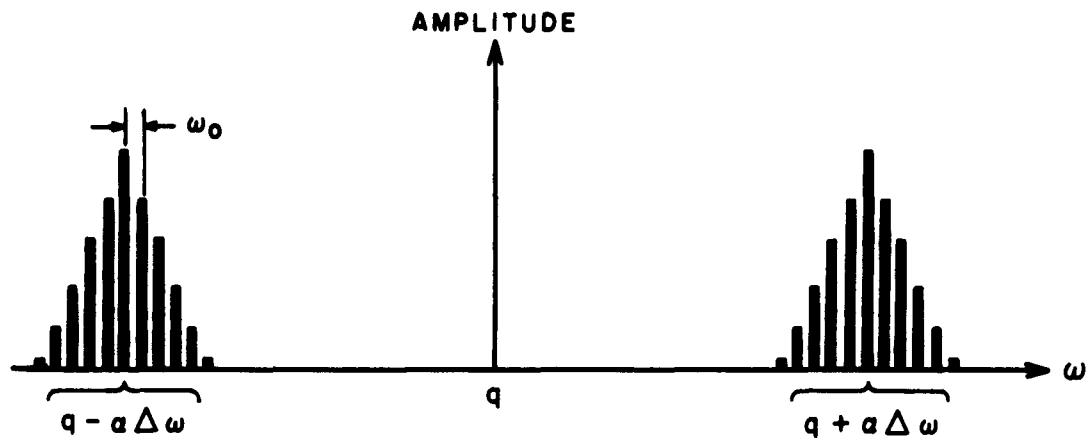
FIG. 10 SPECTRUM OF A SQUARE WAVE OF FREQUENCY ω_0 AFTER FREQUENCY MODULATION WITH CARRIER FREQUENCY q
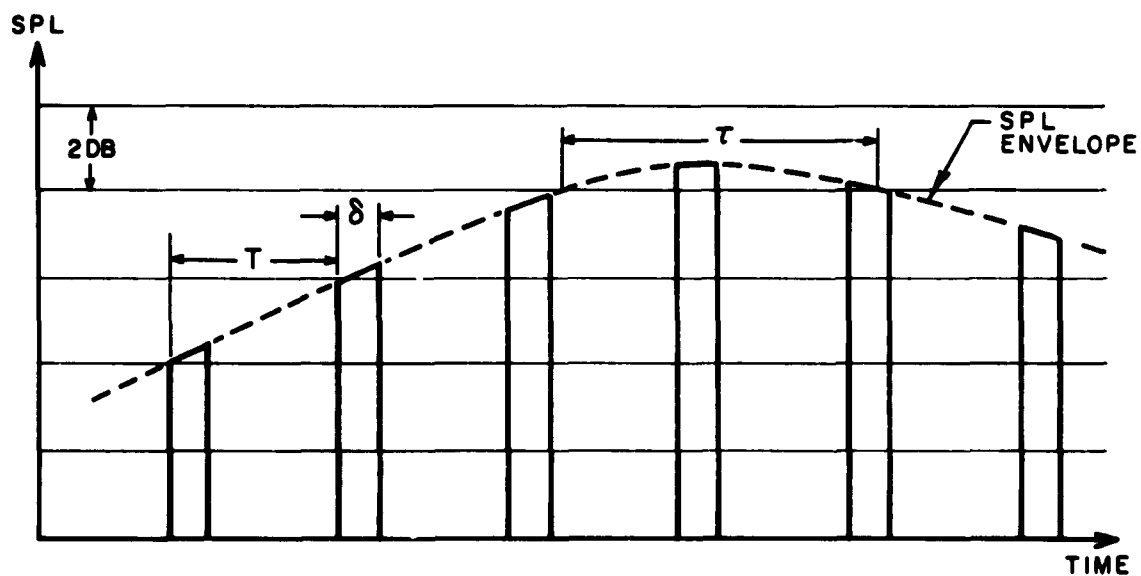
FIG. 11a NOMENCLATURE FOR DISCUSSION OF TIME SHARING
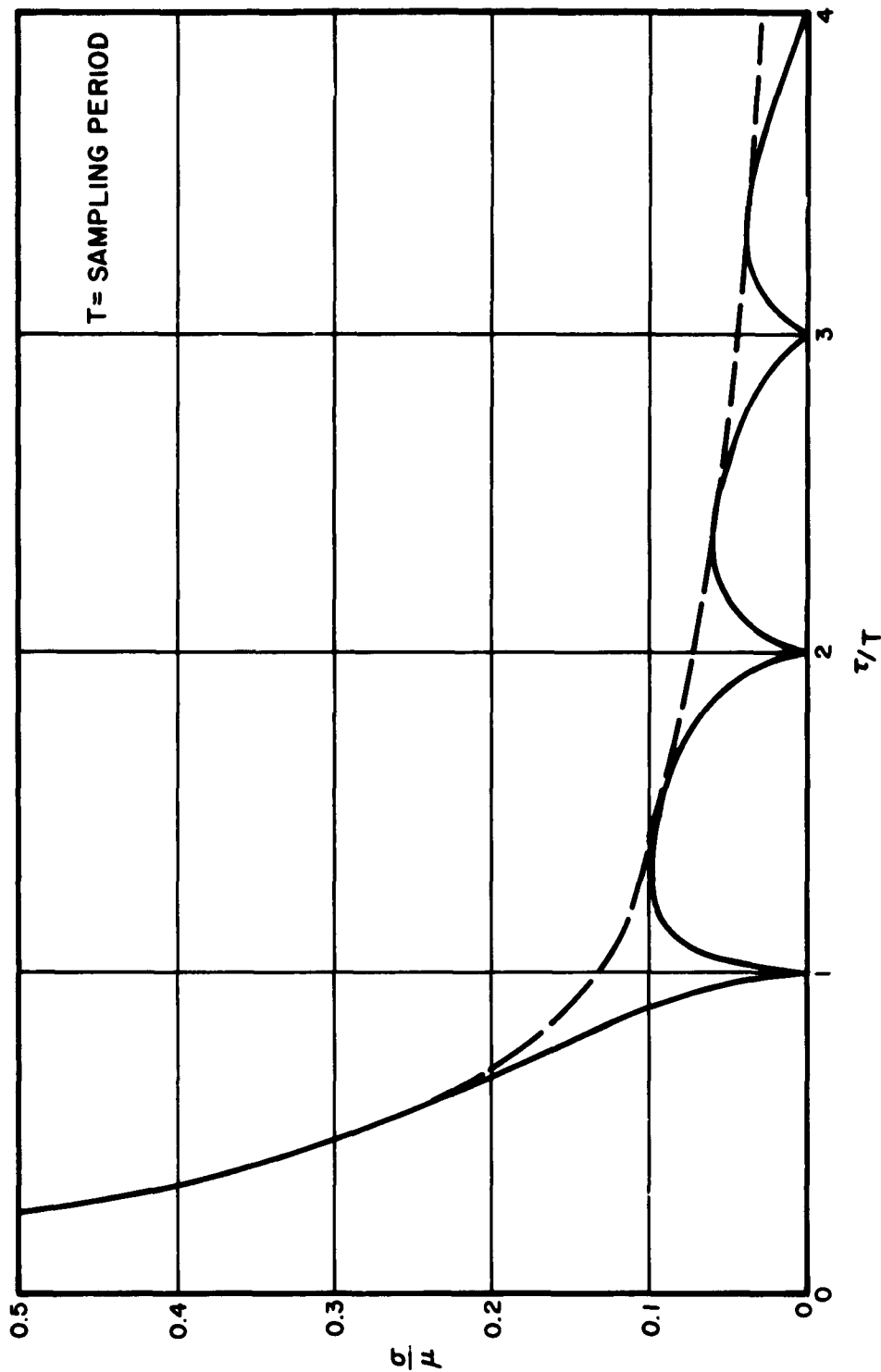
FIG. IIb RATIO σ/μ OF STANDARD DEVIATION TO MEAN NUMBER OF SAMPLES
FOR 12 MAXIMA EACH OF DURATION τ
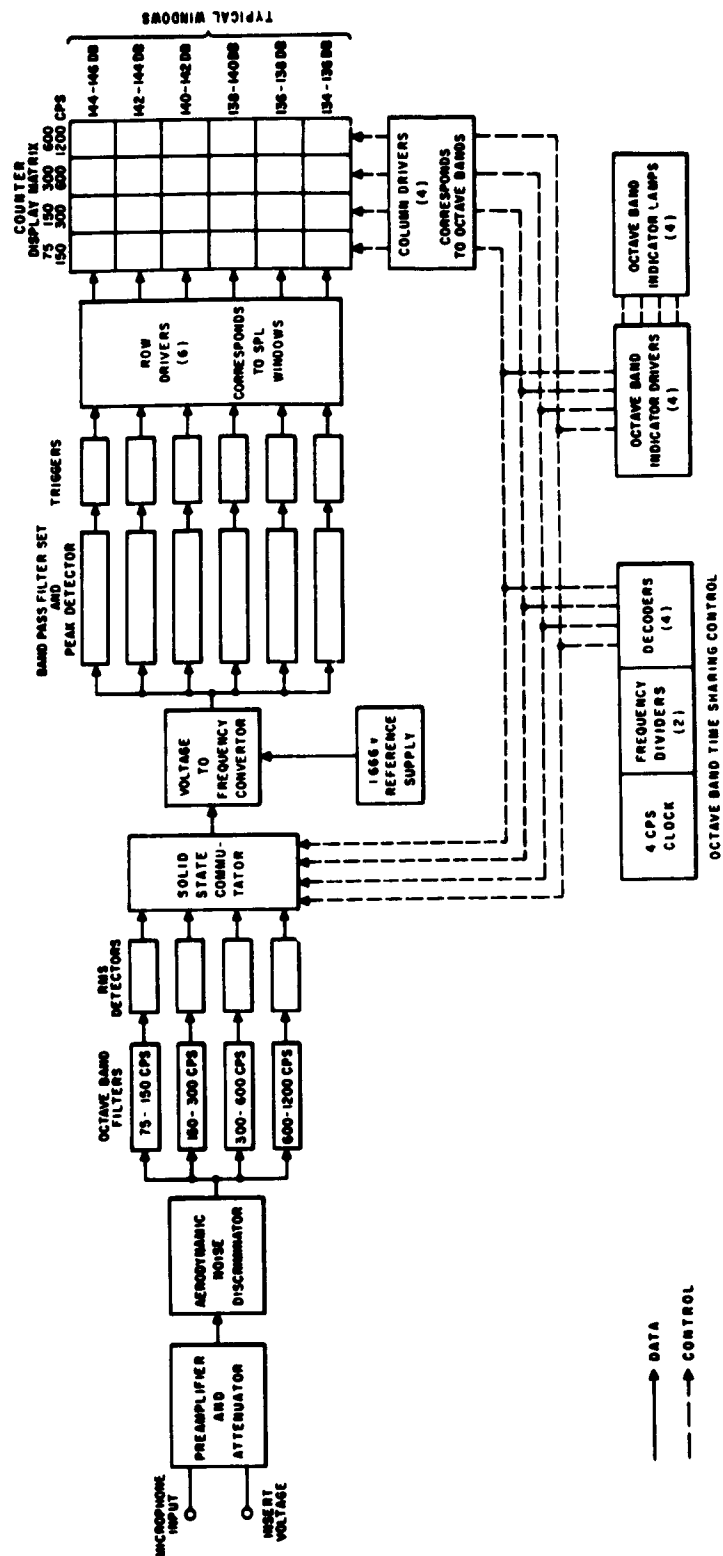
FIG. 12 DIAGRAM OF PRINCIPLE UNITS OF SONIC LIFE HISTORY RECORDER

DATA ACQUISITION

AMPLITUDE
DISCRIMINATOR

TIME SHARING
AND COUNTER
DRIVERS

CALIBRATION
LAMP PACKAGE

IMPULSE
COUNTER
PACKAGE
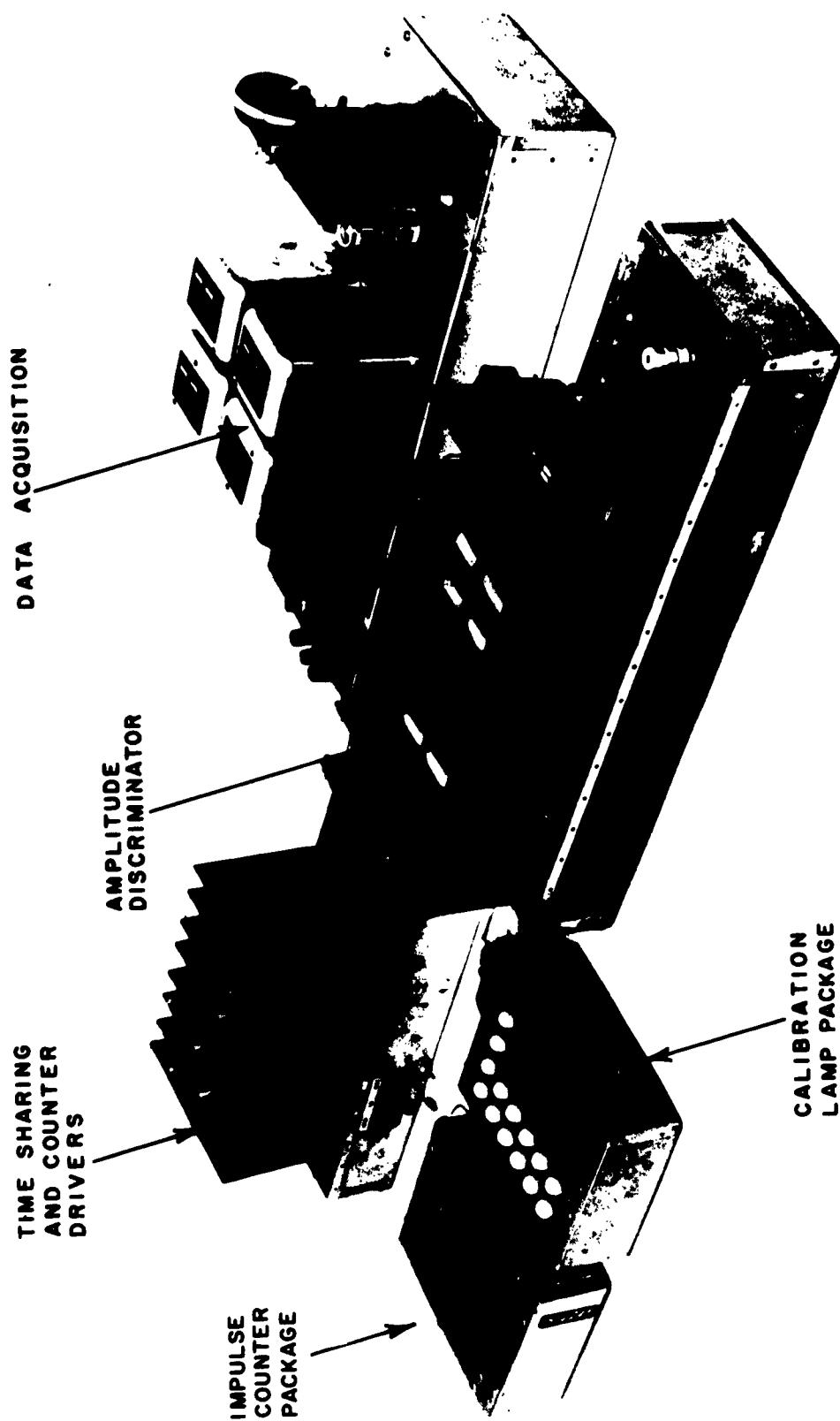
FIG.I3 PHOTOGRAPH OF BREADBOARD SYSTEM
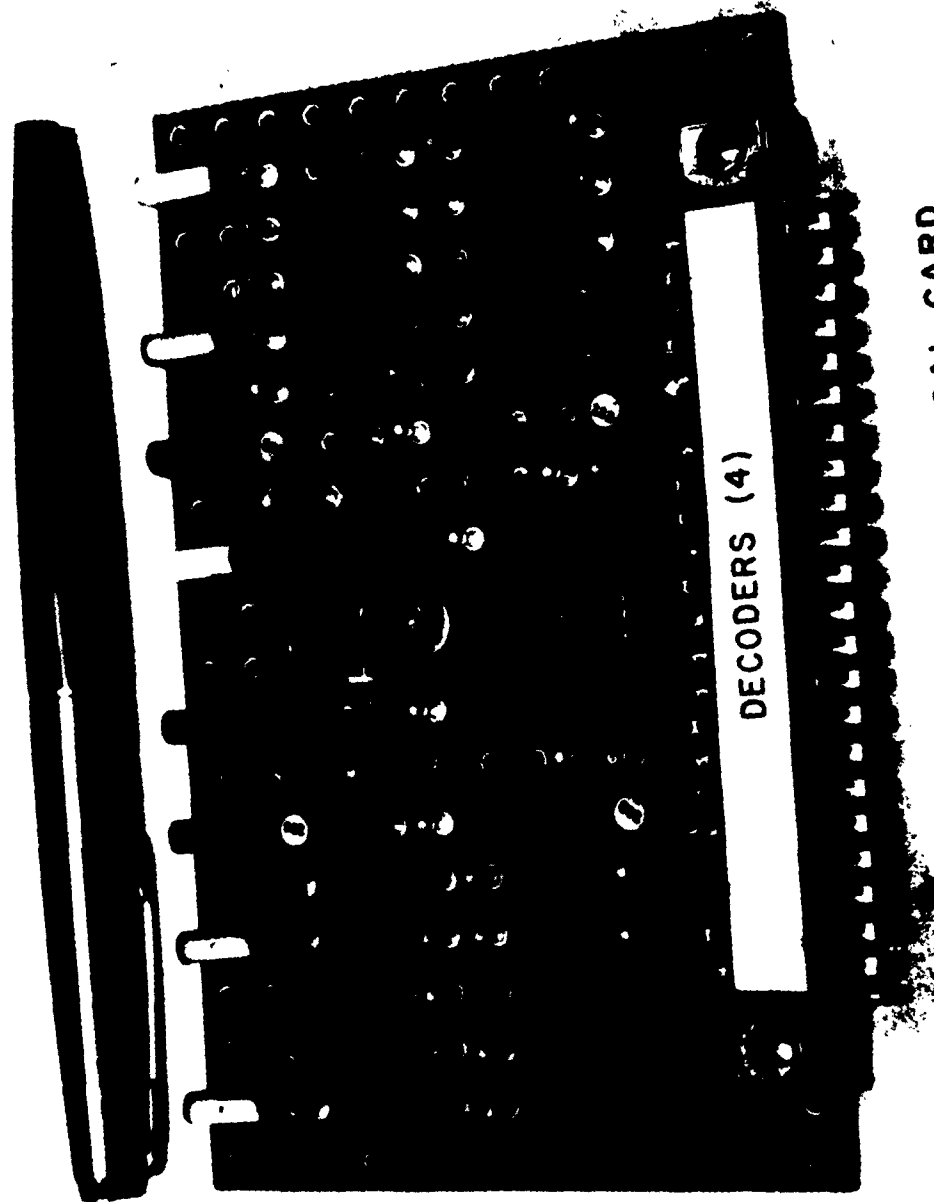
FIG. 14 PHOTOGRAPH OF TYPICAL CARD

DECODERS (4)
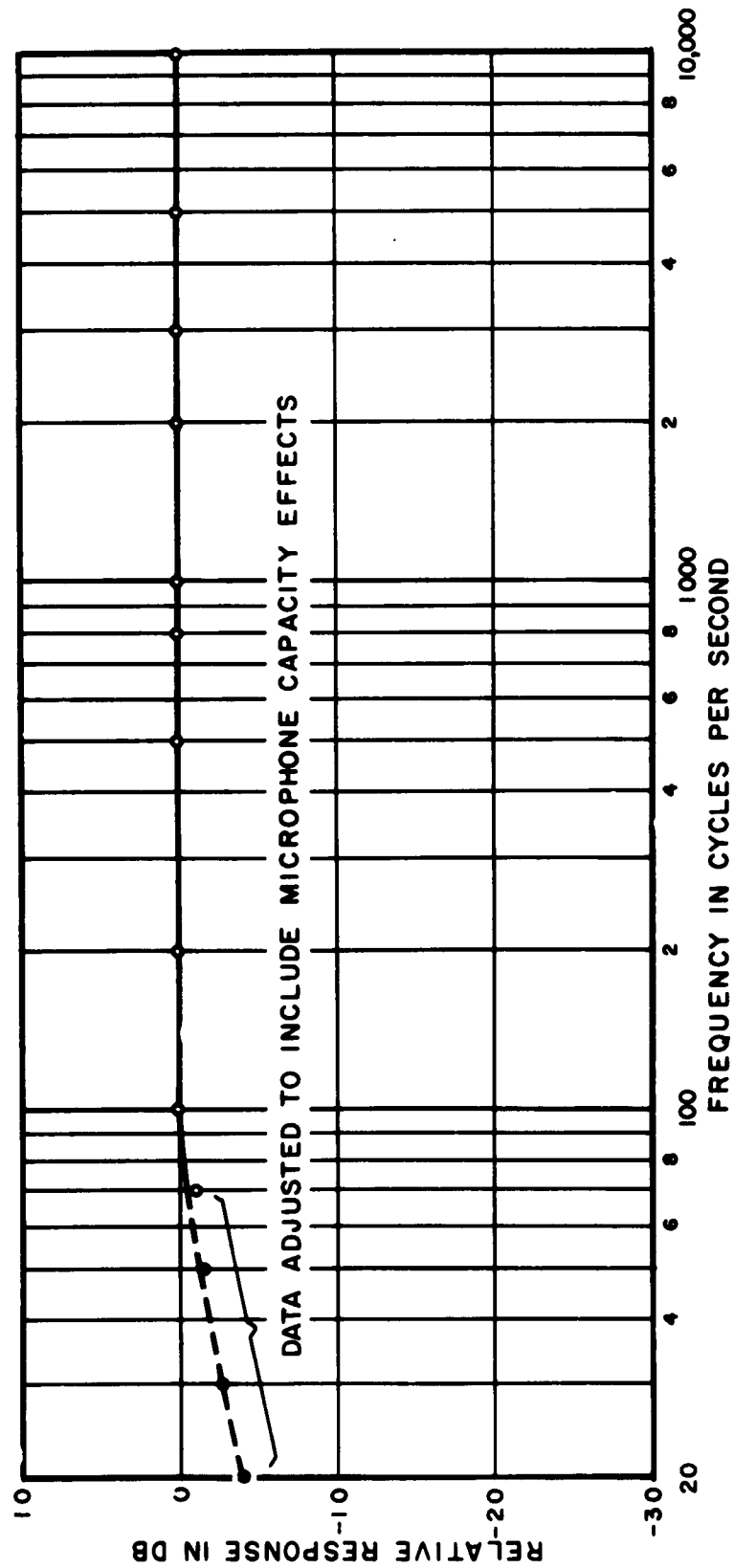
FIG.15   FREQUENCY RESPONSE OF DATA ACQUISITION EQUIPMENT
UP TO OCTAVE BAND FILTERS
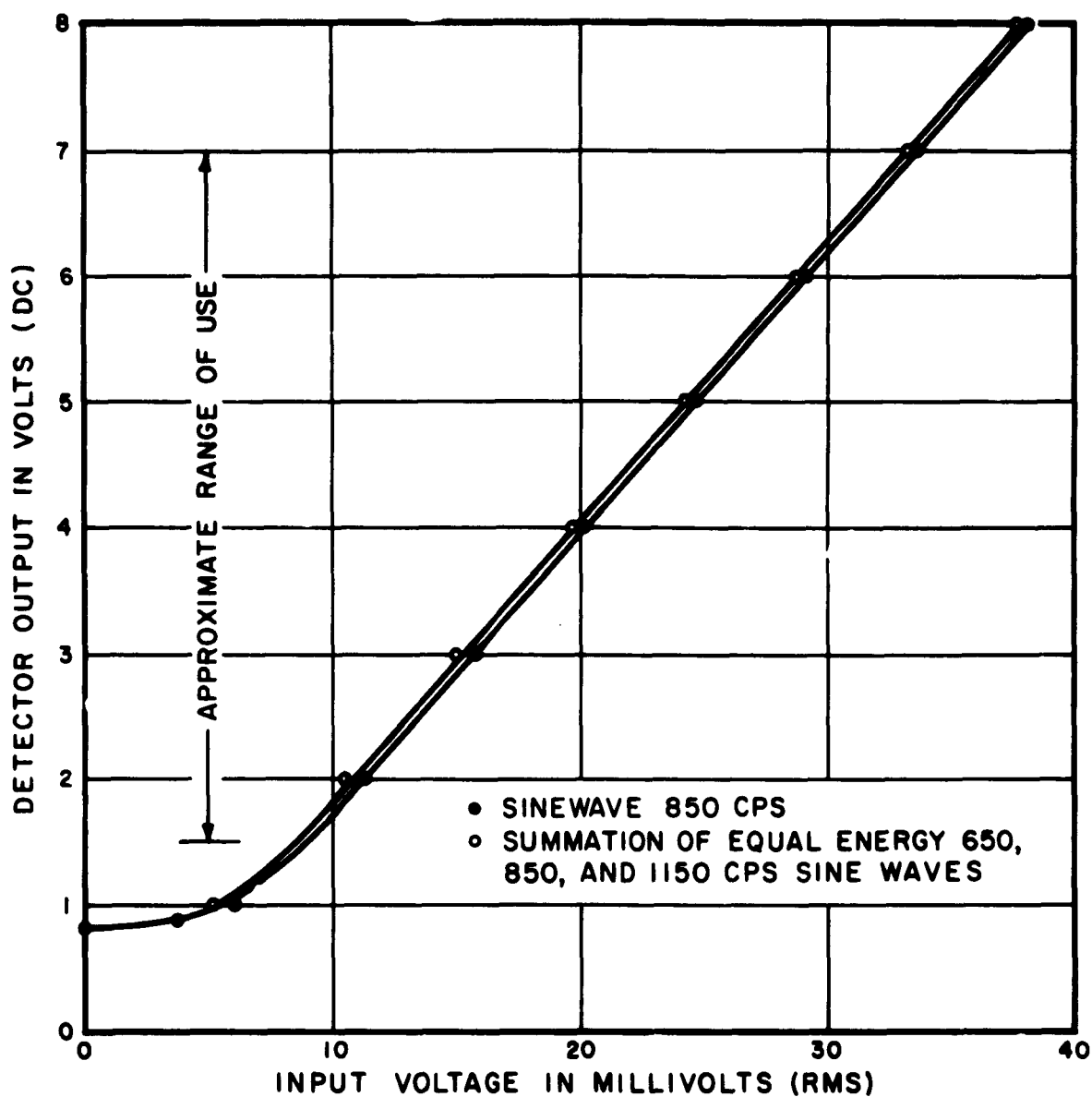
FIG. 16   INPUT VOLTAGE TO DATA ACQUISITION VS.
OUTPUT VOLTAGE FROM RMS DETECTOR

FIG. 17 PHOTOGRAPH OF MICROPHONE VIBRATION MOUNT AND MOLD
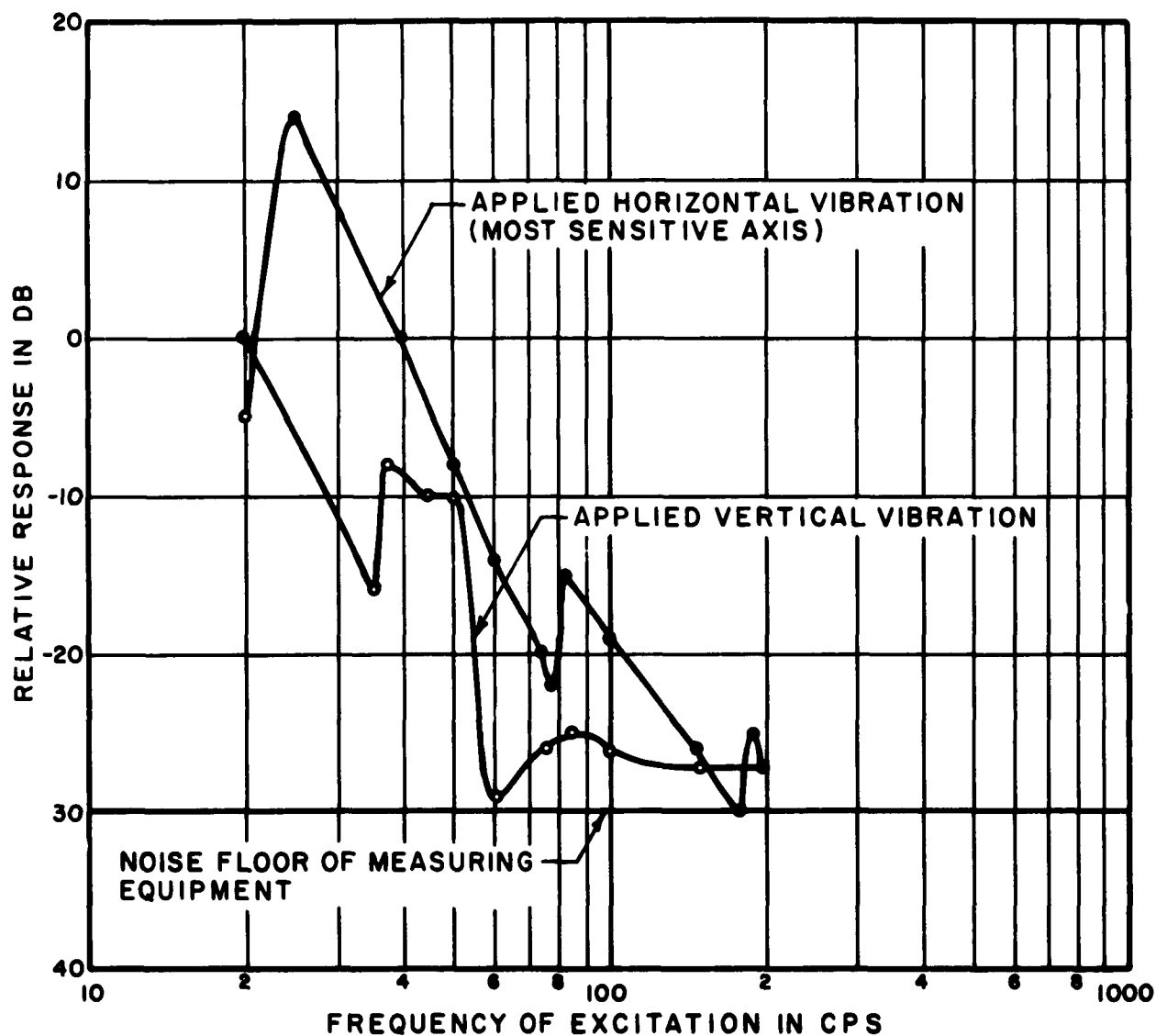
FIG. 18   VIBRATION TRANSMISSION OF MICROPHONE MOUNT
AT I g RMS EXCITATION
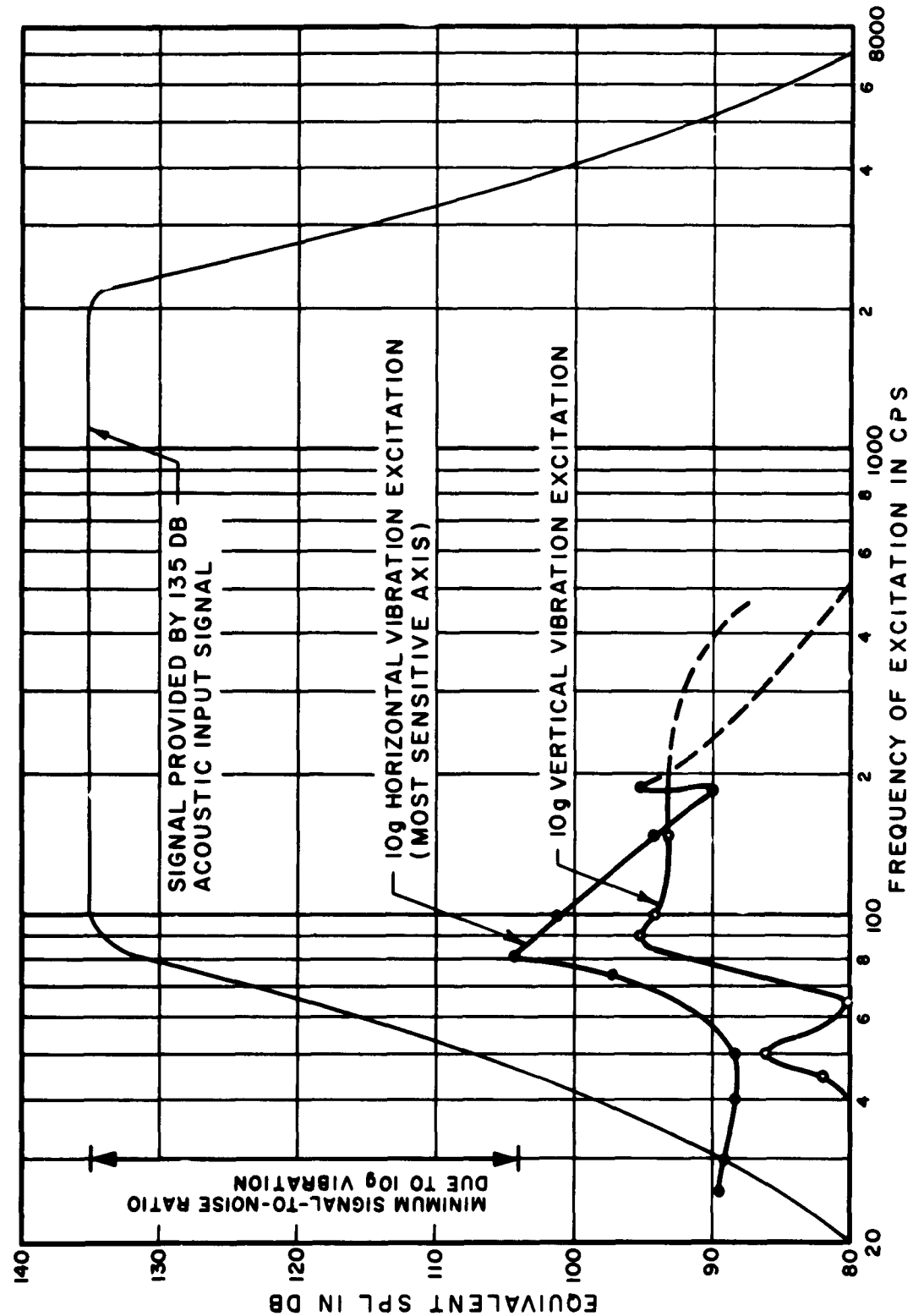
FIG. 19   EXPECTED EQUIVALENT SPL FROM VIBRATION RESPONSE OF
MICROPHONE WITH MOUNT EXCITED AT 10g RMS
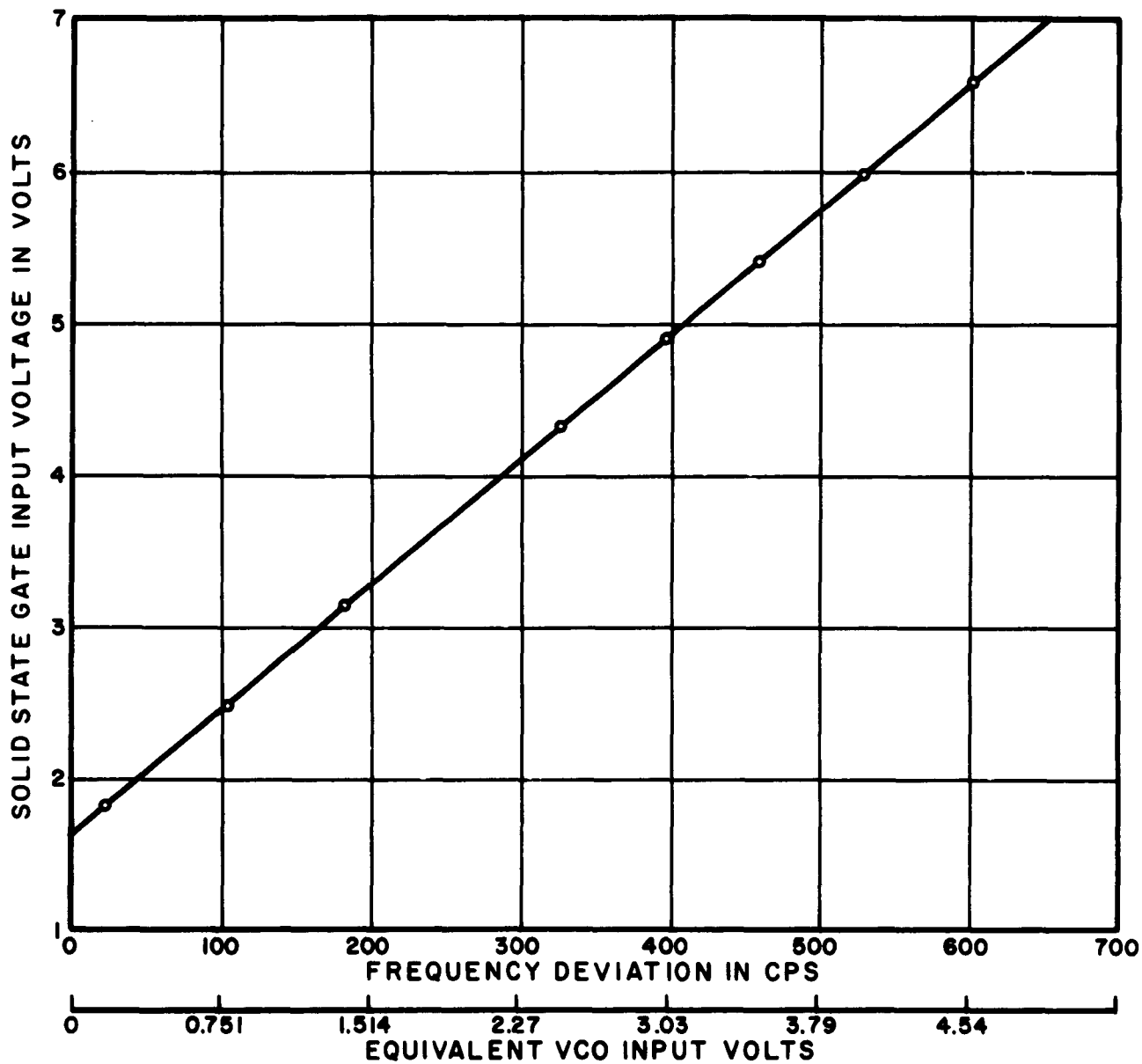
FIG. 20   INPUT VOLTAGE TO SOLID STATE GATES VS.
FREQUENCY DEVIATION OUTPUT OF VCO
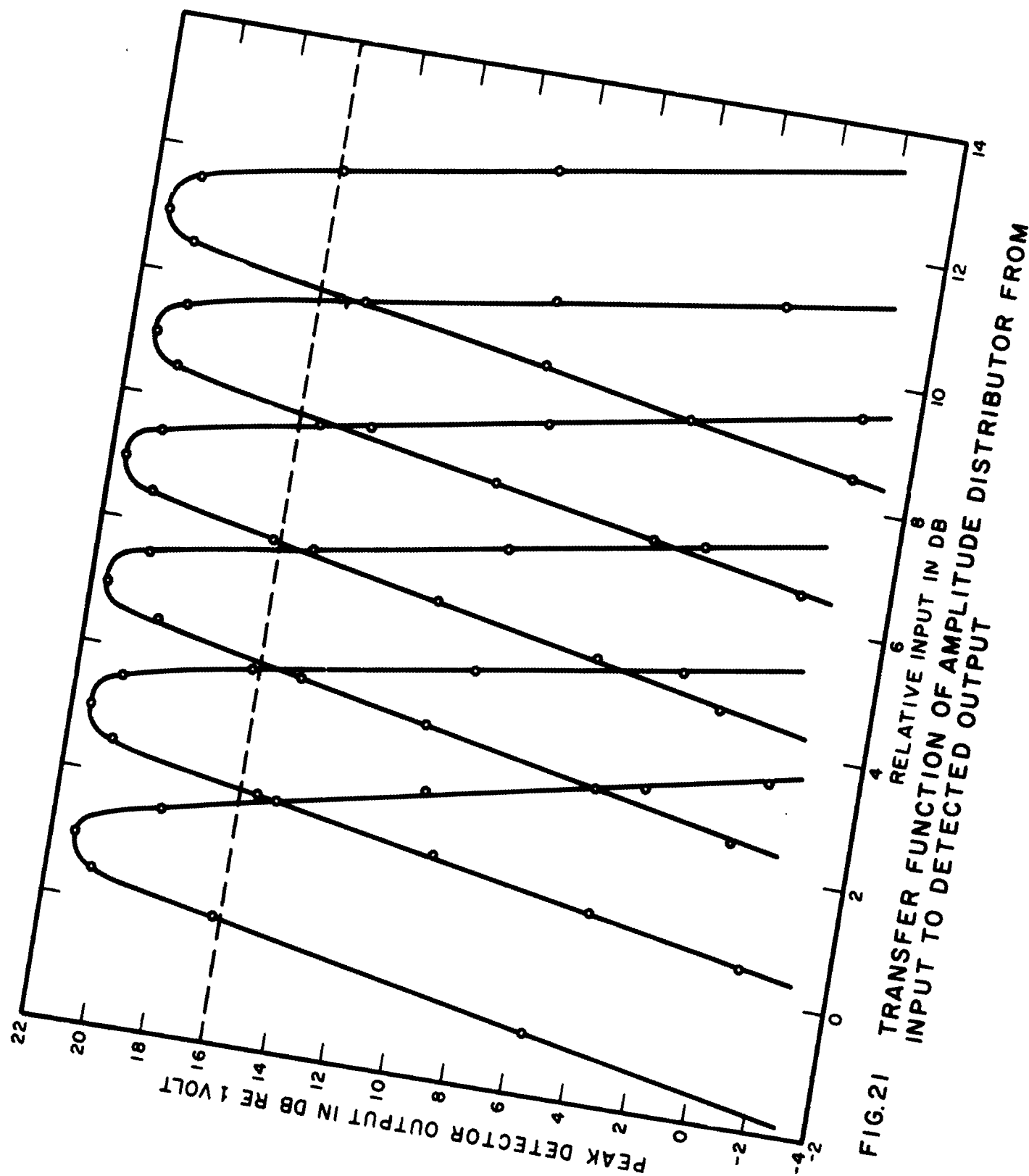
FIG. 21   TRANSFER FUNCTION OF AMPLITUDE DISTRIBUTOR FROM
INPUT TO DETECTED OUTPUT

79
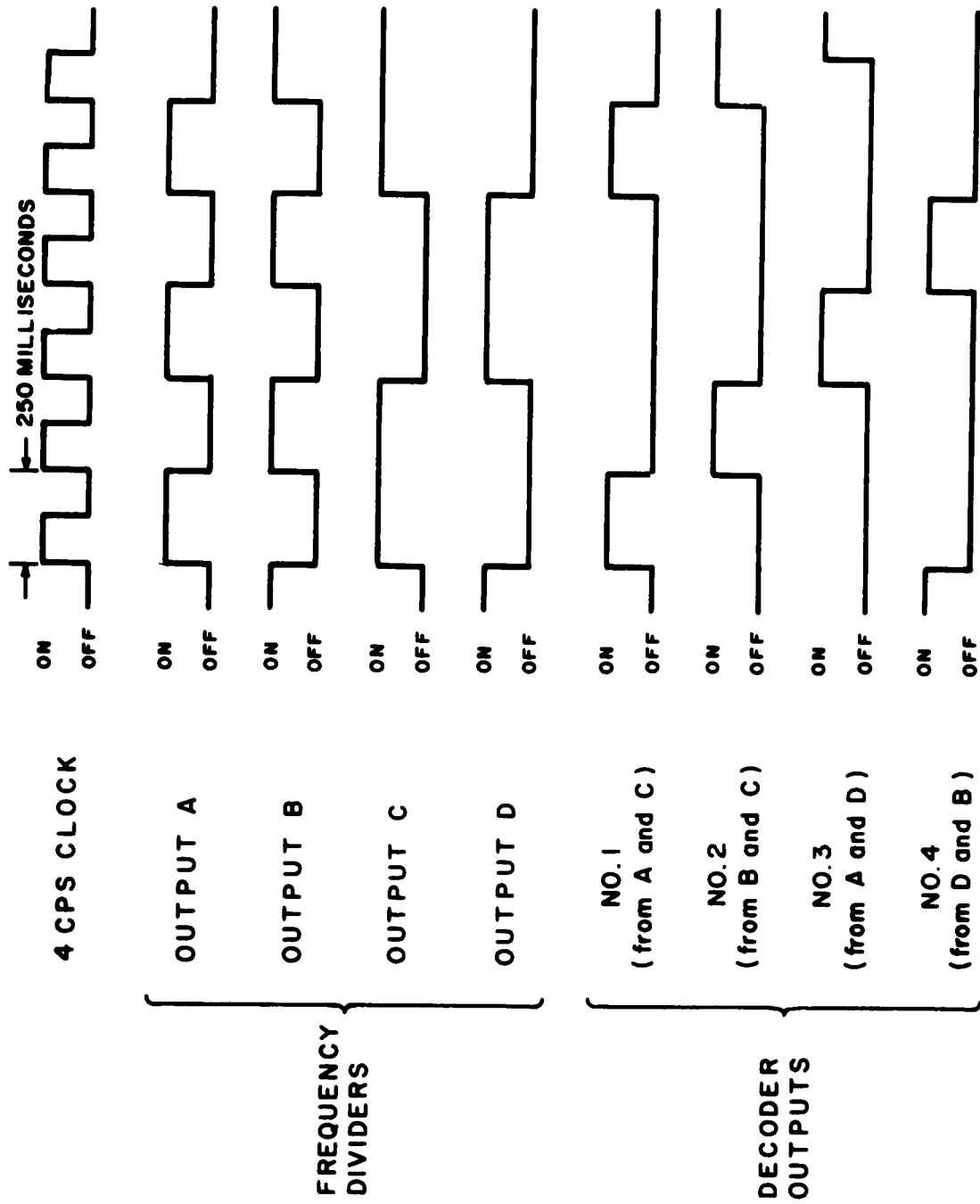
FIG. 22   TIME SHARING CONTROL WAVEFORMS

80

APPENDIX A.

DETAILED CIRCUIT DIAGRAMS

OF THE SONIC RECORDER
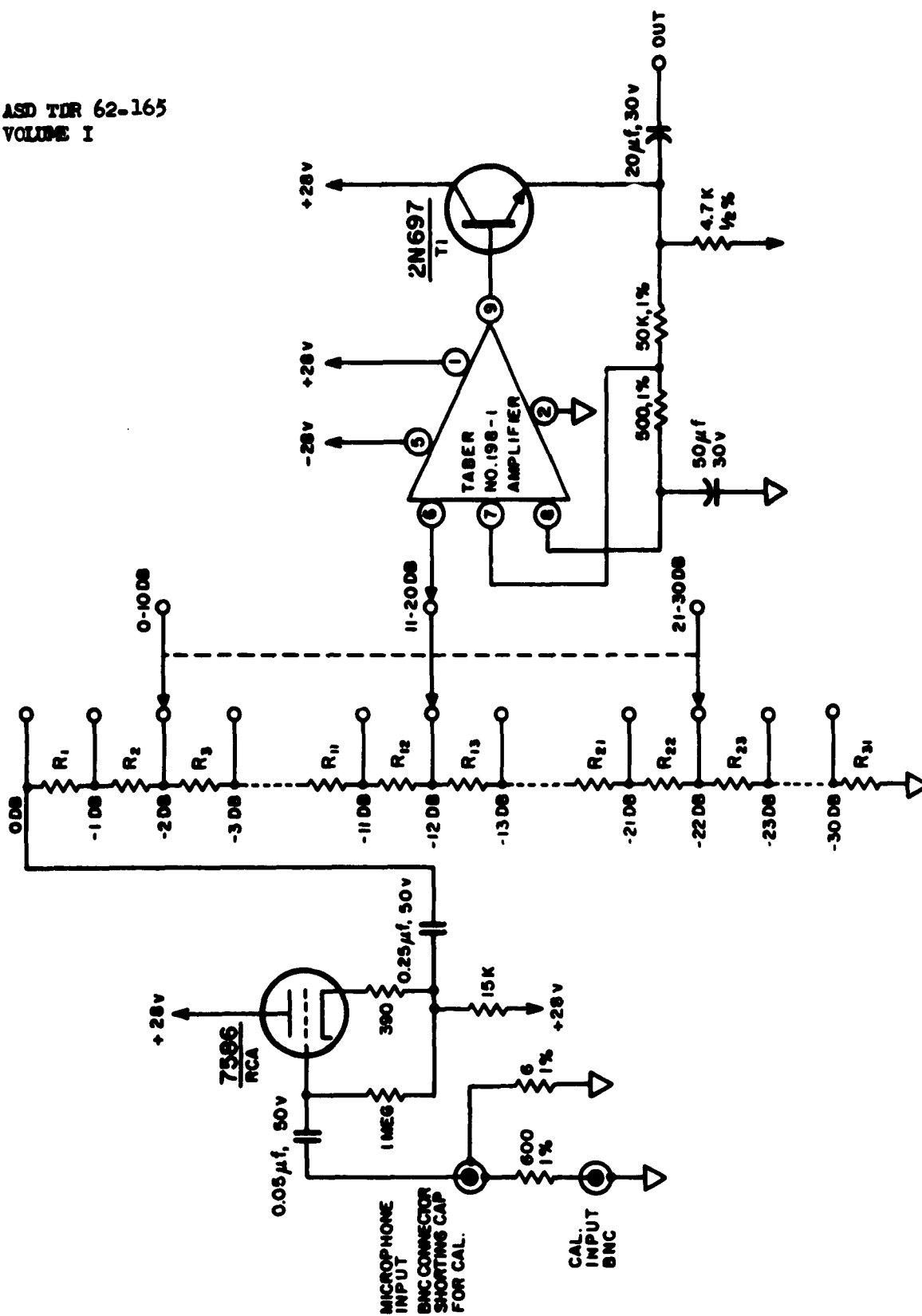
FIG. A-I PREAMPLIFIER AND ATTENUATOR

82

ATTENUATOR RESISTOR VALUES

for Figure A-1

Attenuator Impedance = 2000~

R_1	=	214~	11	68	21	21.4
R_2	=	196	12	60	22	19.6
R_3	=	172	13	56	23	17.2
R_4	=	156	14	48	24	15.6
R_5	=	138	15	44	25	13.8
R_6	=	122	16	38	26	12.2
R_7	=	108	17	36	27	10.8
R_8	=	98	18	30	28	9.8
R_9	=	86	19	28	29	8.6
R_{10}	=	78	20	24	30	7.8

R_{31} = 64~

CONSOLIDATED CONTROLS CORP.
ALTITUDE SWITCH CCC 214 C 50

DYNAMIC PRESSURE
"q" SWITCH

INPUT

OUTPUT

A

B

C

Note: Switch contacts are shown in
normal position when aircraft
is on the ground
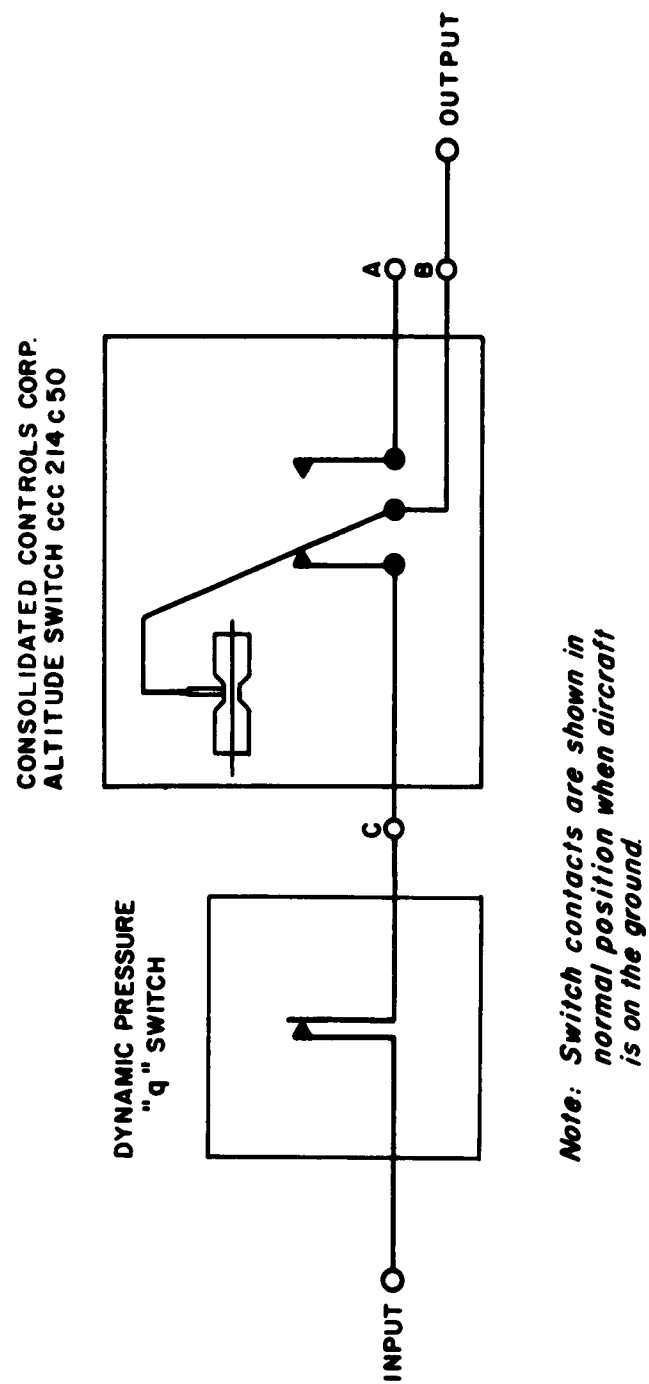
FIG. A-2   AERODYNAMIC NOISE DISCRIMINATOR
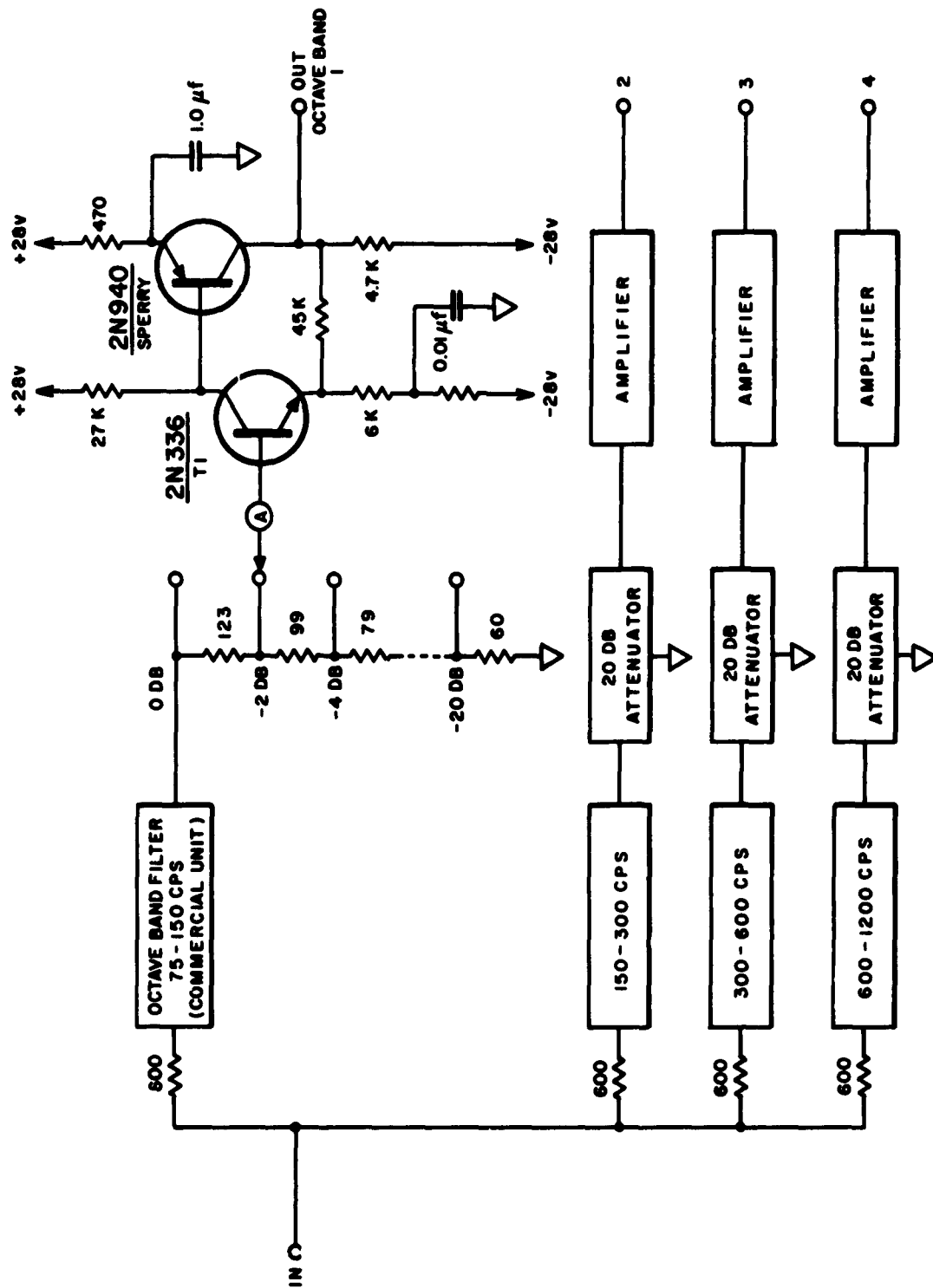
FIG. A-3 OCTAVE BAND FILTERS, ATTENUATORS, AND AMPLIFIERS

85

ATTENUATOR RESISTOR VALUES

for Figure A-3

Attenuator Impedance = 600~

R_1 = 123~

R_2 = 99

R_3 = 79

R_4 = 61

R_5 = 49

R_6 = 39

R_7 = 31

R_8 = 24.5

R_9 = 20

R_{10} = 15.5

R_{11} = 60~
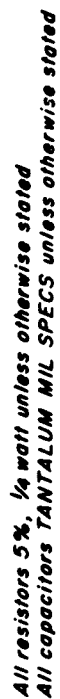
FIG. A-4 QUASI-RMS DETECTOR

All resistors 5%, 1/4 watt unless otherwise stated
All capacitors TANTALUM MIL SPECS unless otherwise stated
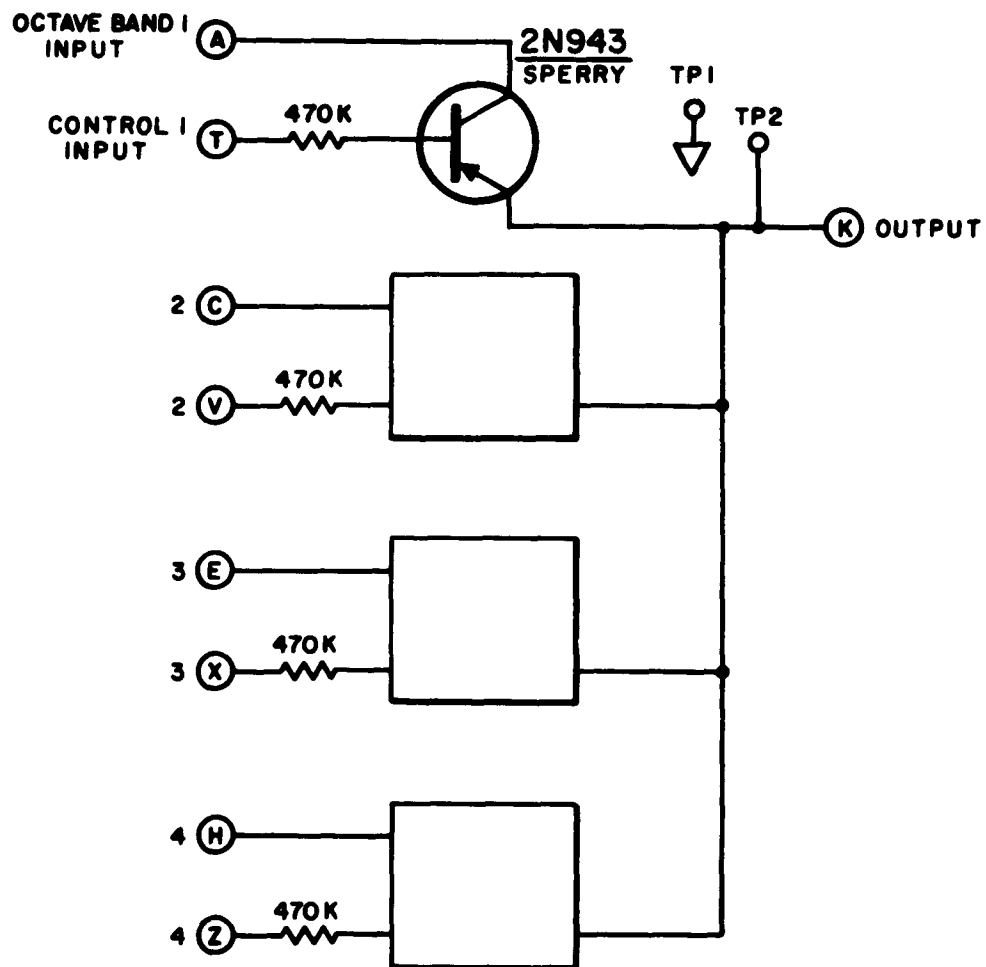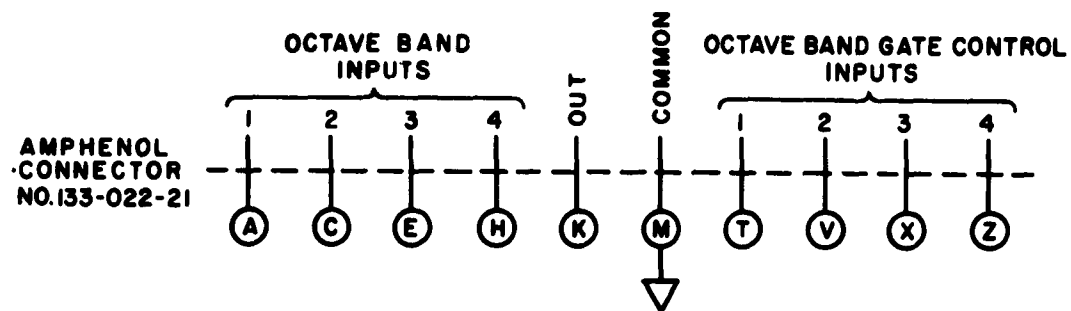
FIG. A-5 SOLID STATE COMMUTATOR

OUT
+1.666 v

+28v

COMMON

-28 v

-25.4 v

AMPHENOL CONNECTOR
NO. 133-022-21

Ⓚ   Ⓛ   Ⓜ   Ⓟ   Ⓡ

*1100
1 w

(IRC TYPE
MEA T-2)

*Exact value is selected to
give 7.5 ma diode currents

IN937A
MOTOROLA

TP 1

IN943A
MOTOROLA

BIAS
CONTROL

(BOURNS
TRIMPOT)

TP 2

*690
½ w

cw   500

Ⓚ OUT
1.666 v

(IRC TYPE
MEF T-2)

-28 v
Ⓟ

IN465
HOFFMAN

Ⓡ OUT
-25.4 v

4.7 K
½ w
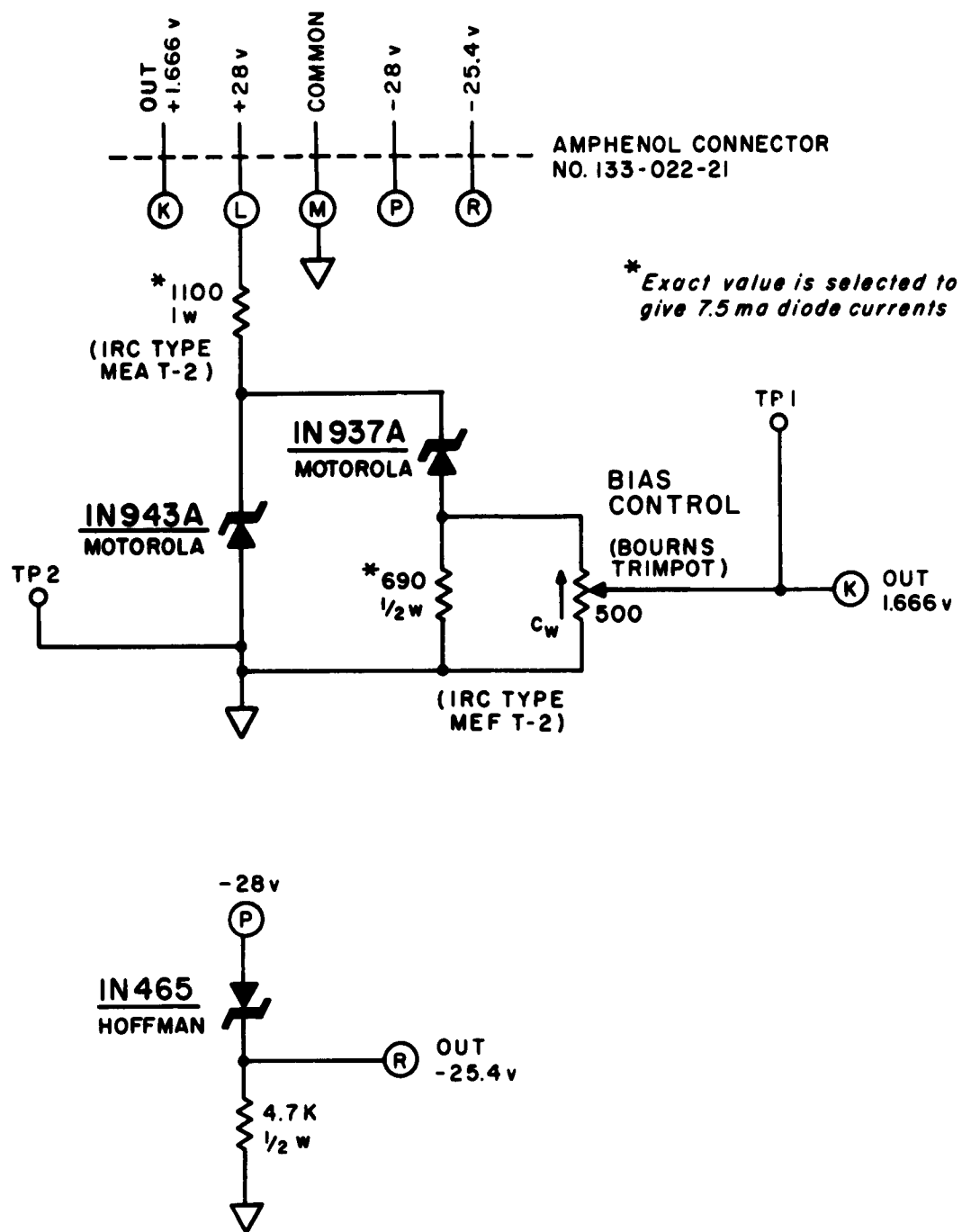
FIG. A-6 1.666 v BIAS SOURCE AND -25.4 v SOURCE
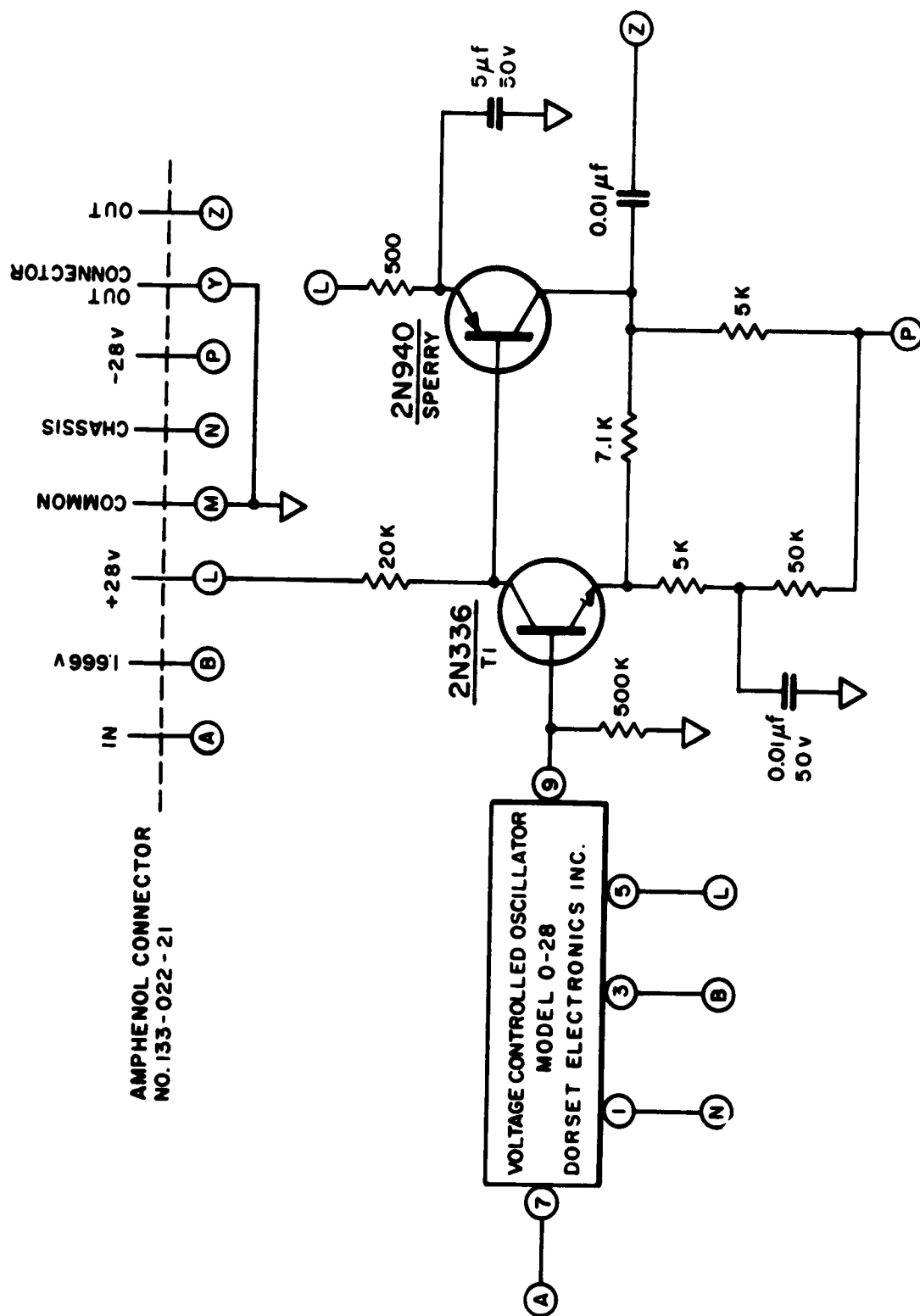
FIG. A-7 VOLTAGE TO FREQUENCY CONVERTER
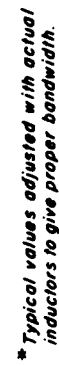
FIG. A-8   BAND PASS FILTER, PEAK DETECTOR AND TRIGGER

BAND PASS FILTER COMPONENT VALUES

for Figure A-8

BAND	FREQ(MC)	$C_1^*(\rho f)$	C_2^*	C_c^*	R_1^*	R_2^*	R_f^{**}
U(shown)	18.70-19.27	17,500	17,500	240	40K	40K	20 K
V	19.27-19.99	16,000	16,000	300	40K	40K	17 K
W	19.99-20.90	15,000	15,000	330	22K	27K	8.2K
X	20.90-22.04	14,000	14,000	360	18K	22K	18 K
Y	22.04-23.48	12,000	12,000	390	20K	20K	10 K
Z	23.48-25.30	10,000	10,000	430	20K	20K	12 K

*   Typical values, adjusted with actual
inductors to give proper bandwidth.

** Typical values, adjusted to give unity
gain in the band, between TP-1 and TP-3.
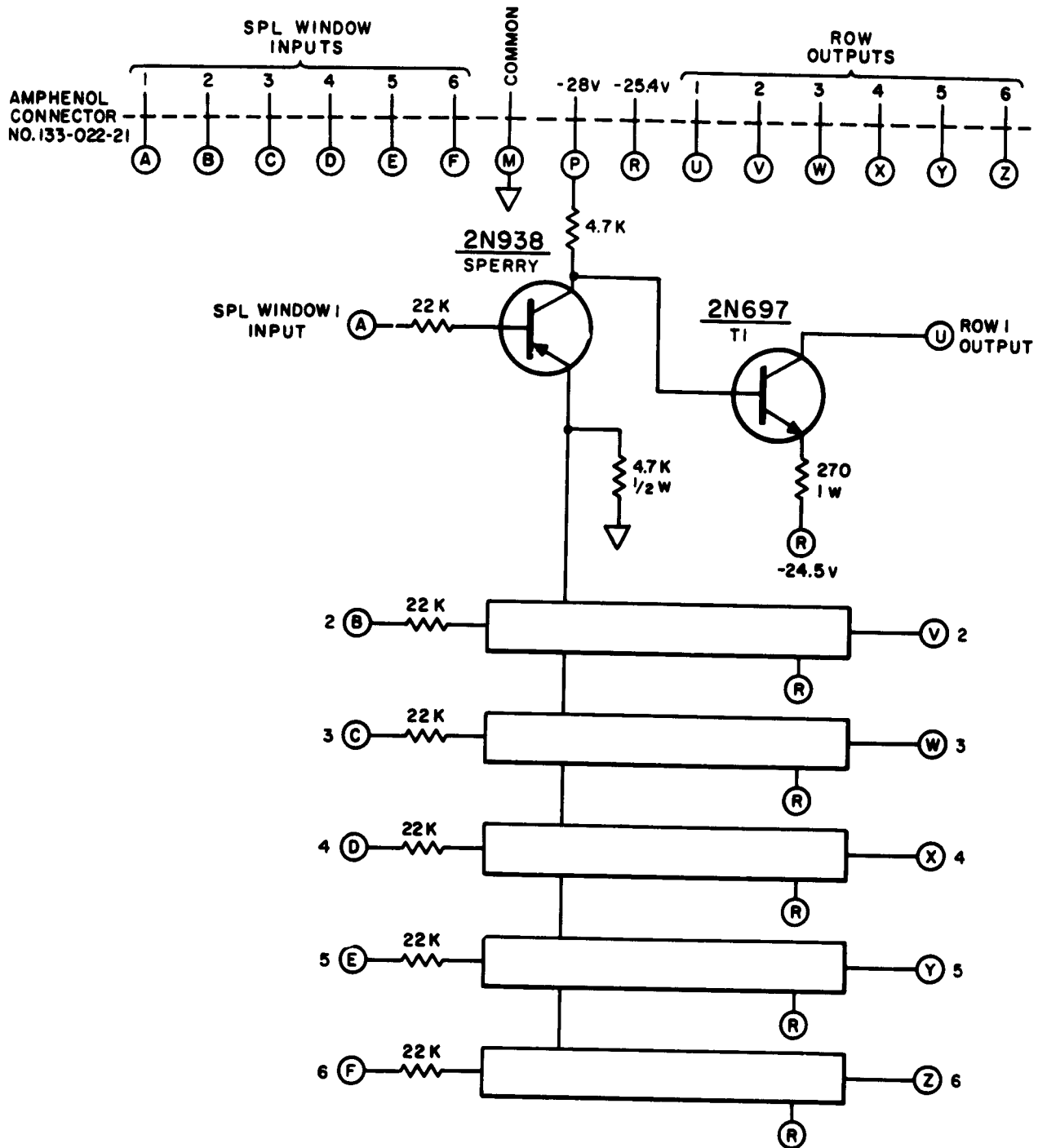
FIG. A-9   COUNTER ROW DRIVERS
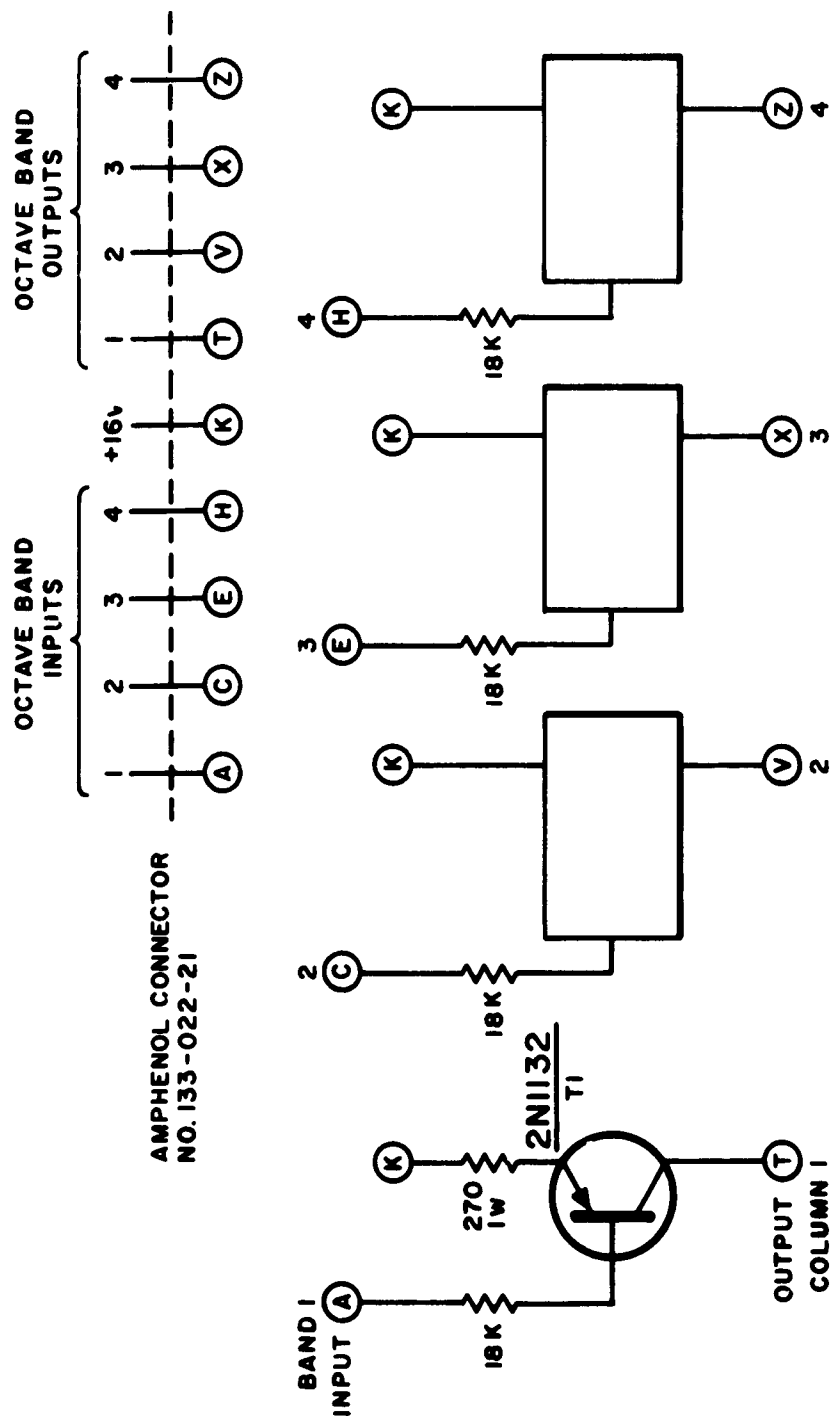
FIG. A-IO   COUNTER COLUMN DRIVERS
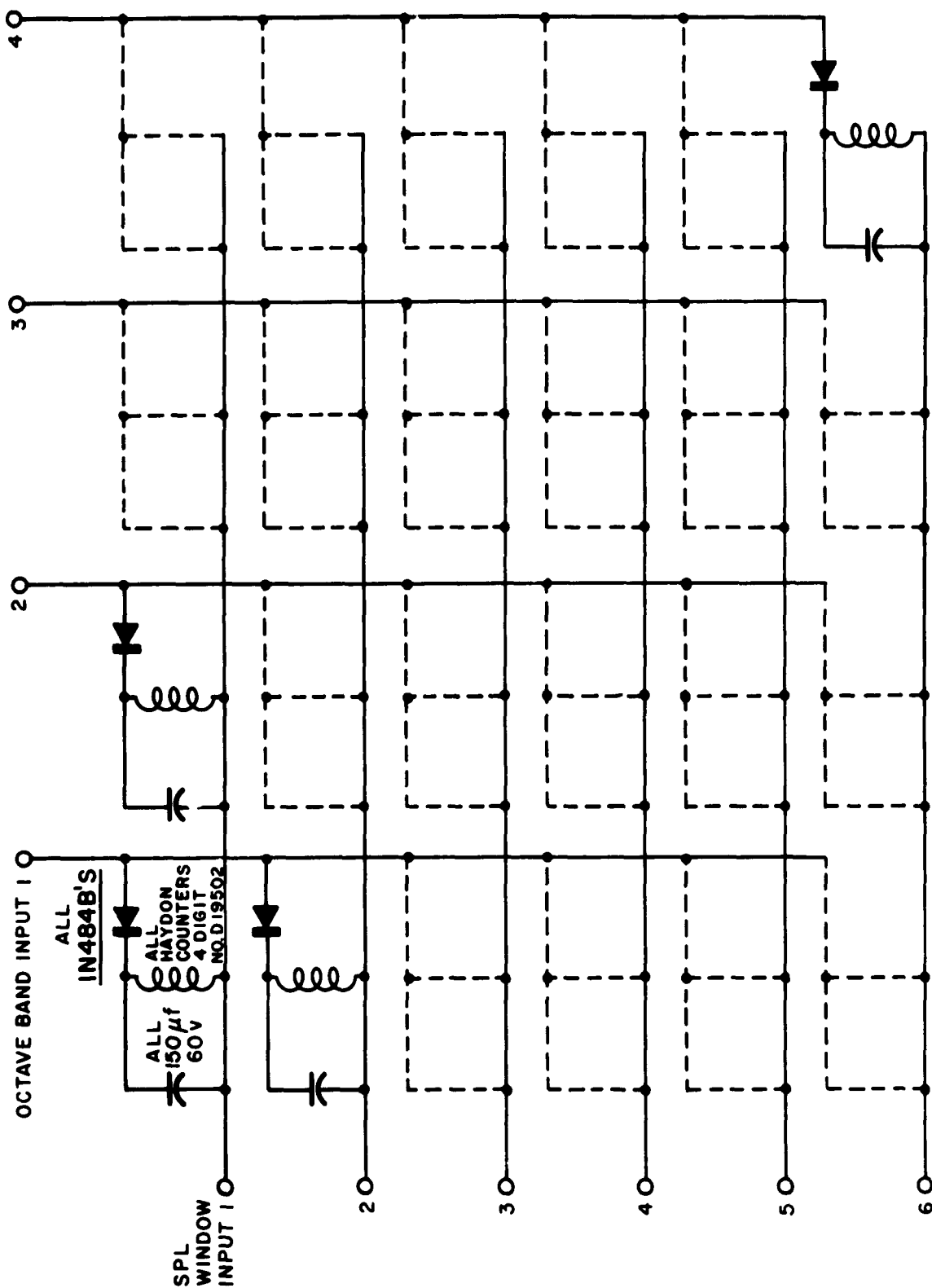
FIG. A-II   COUNTER MATRIX
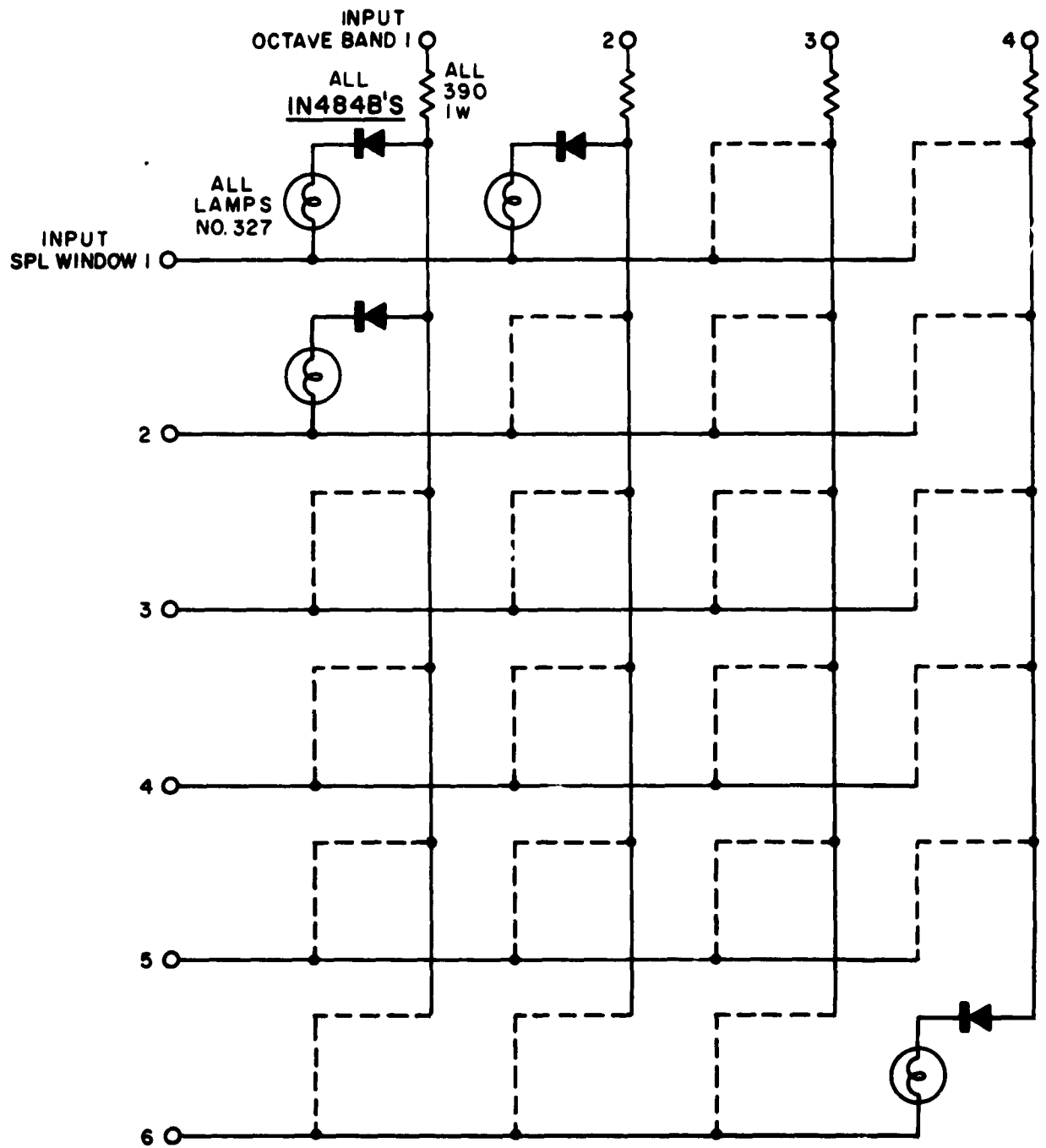
FIG. A-12 LAMP MATRIX
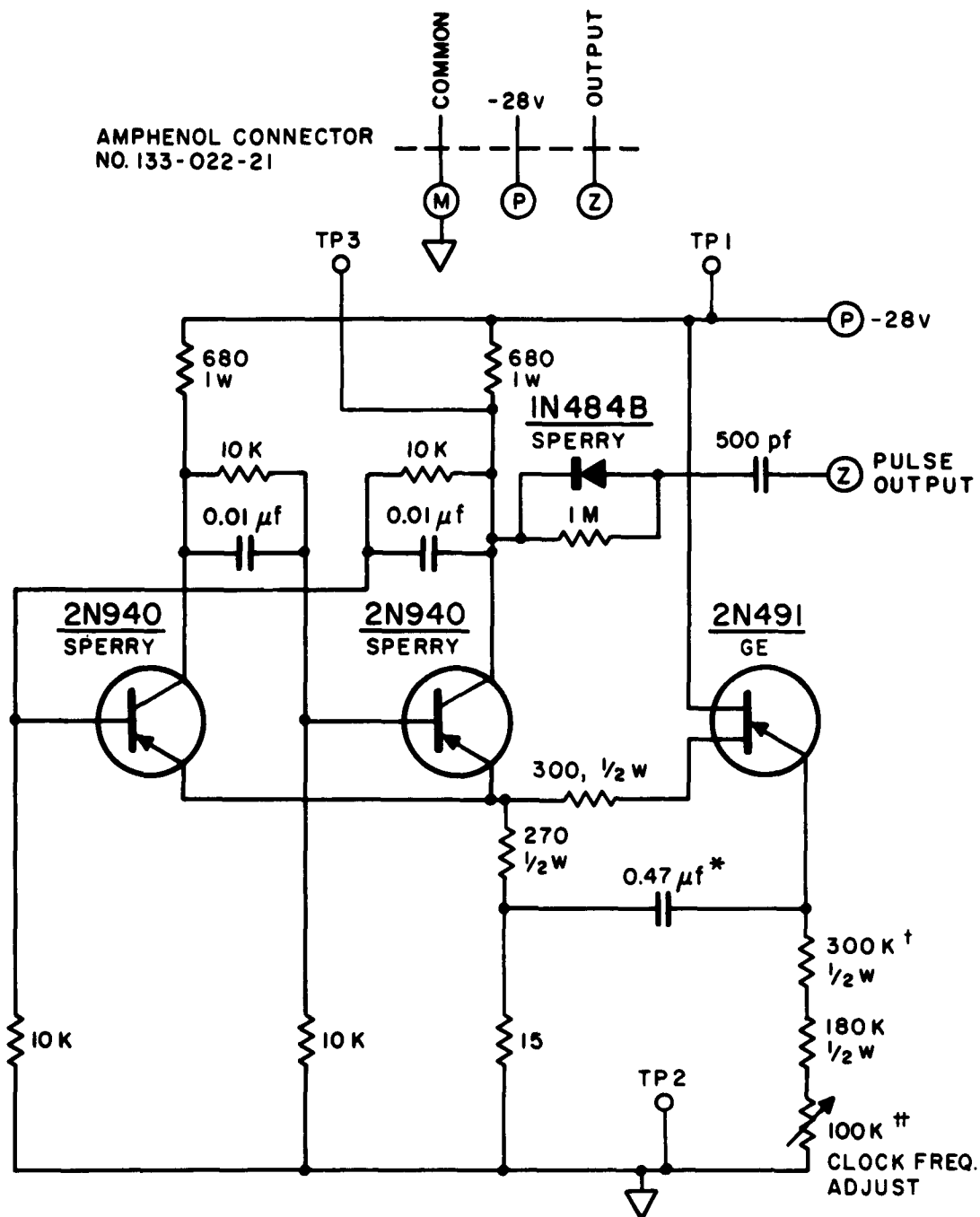
FIG. A-13   4 pps CLOCK
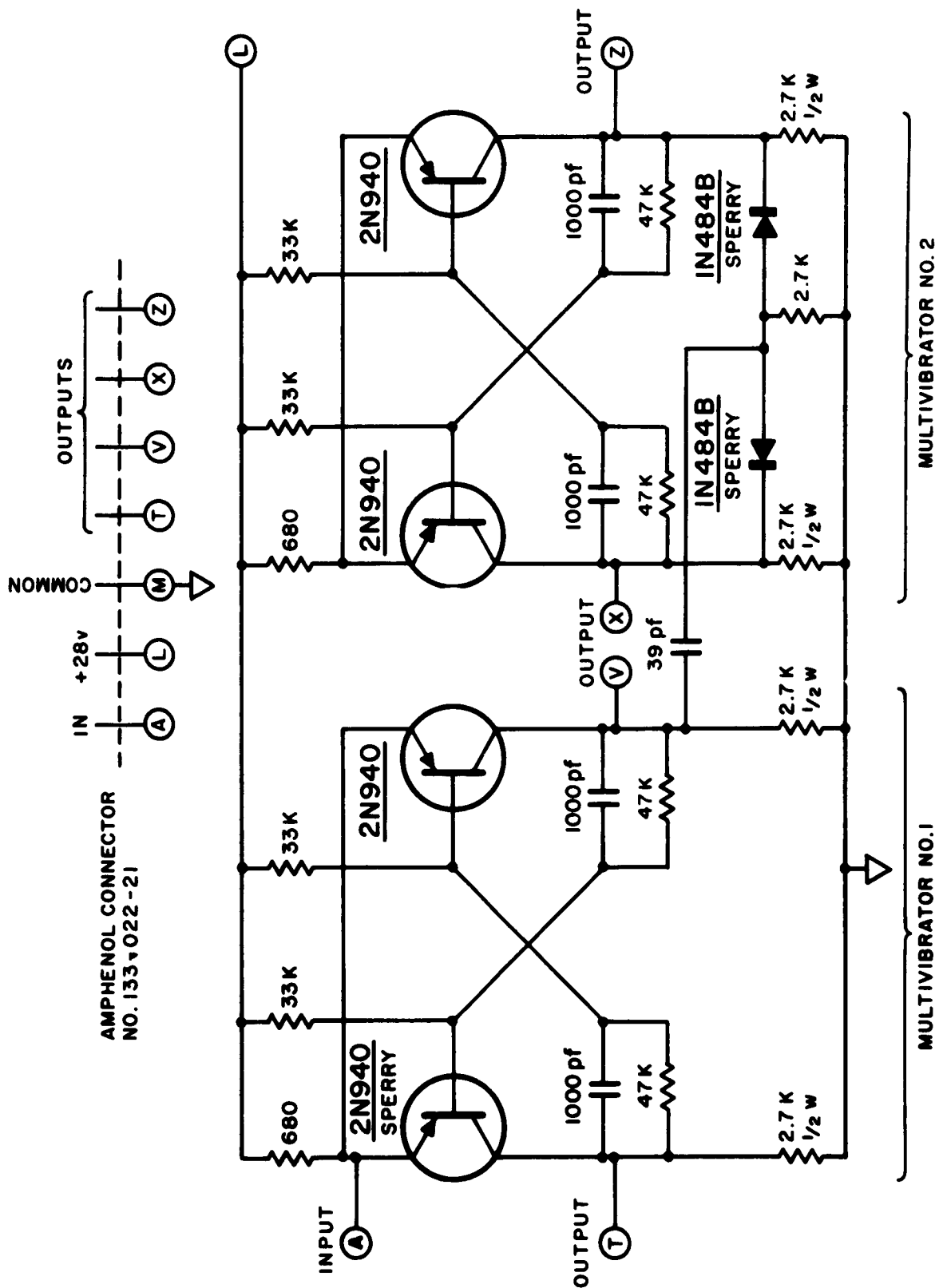
FIG. A-14   BISTABLE MULTIVIBRATORS
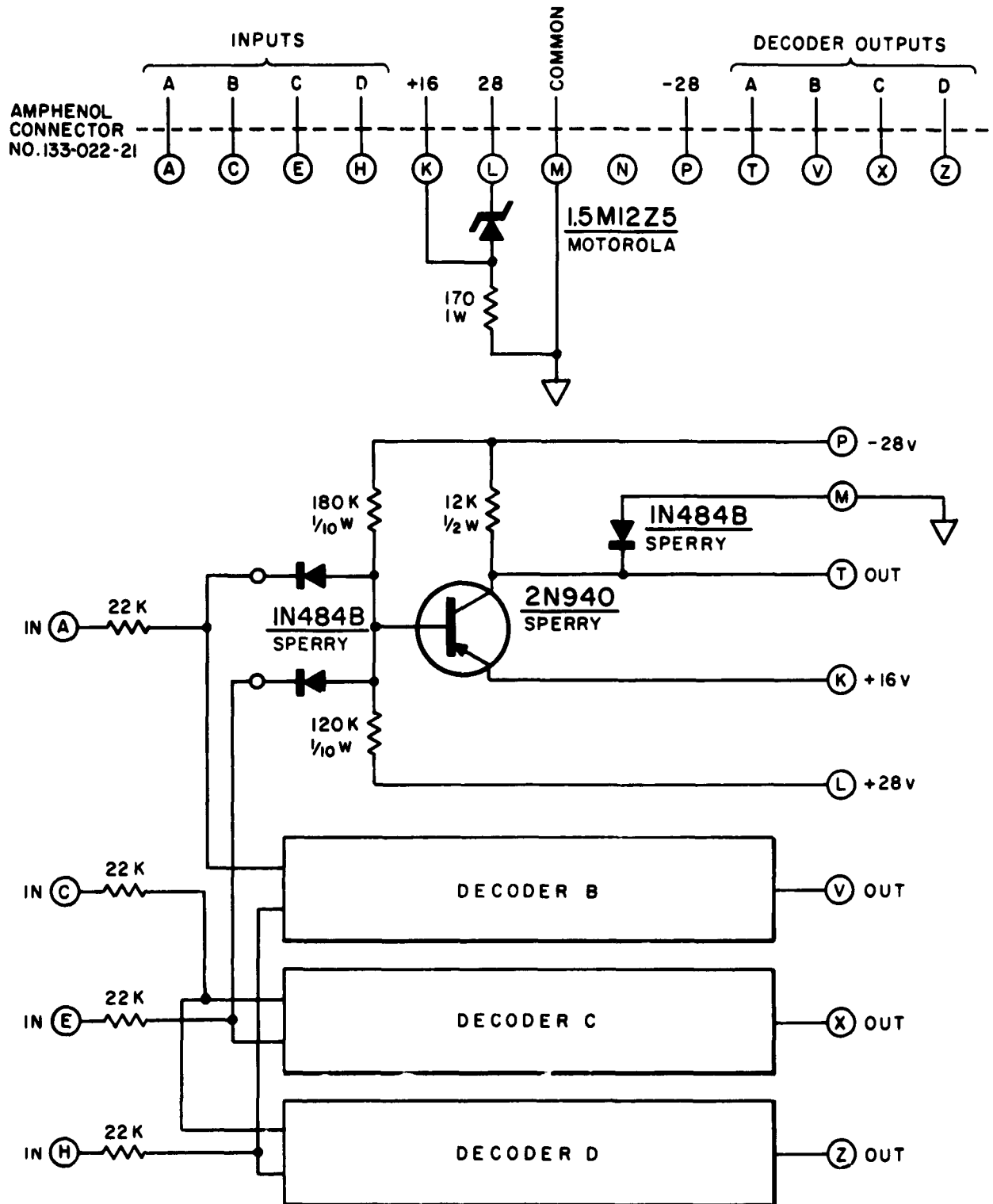
FIG. A-15 DECODER CIRCUITS

99
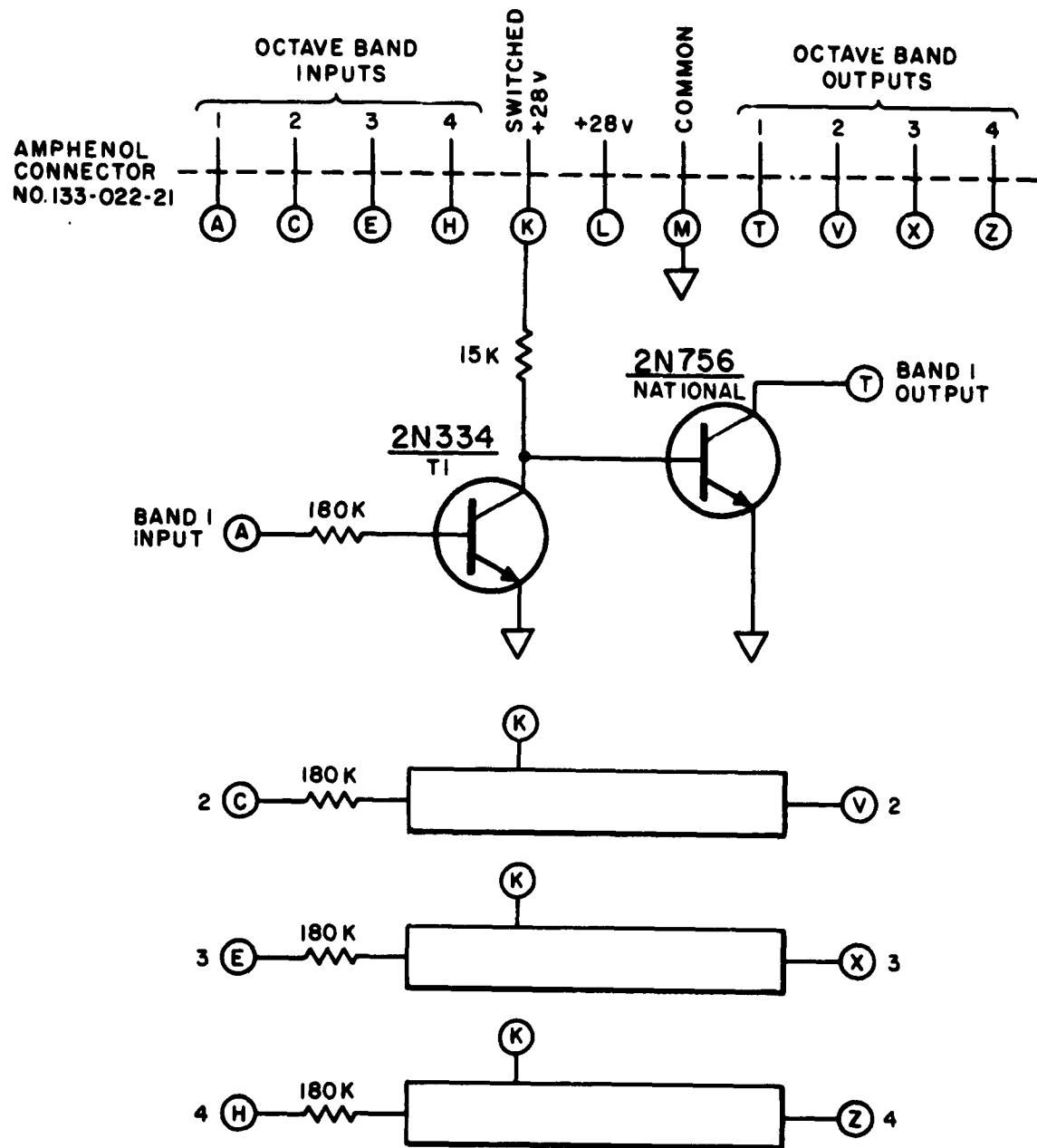
FIG. A-16   OCTAVE BAND INDICATOR LAMP DRIVERS

RUN

INPUT
FROM CLOCK

CAL.

TO FREQUENCY DIVIDERS

STEP (MOMENTARY)

TO PIN K OF
LAMP DRIVER BOARD

RUN

CAL.

+28 V

STEP

NO. 327 LAMPS

TO PIN T
OF FIG. A-16

V

X

Z
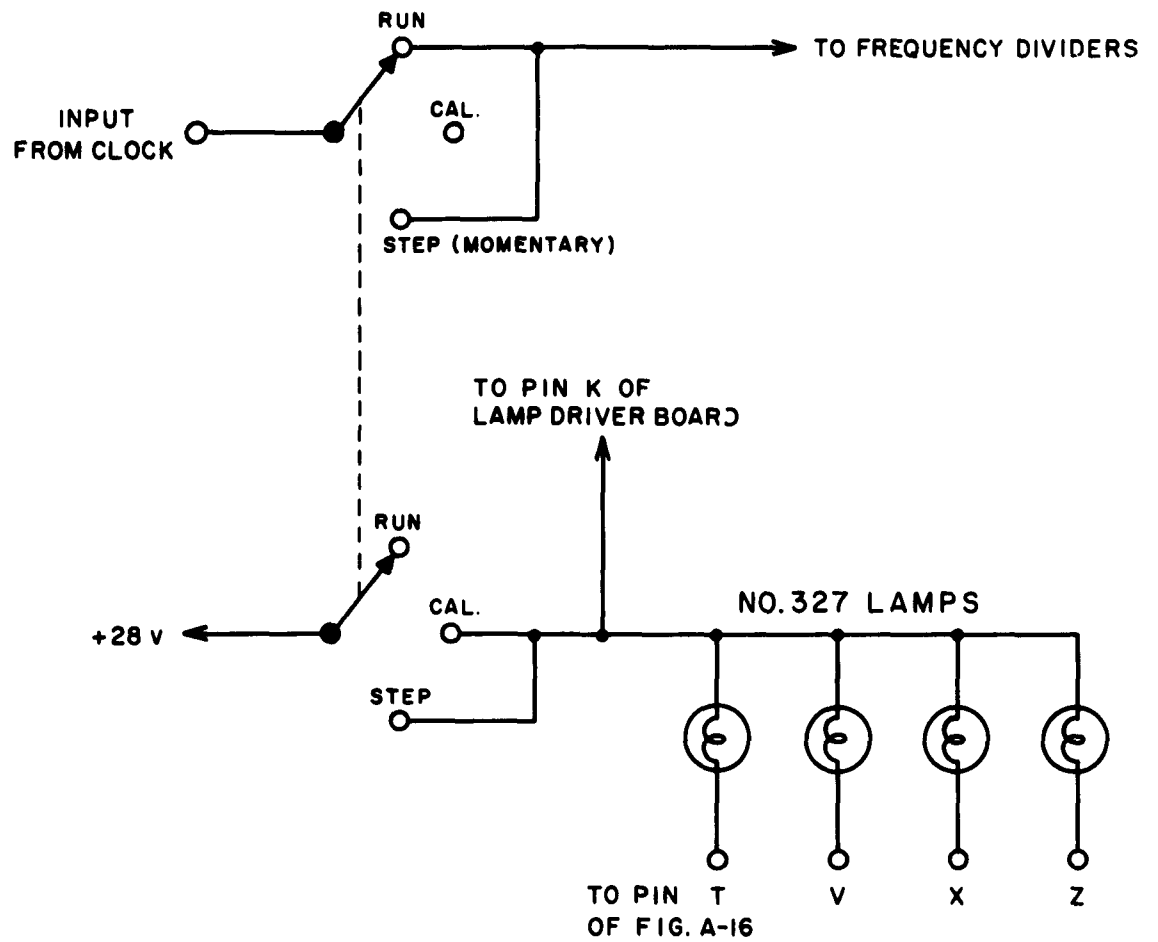
FIG. A-17   OCTAVE BAND INDICATOR LAMPS
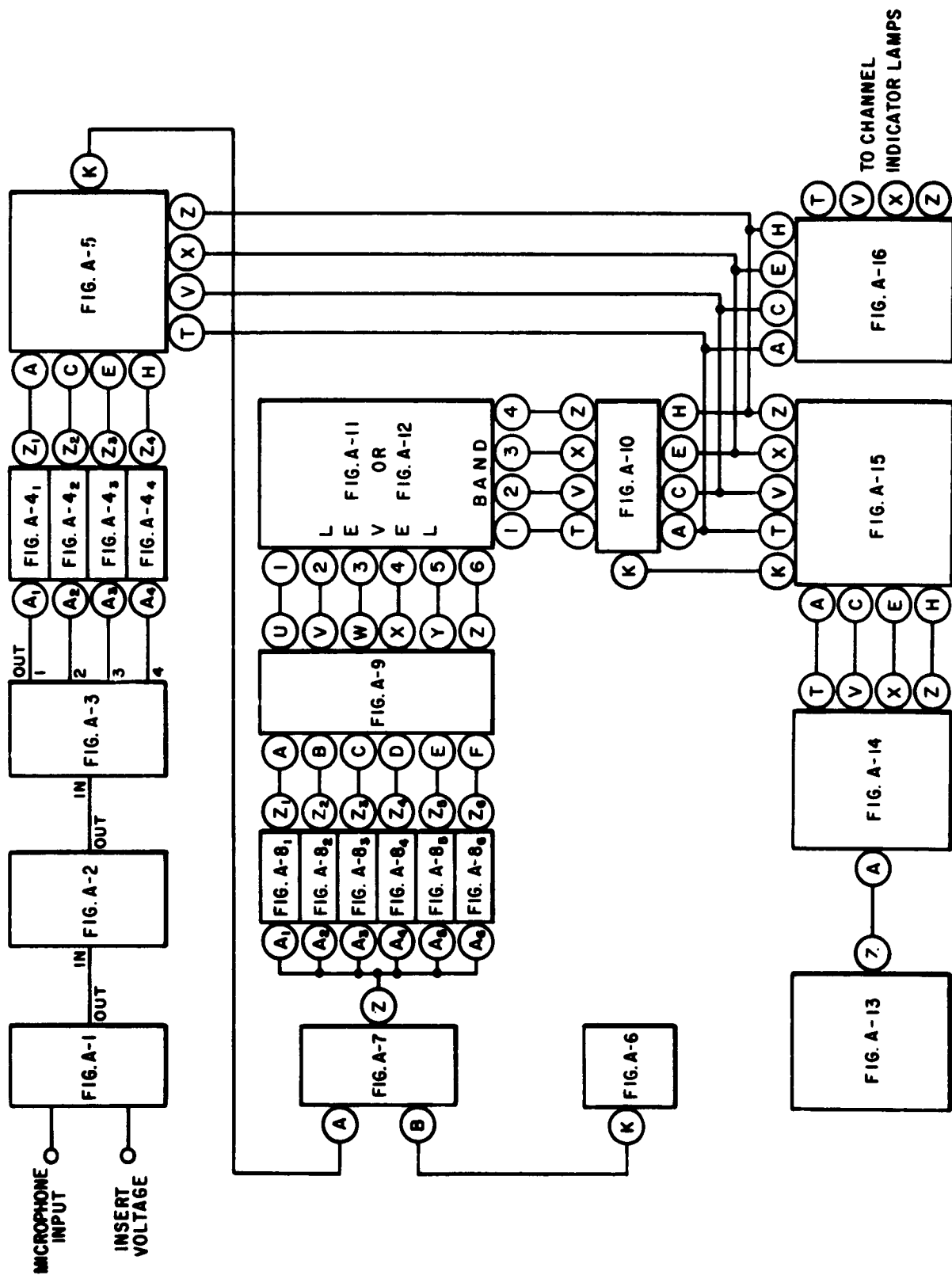
FIG. A-18   SIGNAL INTERCONNECTION DIAGRAM

APPENDIX B.

OPERATIONAL RECOMMENDATIONS FOR THE SONIC RECORDER

A.   INITIAL CHECKOUT AND CALIBRATION PROCEDURES

1.   Calibration Equipment Required

Acoustic Calibrator of approximately 125 db SPL +0.1 db at 400 cps, capable of being used over a microphone flush mounted on an aircraft (or other type of calibrator as may be required for special mountings).

Oscillator in range 75 to 1200 cps capable of supplying 40 volts rms into the 600 ohms at the Insert Voltage Input of Figure A-1.

Decade Attenuator with 10 db, 1 db, and 0.1 db steps.

Electronic Counter capable of counting frequency and periods with five decades minimum and accuracy of +1 count.

DC Voltmeter with input impedance of 1 megohm minimum, range up to 30 volts and intermediate scales and accurate to within +2%.

2.   The controls and adjustments built into the Sonic Recorder are itemized below:

Gain Attenuator: A 30 db precision attenuator in 1 db steps shown in Figure A-1 which controls the effective gain of the Data Acquisition.

Octave Band Attenuator (4 each): A 20 db precision attenuator with 2 db steps shown in Figure A-2 which is used to effect precise differences in gain between the octave band channels and to extend the range of the Gain Attenuator.

Vernier Gain Control (4 each): A continuous potentiometer with a 9 db range shown in Figure A-3 which is used to adjust the gain to match the incremental 1 db levels and provide for gain matching between the four channels.

Bias Control: A continuous potentiometer shown in Figure A-6 which is used to adjust the Bias Supply output to yield a net 1.66 volt bias into the Voltage-to-Frequency Converter.

103

Center Frequency Adjust: A control on the commercial voltage-controlled-oscillator shown in Figure A-7 to set the frequency output.

Deviation Adjust: A control on the commercial VCO shown in Figure A-7 to adjust the sensitivity of the VCO.

Trigger Level Control (6 each): A continuous potentiometer in Figure A-8 which is used to set the trigger levels to correspond to a given peak detector output.

Clock Frequency Adjust: A continuous potentiometer in Figure A-13 which is used to set the clock output frequency.

Run-Cal Switch: A three-position switch shown in Figure A-17 which is used to step between octave band channels during "Calibration" or to continuous sampling during "Run."

> NOTE: The balance Control of Figure A-4 is adjusted to give temperature drift compensation over the range -50°C to 70°C (see Section E.2. of this appendix). This control should not be changed during checkout or calibration.

3. Initial Checkout Procedures

This checkout is to be part of the final tests of a unit before being used in the field. In addition, this procedure would be useful after the instrument has been repaired.

a) Step 1*

Check all chassis interconnections and power connections for correct polarity and value. Turn on power and measure and adjust power supplies to correct voltage.

b) Step 2

Set the initial position of the following controls to:

---

* For a field calibration, disconnect the Elapsed Time Indicator before turning power on.

	Microphone Sensitivity	Setting
Gain Attenuator:	-100 to -110	0 db
	- 90 to -100	10 db
Octave Band Attenuators:	0 db for each octave band channel	
Vernier Gain:	About middle for each octave band	
Run-Cal Switch:	To Cal. on the 300-600 cps channel as shown by the Octave Band Indicator Lamp	

Disconnect the Impulse Counter Package and plug in the Calibration Lamp Package.

c)   Step 3

Apply an input of approximately 0.1 volt rms, 400 cps at the terminal marked "Cal. Input" of Fig. A-1. Monitor the voltage at A of Fig. A-7 (the input of the VCO) with the DC Voltmeter. Increase the insert voltage until the monitor reads approximately 6 volts. With linear graph paper plot the monitor voltage at 6, 4, and 2 volts vs. the insert voltage in volts. Draw a straight line through these points and note accurately the value at which this straight line intercepts the insert voltage axis. This value should be -1.66 volts.

d)   Step 4

If the intercept value is different than -1.66 volts proceed as follows. Note the actual intercept value obtained in Step 3. It is necessary to adjust the bias control of Fig. A-6 so that the intercept coincides with -1.66 volts. If, for example, the intercept were at -1.55 volts, it is apparent that the bias control needs to be more negative by 0.11 volts. This is done by setting the insert voltage to zero and noting the voltage output at the monitor. The bias adjust is then set so the monitor changes by the amount required. For example, if the monitor indicated -0.60 volts and the change desired is 0.11 volts, the bias is adjusted so the monitor output is -0.71 volts.

e)   Step 5

Repeat Step 3 to check adjustment.

f)   Step 6

Repeat Steps 3, 4, and 5 for the other octave band channels.

g)   Step 7

Connect microphone to input of cathode follower. Apply a 125 db sound pressure level at 400 cps to the microphone. Monitor the input "A" to Fig. A-7. Adjust the Octave Band Attenuator to set approximately +1.00 volts at the monitor. Adjust the Vernier Gain Control to yield exactly +1.00 volts at the monitor. (The 1.00 volts is selected for convenience and to be 8 db below full scale.)

h)   Step 8

Remove acoustic calibrator.   Replace microphone with a dummy or add an airtight cap. Apply an insert voltage at 400 cps and adjust the input voltage to yield exactly +1.00 volts at the monitor selected in Step 7.   Record the insert voltage.

Incidentally, the microphone sensitivity at 400 cps is then:

Microphone
Sensitivity $= -125$ db SPL $+ 74$ db -40 db $+ V_{Ins}$ (in db re 1 volt rms)

$$= -91 \text{ db} + V_{Ins} \text{ (db re 1 volt)}$$

where V_{Ins} is the insert voltage in db re 1 volt applied at the "Cal. input." The (-40 db) in the above is derived from the 40 db attenuation between the "Cal. Input" and the equivalent microphone voltage.

i)   Step 9

Set all Octave Band Attenuators at the value established for the 300-600 cps band in Step 7.

j)   Step 10

Using the Run-Cal Switch, advance the recorder to the 600-1200 cps band. Place in "Cal" position. Apply an insert voltage at 1000 cps with an rms level as determined in Step 8.

k) Step 11

Adjust the Vernier Gain for this octave band to yield +1.00 volts at the monitor of Step 7.

l) Step 12

Repeat Steps 10 and 11 by applying 100 cps and 200 cps and adjusting the Vernier Gain for the respective octave bands.

m) Step 13

The recorder is next adjusted to provide the 12 db amplitude windows for each of the four octave bands. The upper edge of the top window for the octave band with the lowest expected levels is used to adjust the overall system gain. An insert voltage amplitude (rms) is selected to be the number of db above the V_{Ins} of Step 8 that the maximum SPL for this octave band is above 125 db. For example, if a calibration is desired to yield the following amplitude windows:

	Lowest	Highest
75 - 150 cps	136-138	146-148
150 - 300 cps	142-144	152-154
300 - 600 cps	144-146	154-156
600 - 1200 cps	142-144	152-154

The levels for the first octave band would be used to adjust the overall gain. The insert voltage would be selected to be 148 minus 125 or 23 db above that recorded in Step 8.

n) Step 14

Set the Gain Attenuator to its lowest value (30 db). Apply the insert voltage determined in Step 13 at the center frequency for the required octave band. Use the Run-Cal switch to advance the recorder to the correct octave band. Adjust the Gain Attenuator until the voltage at the monitor of Step 7 is set at 5.00 volts. For the example cited in Step 13, this would correspond to approximately a setting of 23 db minus 8 db, or 15 db on the Gain Attenuator. The 8 db is the gain necessary to increase the signal from 1.00 volts to 5.00 volts at the VCO.

o)   Step 15

The Octave Band Attenuators are then set for the various maximum amplitudes in the other octave bands. In the example of Step 13, this would correspond to 6 db more attenuation for the 150-300 cps band, 8 db more attenuation for the 300-600 cps band, and 6 db more attenuation for the 600-1200 cps band.

p)   Step 16

Under the conditions at the completion of Step 14, i.e., 5.00 volts at the monitor, read the output frequency from TP-1 of Fig. A-8 on an electronic counter. Check that the frequency is 25,300 cps. If not, apply zero volts to the VCO as indicated by the DC Voltmeter monitoring input "A" to Fig. A-7 by decreasing the insert voltage by 12 db. Adjust the output frequency to be 18,700 cps with the Center Frequency control on the VCO. Next apply 5.00 volts again. Adjust the VCO Sensitivity until the output is 25,300 cps.

q)   Step 17

Monitor TP-4 of Fig. A-8 with a DC Voltmeter for the bandpass filter corresponding to the lowest band. Adjust the insert voltage from zero until the voltage at TP-4 is 6.00 volts. Observe the lamp corresponding to the amplitude level in the lamp package. Move the Trigger Level Control in a counter-clockwise direction until the lamp is off. Recheck and readjust the monitor to 6.00 volts. Carefully move the Trigger Level Control clockwise until the lamp just turns on.

r)   Step 18

Repeat Step 17 for all six bandpass filters.

s)   Step 19

Place the Run-Cal Switch into "Run" position with one of the readout lamps on. Observe that the lamps cycle across the octave bands.

t)   Step 20

Monitor the output "V" of Fig. A-14 with the electronic counter examining the period of the output. Adjust the Clock Frequency Control for a period of 0.500 seconds.

u)   Step 21

Turn power off. Disconnect insert voltage. Reactivate the
Elapsed Time Indicator and microphone. Replace the Lamp Readout
Package with the Counter Readout Packages. Record the number of
counts in each counter on the appropriate forms.

v)   Step 22

Set Elapsed Time Indicator to zero.

w)   Step 23

Take static pressure switch and dynamic pressure switch of
Fig. A-2 to laboratory and check their settings.

4.   Field Calibration Procedure

A field calibration would consist essentially of checking some
of the steps listed for initial checkout. This would include Steps
1 to 3, 7 to 15, 19, and 21.

The omitted steps include those required to determine the
detector intercept point for the four detectors, the adjustment of
the six trigger levels, the adjustment of the clock frequency, and
the calibration of the static and dynamic pressure switches.

The first few calibrations of the first instrument constructed
will want to be more extensive, enough to encompass all of the
Initial Checkout Procedure. This will serve as a check to establish
the critical Steps to be included in the Field Calibration Procedure.

B.   POWER SUPPLY REQUIREMENTS

The complete breadboard system is designed around 28 volts dc
for B+ and B- supply voltages. Three individual sets of supplies
are recommended since decoupling is required and it is optimum for
separate supplies. Also the currents can be balanced between
supplies very nicely. The following power supplies specifications
are recommended.

$\pm$28 volts dc regulated to within $\pm$0.05% for line and

$\pm$0.1% for load variations.

The three different supplies would be utilized in this manner.

1. **Supply 1**

   Provide +28 volts to Figs. A-1, A-3, and A-4. The current load is expected to be 130 ma maximum.

2. **Supply 2**

   Provide +28 volts to Figs. A-6, A-7, and A-8. The current load is expected to be 150 ma maximum.

3. **Supply 3**

   To provide +28 volts to Figs. A-9, A-10, A-13, A-14, A-15, A-16, and A-17. The current load is expected to be 100 ma at maximum since only one lamp or counter of the matrix is to actuate at a time.

   Inquiries to power supply manufacturers have indicated that these supplies can be provided in small packages to the regulation desired. For example, one supply is available which contains both +28 volts at .05% line regulation and 0.1% load regulation at 150 ma in a package approximately 3" x 3" x 4" and a weight of 1 lb. This particular supply was used in the Polaris program for operating temperatures from 0°C to +50°C and storage at -65°C to +85°C. The manufacturer states that it can be easily converted to silicon transistors and operate at higher temperatures if required. Other supplies with silicon components are available at ±0.1% regulation and 250 ma loads with a ±28 volt supply in a package 6" x 4" x 5".

C. MICROPHONE

   A flush mounted ceramic microphone has been selected for use with the recorder system. This selection is based upon obtaining a reliable and rugged unit for this application. The flush mount is considered necessary if the microphone is mounted on the external skin of an aircraft. Otherwise the turbulence resulting when the microphone is exposed to a high air velocity would create measurement problems. The ceramic type of microphone is simpler and more rugged than the condenser and diaphragm types. In addition the signal conditioning equipment is simpler since the capacities are higher and no bias voltage is required. The ability of the ceramic microphone to match the desired maximum SPL limits and withstand the high temperatures and high humidity expected strongly recommends it for this application.

   Microphones from many manufacturers have been considered. In general, three requirements classified the units acceptable for this application: a) flush mounting, b) vibration sensitivity, and

c) temperature sensitivity. The vibration sensitivities of most ceramic microphones is of the order of 130 db equivalent SPL per g rms up to 1000 cps. One exception to this is the Gulton P420-M6 which employs internal vibration cancellation with a second ceramic element. A reduction of the vibration sensitivity to about 105 db equivalent SPL per g was measured on one sample of this microphone.

Lead zirconate offers a low temperature sensitivity compared to other ceramic elements. Measurements made by the Clevite Research Center indicate that a voltage sensitivity change of .013 db/C^o can be realized between -60 and +60ºC. The Atlantic Research LC-60 employs this element; however, the vibration response of this unit is of the order of 129 db equivalent SPL per g below 1000 cps. The temperature sensitivity of the Gulton P420-M6 is quoted as .017 db/C^o, which is comparable to the lead zirconate element.

The microphone selected is the Gulton P420-M6 which has the following specifications as stated by Gulton in literature published in June, 1961.

Sensitivity:	-102 db re 1 volt/μbar
Linearity:	±0.5 db up to 190 db SPL
Frequency Response:	±2 db from 2 cps to 6000 cps
Vibration Sensitivity:	90 db equivalent SPL for 1 g rms
Capacitance:	2400 pfd
Static Pressure:	greater than 30 psi
Operating Temperature:	-54^oC to $+120^oC$ yields less than +1.5 db change of sensitivity, (or about 0.017 db/C^o).

Some tests have been conducted to establish some of the specifications of one sample of this microphone. These yield the following data:

ASD-TDR-62-165
Volume I

Sensitivity:	-103.6 db re 1 volt/μbar
Frequency Response (+0.2 db):	20 cps to 3000 cps
Vibration Sensitivity:	105 db equivalent SPL for 1 g rms between 20 cps and 2000 cps
Capacitance:	2300 pfd

In addition the variation of sensitivity with ambient pressure
was briefly investigated. Ambient pressures down to 2 psia were reached.
No permanent shift of sensitivity of the microphone was noted. Changes
from 29 to 21 inches of mercury yielded a change of +1 db in the fre-
quencies between 100 and 1400 cps. This corresponds to a change from
sea level to about 9000 ft. If linearity were assumed in this range,
this is equivalent to +0.11 db/1000 ft.

The contribution of this error should be small since the jet noise
reduces rapidly as the vehicle gains speed and altitudes close to the
ground are most significant for the high SPL's. Since most runways
are probably below 3000 ft., this might correspond to an uncertainty
of +0.3 db, which is relatively small compared to and uncorrelated with
the temperature errors.

Care must be exercised in the mounting of the microphone to the
aircraft since the external case of the microphone is its ground. Common
mode voltages could cause significant problems if the microphone is
grounded at the installation. It is necessary that the microphone case
not make electrical contact with the airframe at its installation.

D. ELAPSED TIME INDICATOR

Many Elapsed Time Indicators are available for operation in this
application. One that seems well suited is the A.W. Haydon 19200
series. These are similar in construction and environmental specifica-
tion to the impulse counters, i.e., -54°C to +85°C, and 10 to 2000 cps
at 20 g. Four digits are again available and can be used down to a
0.1 hour resolution. Maximum elapsed time error is +0.1 hour at 400
cps and 104 to 124 volts. The weight of the unit is 3/4 of an ounce;
the volume is 0.25 cubic inches.

E. RMS-DETECTOR CIRCUIT; DESIGN AND TEMPERATURE COMPENSATION

1. Experimental Design

The detector handles two types of signals: a pure tone for cali-
bration and octave bands of random noise from data.

The detector circuit shown in Fig. A-4 is a quasi rms type which
will give accurate rms readings of pure tone or random gaussian noise.
Thus no correction is needed during calibration which is an advantage
over a true-rectified average circuit. Yet the present circuit is much
simpler than a true rms circuit.

ASD-TDR-62-165
Volume I

The detecting action partially clips the positive and negative
peaks. The clipping level is set by the charge accumulated in the
capacitors. Simultaneously the second capacitor measures the peak-
to-peak value of the clipped signal. As the signal becomes more
and more clipped, the peak-to-peak value approaches a definite value
dependent on the waveform average power. This is insured by the
series resistor which prevents the sudden charging of either
capacitor, and by the output load which imposes a constant drain
of charge from the capacitor.

The detector was designed experimentally as follows:

a)   Select a detector load (in this case 27K).

b)   Select equal capacitors, whose value will yield an
acceptable discharge time constant; 100 μf gives about 2.7 seconds.

c)   Adjust the series resistor to give equal dc output for the
same applied true rms of a sine wave or an octave band of noise.

The curve of Fig. B-1 shows that for a given load R_L the series
resistor R can be adjusted to give equal dc output for the same rms
value of input sine wave or octave band of noise.

2.   Temperature Compensation

The temperature drift in detector occurs from the offset voltage
of the silicon diodes while conducting. The silicon diode is
equivalent to an ideal diode in series with a resistor and battery,
the battery being the offset voltage. This offset varies with con-
duction current and temperature. The offset voltage of silicon
diodes has a negative temperature coefficient, resulting in an
increase of the detector output with increasing temperature. This
change of offset voltage for a silicon diode is typically 0.25 volts
over the temperature range of $-50°C$ to $+100°C$. Since two such diodes
are used, twice this voltage change will appear at the detector output.

The emitter follower at the detector output has also a tempera-
ture drift. This drift is primarily caused by the temperature
coefficient of V_{BE} (the forward voltage drop across the base-emitter
diode of the transistor) and the temperature coefficient of I_{CBO}
(base current for open circuited emitter: $I_E = 0$).

113

In addition, the β of the silicon transistors has a positive temperature coefficient of approximately 0.5% per C^o. When an emitter follower circuit is used, the net gain change becomes approximately

$$\Delta G = \frac{\beta(1+\gamma t)}{1+\beta(1+\gamma t)} = \left(1 - \frac{1}{\beta}\right) + \frac{\gamma T}{\beta}$$

By selecting high β transistors ($\beta > 50$), the temperature coefficient γ is reduced by the factor $\frac{1}{\beta}$ and becomes negligible.

Since I_{CBO} has a strong exponential dependence on temperature, it is wise to select a transistor having a very small I_{CBO} at room temperature (such as the type 2N940 or 2N943).

Since:

$$I_{CBO} = A_o\, e^{k(\Delta T)}$$

where,

$A_o = I_{CBO}$ at $25^o C$

ΔT = temperature change in C^o measured from $25^o C$

$k = 0.06$ to 0.094

It follows that for $\Delta T = +50^o C$, $e^{k\Delta T}$ becomes 20 to 100 depending on the value of k chosen. If the voltage change introduced by the change in I_{CBO} flowing in the detector load resistor (27K) is to be less than 50 millivolts, it follows that I_{CBO} at room temperature should be less than .01 microampere. Many transistors satisfy this condition.

The temperature coefficient of V_{BEO} is negative with a slope of about -2.5 mv/C^o. In a PNP emitter follower configuration, the emitter voltage decreases with increasing temperature, thus providing already a partial compensation for the rise of detector voltage with temperature.

The final overall compensation is obtained by adding a small zener diode in series with the output of the emitter follower. This solution is discussed in the following paragraphs.

ASD-TDR-62-165
Volume I

F.   IMPROVED INPUT CIRCUIT

The cathode follower of Fig. A-1 can be replaced by a unipolar
(field effect) transistor. These transistors are now available only
in sample quantities and their reliability has not been well estab-
lished. However, their high input impedance and low electrical noise
make them ideal for this application. In addition, they have a much
lower vibration sensitivity than the nuvistor vacuum tubes. The
available types of unipolar transistors are all silicon units.

A preamplifier circuit, using a unipolar transistor is shown
in Fig. B-2. A better frequency response than the cathode follower
of Fig. A-1 is obtained. The electrical noise, in octave bands from
75 to 1200 cps is less than -100 db re 1 volt re the input, with a
1500 $\mu\mu$f capacitor replacing the microphone.

These results show that the circuit of Fig. B-2 should be used
in preference to the cathode follower section of Fig. A-1 as soon as
the unipolar transistors are commercially available and their relia-
bility well established.

116
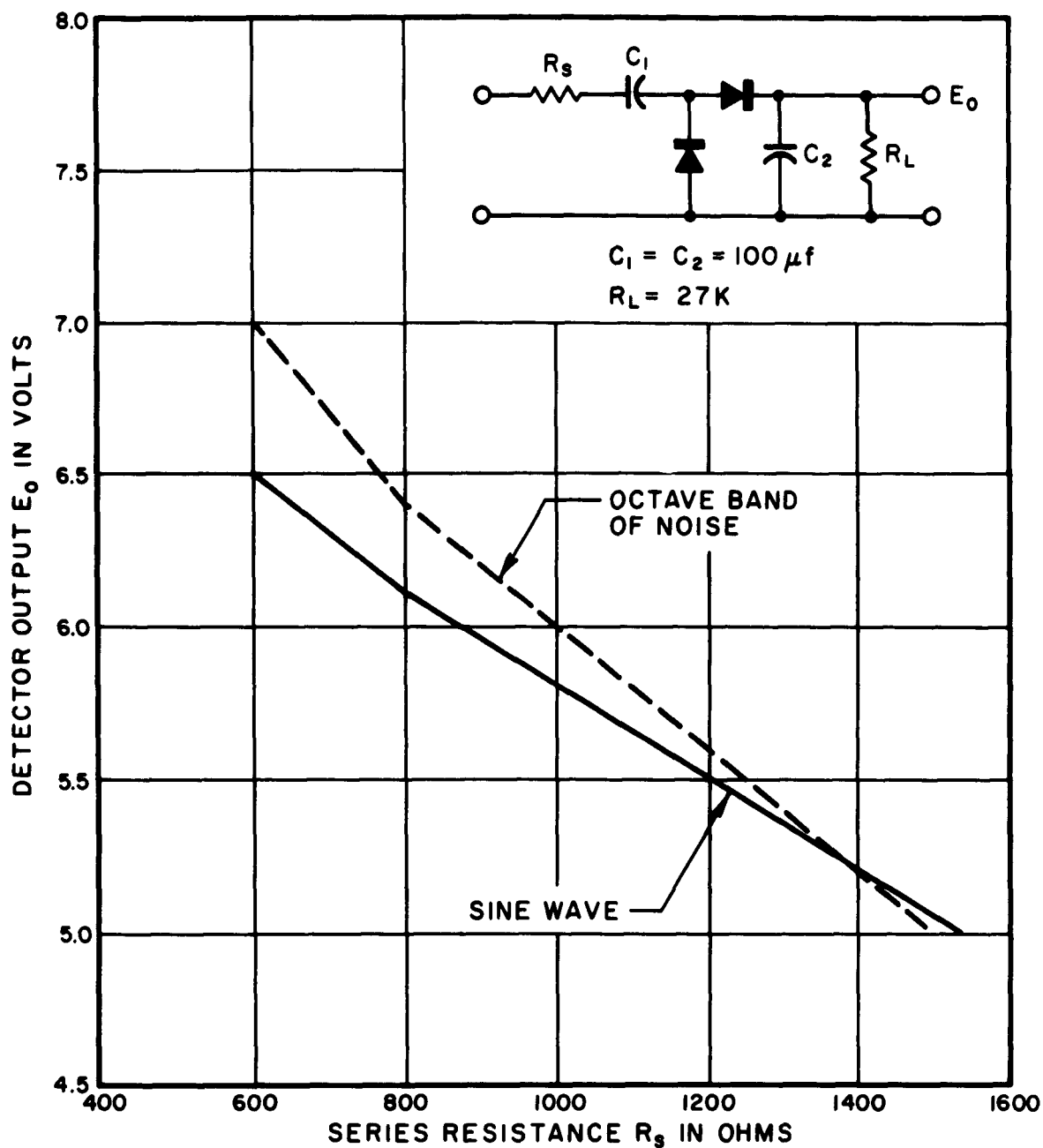
FIG. B-I   DETECTOR OUTPUT AS A FUNCTION OF THE
SERIES RESISTOR R_s. INPUT VOLTAGE
4.0 VOLTS RMS

FIG. B-2   IMPROVED INPUT CIRCUIT

118

Aeronautical Systems Division, Dir/Aero-mechanics, Flight Dynamics Lab, Wright-Patterson AFB, Ohio.
Rpt No. ASD-TDR-62-165, Vol I. STUDY OF A SONIC LOAD RECORDER. Interim report, Nov 62, 118p. incl illus., tables, 15 refs.

Unclassified Report

The feasibility of a compact instrument to measure the accumulated acoustic exposure of a flight vehicle is considered. The output data of the instrument will aid the estimation of fatigue life. A study of the conditions and parameters involved together with general requirements of the instrument is presented. Design criteria are discussed such as techniques for amplitude analysis, sampling and

(over)

accumulation of data in a directly readable and usable form. A specific design of a breadboard model of the sonic recorder is given with test and performance data under laboratory conditions. A discussion of the effects of temperature, vibration, and power supply variations is also included. Complete circuit diagrams are provided.

1. Acoustics
2. Recording systems
3. Noise analyzers
4. Fatigue (mechanical)
I. AFSC Project 1370, Task 137005
II. Contract AF33(616)-7789
III. Bolt Beranek and Newman, Inc., Cambridge, Mass.
IV. J. H. Ball, et al.
V. BBN Report 902
VI. Aval fr OTS
VII. In ASTIA collection

Aeronautical Systems Division, Dir/Aero-mechanics, Flight Dynamics Lab, Wright-Patterson AFB, Ohio.
Rpt No. ASD-TDR-62-165, Vol I. STUDY OF A SONIC LOAD RECORDER. Interim report, Nov 62, 118p. incl illus., tables, 15 refs.
Unclassified Report

The feasibility of a compact instrument to measure the accumulated acoustic exposure of a flight vehicle is considered. The output data of the instrument will aid the estimation of fatigue life. A study of the conditions and parameters involved together with general requirements of the instrument is presented. Design criteria are discussed such as techniques for amplitude analysis, sampling and
(over)

accumulation of data in a directly readable and usable form. A specific design of a breadboard model of the sonic recorder is given with test and performance data under laboratory conditions. A discussion of the effects of temperature, vibration, and power supply variations is also included. Complete circuit diagrams are provided.

1. Acoustics
2. Recording systems
3. Noise analyzers
4. Fatigue (mechanical)
I. AFSC Project 1370, Task 137005
II. Contract AF33(616)-7789
III. Bolt Beranek and Newman, Inc., Cambridge, Mass.
IV. J. H. Ball, et al.
V. BBN Report 902
VI. Aval fr OTS
VII. In ASTIA collection